

Utah State University

DigitalCommons@USU

All Graduate Theses and Dissertations

Graduate Studies

5-2013

Novel Aminoglycosides: Bioactive Properties and Mechanism of Action

Sanjib K. Shrestha
Utah State University

Follow this and additional works at: <https://digitalcommons.usu.edu/etd>



Part of the [Biology Commons](#)

Recommended Citation

Shrestha, Sanjib K., "Novel Aminoglycosides: Bioactive Properties and Mechanism of Action" (2013). *All Graduate Theses and Dissertations*. 2073.
<https://digitalcommons.usu.edu/etd/2073>

This Dissertation is brought to you for free and open access by the Graduate Studies at DigitalCommons@USU. It has been accepted for inclusion in All Graduate Theses and Dissertations by an authorized administrator of DigitalCommons@USU. For more information, please contact digitalcommons@usu.edu.



NOVEL AMINOGLYCOSIDES: BIOACTIVE PROPERTIES AND MECHANISM OF
ACTION

by

Sanjib K. Shrestha

A dissertation submitted in partial fulfillment
of the requirements for the degree

of

DOCTOR OF PHILOSOPHY

in

Biology

Approved:

Jon Y. Takemoto, PhD
Major Professor

Michelle M. Grilley, PhD
Committee Member

Charles D. Miller, PhD
Committee Member

Dennis L. Welker, PhD
Committee Member

Cheng-Wei Tom Chang, PhD
Committee Member

Mark R. McLellan, PhD
Vice President for Research
and Dean of Graduate School

UTAH STATE UNIVERSITY
Logan, Utah

2013

Copyright © Sanjib K. Shrestha 2013

All Right Reserves

ABSTRACT

Novel Aminoglycosides: Bioactive Properties and Mechanism of Action

by

Sanjib K. Shrestha, Doctor of Philosophy

Utah State University, 2013

Major Professor: Dr. Jon Y. Takemoto
Department: Biology

Fungicide discovery is relatively neglected when compared to the investment in the development of antibacterial, antiviral, and anti-cancer therapeutics. Due to extensive use of currently available fungicides in agriculture and medicine, resistance is emerging among plant and animal pathogenic fungi. This necessitates the search for novel antifungal agents that are effective and less toxic and that do not promote resistance.

FG08 and K20 are novel aminoglycoside analogs synthesized from kanamycin B and A, respectively. The antimicrobial properties of these analogs were tested *in vitro* against a wide range of agriculturally and clinically important fungal pathogens. Both compounds showed broad-spectrum antifungal properties, but they did not inhibit bacteria such as *Escherichia coli* and *Staphylococcus aureus*. The hemolytic activities and cytotoxicities of FG08 and K20 were also evaluated. They showed no toxicity or lowered toxicity against animal cells at their antifungal minimum inhibitory concentrations (MICs).

The fungicidal mechanisms of action of FG08 and K20 were examined using intact cells of *Saccharomyces cerevisiae*, *Cryptococcus neoformans*, hyphae of *Fusarium graminearum*. FG08 and K20 caused SYTOX Green dye uptake and potassium efflux by intact cells, indicating that they increase plasma membrane permeability. FG08 and K20 also caused leakage of pre-loaded calcein from small unilamellar vesicles (SUVs) composed of lipids that mimic the lipid composition of fungal membranes, further suggesting increased membrane permeability as their mechanism of action.

The synergistic interactions of K20 with six azoles (such as itraconazole, and fluconazole) were investigated against a wide array of fungal pathogens. The *in vitro* results revealed strong synergy between K20 and azoles against plant and human pathogenic fungi. Their synergies were further confirmed by time kill curves and disk diffusion methods.

In conclusion, FG08 and K20 are broad-spectrum antifungal agents that do not inhibit bacteria. At their antifungal MICs, they are not toxic to animal cells, but they inhibit fungi by interacting with the fungal plasma membrane, leading to pore formation. These novel aminoglycoside analogs appear attractive for applications as fungicides in agriculture and medicine.

PUBLIC ABSTRACT

Novel Aminoglycosides: Bioactive Properties and Mechanism of Action

by

Sanjib K. Shrestha, Doctor of Philosophy

Utah State University, 2013

Major Professor: Dr. Jon Y. Takemoto
Department: Biology

More than 90% of crop diseases are due to fungal infections, which globally cause enormous economic losses. Fungal infections in humans and animals have also become a serious concern, especially in immunocompromised individuals. However, only a few new fungicides have been introduced since the mid-1980s, and concerns with inconsistent and declining effectiveness due to resistance, environmental impacts, animal and human toxicity, and costs continue to challenge the use of available fungicides. There is a serious and persistent need for new antifungal agents that are more effective, eco-friendly, less toxic, and available at reasonable cost.

This study reveals two novel aminoglycosides, FG08 and K20, that are synthesized from kanamycin B and A, respectively. Kanamycin B and A are aminoglycoside antibiotics that kill bacteria. In contrast, FG08 and K20 showed broad-spectrum antifungal activities against a wide range of agriculturally and clinically important fungal pathogens, but they did not inhibit bacteria. They showed no or lowered

toxicities against animal cells at their antifungal minimum inhibitory concentrations (MICs). They inhibit fungi by interacting with the fungal plasma membrane, leading to pore formation. K20 can be produced on a large scale, which makes it feasible to develop as a fungicide for commercial application. Additionally, K20 showed synergistic antifungal interaction with azoles against various fungi. Azoles are today's most widely used antifungal agents to treat fungal infections in agriculture and medicine. In conclusion, this research has helped discover a new class of broad spectrum fungicides, which appear attractive for application as crop disease protectants and therapeutics against serious fungal infections in immunocompromised humans.

DEDICATION

This dissertation is dedicated to my loving parents, **Sanat K. Shrestha** and **Niranjana K. Shrestha**, and my uncle **Prof. Dr. Krishna K. Shrestha**.

ACKNOWLEDGMENTS

Foremost, I would like to express my sincere gratitude to my advisor, Dr. Jon Y. Takemoto, for the continuous support of my PhD study and research, for his motivation, enthusiasm and immense knowledge. I appreciate his willingness to permit me the freedom to explore different avenues of research while I was working in his laboratory. I deeply appreciate his persistence in pushing me to re-examine, rethink, and rewrite so as to produce the best work possible. I have been amazingly honored to have him as an advisor; without his support this dissertation could not have been completed.

I would specially like to thank Dr. Michelle Grilley for her endless guidance, insightful comments, and constant encouragement throughout my doctoral program. I would like to convey my deepest appreciation and respect to all members of my committee, Dr. Cheng-Wei Tom Chang, Dr. Bradley R. Kropp (former committee member), Dr. Charles Miller, and Dr. Dennis Welker (new committee member) for their support, time, understanding, and encouragement through all these years. I owe special thanks to Lynnette Takemoto for her technical support and personal advice. I am also grateful for the support from Dean Scott Hinton, Dr. Ronald Sims, and Dr. Dong Chen of the Synthetic Biomanufacturing Institute, USU.

I also thank and acknowledge all of my lab mates in Dr. Takemoto's laboratory who made my work here greatly enjoyable. Special thanks to Christine Dhiman, Thomas Anderson, Dr. Mekki Bensaci, and Yukie Kawasaki. I would also like to thank my colleagues in the Dewald and Chang laboratories, Dr. Sitaram Harihar, Dr. Almut Volmer, Dr. Marina Fosso, and Jaya Shrestha for their friendship and help.

I would like to thank my parents for their endless love, support, and sacrifices they have done for me. I am extremely grateful to my elder sisters, Menuka Shrestha and Medina Shrestha, for their constant support and encouragement they have provided me during these years. In addition, I would like to deeply appreciate my sweet brother, Rajeev K. Shrestha, for taking good care of our parents, business, and everything back home. I am very fortunate to have him as a brother. Special thank go to my dear son, Sanil Shrestha, for being my strength and origin of happiness. Last but not least, I wish to thank my beloved wife, Nika Shrestha, for her unconditional love, support, and patience. She was always there consoling me and stood by me through the good times and bad. Without you, my dear, I could not have achieved this.

Sanjib K. Shrestha

CONTENTS

	Page
ABSTRACT.....	iii
PUBLIC ABSTRACT	v
DEDICATION.....	vii
ACKNOWLEDGMENTS	viii
LISTS OF TABLES.....	xii
LISTS OF FIGURES	xiii
LISTS OF ABBREVIATIONS.....	xv
CHAPTER	
1. INTRODUCTION AND LITERATURE REVIEW	1
THE FUNGI.....	1
ANTIFUNGAL AGENTS	2
ANTIFUNGAL DRUG COMBINATION THERAPY	8
AMINOGLYCOSIDES	9
JUSTIFICATION AND OBJECTIVES	14
REFERENCES	16
2. MEMBRANE LIPID-MODULATED MECHANISM OF ACTION AND NON CYTOTOXICITY OF NOVEL FUNGICIDE AMINOGLYCOSIDE FG08.....	27
ABSTRACT.....	27
INTRODUCTION	28
MATERIALS AND METHODS.....	30
RESULTS	35
DISCUSSION.....	37
CONCLUSIONS.....	41
REFERENCES	41
3. NOVEL AMINOGLYCOSIDE K20: ANTIFUNGAL PROPERTIES, MECHANISM OF ACTION, AND SUPPRESSION OF MURINE	

PULMONARY <i>CRYPTOCOCCUS NEOFORMANS</i> INFECTION.....	55
ABSTRACT.....	55
INTRODUCTION	56
MATERIALS AND METHODS.....	58
RESULTS	65
DISCUSSION.....	68
REFERENCES	71
4. ANTIFUNGAL SYNERGISM BETWEEN AMINOGLYCOSIDE K20 AND AZOLES ANTIFUNGALS	86
ABSTRACT.....	86
INTRODUCTION	87
MATERIALS AND METHODS.....	89
RESULTS	93
DISCUSSION.....	95
REFERENCES	98
5. SUMMARY AND FUTURE DIRECTIONS.....	106
REFERENCES	110
APPENDICES	112
A. Chemo-enzymatic synthesis of a novel aminoglycoside analog, FG08	113
B. The effect of K20 on the dimorphic transition of <i>C. albicans</i>	120
C. Bioactivity of novel aminoglycoside, FG03	122
CURRICULUM VITAE.....	130

LIST OF TABLES

Tables	Page
2-1. Growth susceptibilities of yeast sphingolipid biosynthetic mutants to FG08.....	45
3-1. Minimal inhibitory concentrations (MICs) of K20 and kanamycin A against bacteria and fungi	75
4-1. Suceptiblility of fungal strains to K20 and azoles alone and in combination.....	103

LIST OF FIGURES

Figure		Page
1-1	Structures of kanamycin A and B	26
2-1	Structures of aminoglycosides kanamycin B and FG08.....	46
2-2	Membrane perturbation effects of FG08 on intact cells of <i>S. cerevisiae</i> strain W303C	47
2-3	Effect of FG08 on SYTOX Green dye staining of <i>S. cerevisiae</i> strain W303C and isogenic sphingolipid biosynthetic mutants	48
2-4	Phase contrast microscope images of FG08 effects on the cell internal structure of <i>S. cerevisiae</i> strain W303C.....	49
2-5	Dose-dependent effect of FG08 on cellular K ⁺ efflux by <i>S. cerevisiae</i> strain W303C	50
2-6	Effect of FG08 on calcein release from SUVs that mimic glycerophospholipid and sterol compositions of fungal, bacterial, and mammalian cell plasma membranes	51
2-7	Disk-diffusion antifungal assays of FG08 against <i>S. cerevisiae</i> W303C and sphingolipid biosynthetic mutants	52
2-8	Mammalian cell cytotoxicities of FG08	53
2-9	Effect of FG08 on SYTOX Green dye staining of C8161.9 cells	54
3-1	Structures of aminoglycosides kanamycin A, FG08, and K20.....	76
3-2	Microscopic images of <i>F. graminearum</i> and <i>C. neoformans</i> H99 suspended and incubated in PDB in microtiter plate wells of MIC microbroth dilution assays	77
3-3	Time kill curves for <i>C. neoformans</i> H99 at different concentrations of K20	78

3-4	Hemolytic activity of K20 (white bars) against sheep erythrocytes after 1 h exposure at 37°C	79
3-5	Mammalian cell cytotoxicities of K20.....	80
3-6	Dose-dependent membrane perturbation effects of K20 on <i>C. neoformans</i> H99	81
3-7	Dose-dependent membrane perturbation effects of K20 on <i>F. graminearum</i>	82
3-8	Effect of K20 on calcein release from SUVs that mimic fungal plasma membranes.....	83
3-9	Mean percent weight change in groups of mice receiving treatments of K20.....	84
3-10	Mouse pulmonary fungal burden at day 15 post <i>C. neoformans</i> infection as assessed by plating for CFU	85
4-1	Time kill curves of ITC or FLC and K20 alone and in combination against azole-R <i>C. albicans</i> 10231.....	104
4-2	Disk diffusion assay showing synergistic interaction of K20 with POS or ITC against azole-R <i>C. albicans</i> 64124and azole-S <i>C. albicans</i> MYA 2876.....	105

LIST OF ABBREVIATIONS

AMEs	aminoglycoside modifying enzymes
CLSI	Clinical and Laboratory Standards Institutes
CFU	colony forming unit
CLZ	clotrimazole
2DOS	2-deoxystraptamine
DMEM	Dulbecco's Modified Eagle Medium
DNFB	dinitrofluorobenzene
FBS	fetal bovine serum
FIC	fractional inhibitory concentration
FICI	fractional inhibitory concentration index
FITC	fluorescein isothiocyanate
FLC	fluconazole
HC50	fifty percent hemolytic concentration
HPLC	high performance liquid chromatography
HRP	horseradish peroxidase
IPC	inositolphosphorylceramide
ITC	itraconazole
KTZ	ketoconazole
LB	Luria-Bertani
LC50	fifty percent lethal concentration
MET	metconazole

MIPC	mannosyl-inositol-phosphorylceramide
M(IP) ₂ C	mannosyl-diinositol-phosphorylceramide
MIC	minimum inhibitory concentration
MTT	3-(4,5-dimethylthiazol-2-yl)-2,5-diphenyltetrazolium bromide
NaDodSO ₄	sodium dodecyl sulfate
NCCLS	National Committee on Clinical Laboratory Standards
PC	phosphatidylcholine
PDB	potato dextrose broth
PDA	potato dextrose agar
PE	phosphatidylethanolamine
PMFS	phenyl methyl sulfonyl fluoride
PI	phosphatidylinositol
POS	posaconazole
PS	phosphatidylserine
PVDF	polyvinylidene difluoride
SOB	super optimal broth
SRE	syringomycin E
SUV	small unilamellar vesicle
VOR	voriconazole
YPD	yeast extract-peptone-dextrose

CHAPTER 1

INTRODUCTION AND LITERATURE REVIEW

THE FUNGI

Fungi are ubiquitous organisms present in the environment that are unavoidable. It is estimated that there are 250,000 to 300,000 species of fungi [1]. In nature, they play important roles in the carbon cycle where they act as decomposers of organic materials along with other microorganisms such as bacteria. Fungi are either unicellular or multicellular and can be grouped on the basis of morphology as either yeasts or molds. Yeasts are a unicellular form of fungi that can divide by budding. They produce round, pasty or mucoid colonies on solid medium. In contrast, molds are multicellular, multinucleated, filamentous forms of fungi that produce thread-like hyphae that intermingle to form a mat-like structure called a mycelium [2].

Fungi are able to grow parasitically on plants, animals, humans and other fungi. Plant pathogenic fungi can cause severe damage and loss to agriculture, causing diseases such as late blight of potato, chestnut blight and Dutch elm diseases. More than 90% of crop diseases are due to fungal infections which globally cause enormous economic losses. Fungal diseases destroy > 125 million tons/year of the top five foods (rice, wheat, maize, potatoes and soybean) that could feed more than 600 million people [3]. Fungi have long been understood to be a widespread threat to plants [3]; however, appreciation of their threats to animal and human health is increasing due to increasing occurrences of systemic mycoses that are becoming significant causes for morbidity and mortality in humans. Approximately 150 species of fungi are known as primary pathogens in humans,

several of which may be fatal if left untreated. *Candida* species have been reported as the fourth most common cause of nosocomial bloodstream infections in the United States; however, other fungi such as *Cryptococcus* spp., *Aspergillus* spp., *Fusarium* spp., and *Scedosporium* spp. are emerging pathogens that pose direct threats to human health [4]. The frequency of invasive fungal infections has increased due to a growing immunocompromised population, as a result of increases in rates of HIV infection, organ transplantation and cancer chemotherapy [5].

ANTIFUNGAL AGENTS

Fungicides are biocidal chemical compounds or biological organisms that specifically kill fungi. Fungicides have been used extensively for over 200 years to protect plants against diseases caused by fungi. Direct application of fungicides has been a major way to control fungal diseases and it plays an important role in crop protection. More than 150 different fungicidal compounds are currently used with a global market value of about 6 billion U.S. dollars, accounting for almost 20% of the agrochemicals market [6]. According to the U.S. Environmental Protection Agency (EPA) approximately 244,000 tons of fungicides and 37,000 tons of fungicides were sold worldwide and in the United States, respectively [7]. Similarly, therapeutic antifungal agents are also used either topically or systemically to treat mycoses in humans. These antifungals have revolutionized the treatment options of fungal infections in medicine. In 2011, the estimation of the global market for antifungal therapeutics was valued at \$10.7

billion and is expected to reach \$12.2 billion in 2016. In 2011, the market for antifungal therapeutics in U.S. alone was valued nearly \$4.5 billion and is expected to total nearly \$4.9 billion in 2016.

Moreover, fungi are complex organisms that share many biochemical targets with other eukaryotic cells. Due to this reason, the development of new antifungal agents remains a major challenge. Although antifungal agents have been pursued for decades, there are limited numbers of effective drugs available to fight against invasive fungal infections. Concerns with inconsistent and declining effectiveness due to resistance, environmental impacts, animal and human toxicity and costs continue to challenge their use. Thus, there is a serious need for the development of new antimicrobials that are more effective, eco-friendly, less toxic and have low incidences of fungal resistance.

Antifungal agents in medicine

Over the years, a number of antifungal agents have been discovered and assessed for use in the treatment of systemic mycoses. Among them, the polyenes, imidazoles, triazoles, allylamines, griseofulvin, and 5-fluorocytosine have proved to be most useful antifungal agents. These drugs can be divided into four broad groups on the basis of their molecular mechanism of action. These antifungal agents either inhibit ergosterol synthesis, impair membrane barrier function, interact with microtubules or inhibit macromolecule synthesis.

Polyenes

Over the past few decades, polyene antifungals have been important for the treatment of invasive fungal infections in medicine. Amphotericin B, nystatin, and natamycin represent the polyene class of antifungal agents. Among them, amphotericin B is the only polyene antibiotic that has been successfully developed as a systemic antifungal agent against systemic mycoses. Amphotericin B is a broad-spectrum antifungal agent produced by *Streptomyces nodosus* [8] that exerts its antifungal activities by binding preferentially to ergosterol in the fungal cell membrane, as compared to cholesterol in the human plasma cell membrane. It destabilizes the fungal plasma membrane by pore formation leading to the leakage of intracellular components such as K^+ ions and eventually cell death [9]. Amphotericin B still remains a gold standard for the treatment of invasive fungal infections. However, the use of amphotericin B is limited by its inherent toxicity [10].

Pyrimidines

5-fluorocytosine (5-FC) and 5-fluorouracil (5-FU) are two pyrimidines that are synthetic structural analogs of DNA nucleotide cytosine. 5-FC was synthesized in 1957 by Duschinsky et al. 1960, initially as an antitumor agent, but later discovered for its antifungal potential to treat fungal infections such as cryptococcosis and candidiasis [11, 12]. It also exerts broad spectrum antifungal activities against *Candida*, *Cryptococcus* and *Aspergillus* species. 5-FC enters the fungal cell through active transport on ATPases. It is then converted to active 5-fluorouracil (5-FU) by fungal cytosine deaminase to active 5-fluorouracil (5-FU) which is incorporated into RNA causing faulty RNA synthesis.

However, monotherapy with 5-FC is not advisable because it is thought to promote the development of fungal resistance. But it has been effectively used in combination with amphotericin B or azoles [13].

Azoles

Azoles are by far most widely used antifungals in clinical practice as well as in agriculture. They are also the most widely studied antifungal agents regarding their mode of action, pharmacological properties and mechanism of resistance. There are two classes of azoles, imidazole and triazoles. Benzimidazole were the first imidazole discovered by Woolly (1944) as an antifungal agent [14]. Many other agricultural and medical azoles were subsequently developed based upon the azole ring.

Triazoles, a subset of the azole drugs, were developed in the 1980s and 1990s and that have wide spectrum of activity and also an excellent safety profile [15]. Azoles exert inhibitory effects on fungi by inhibiting the enzyme lanosterol-14-alpha- demethylase, which is responsible for converting lanosterol to ergosterol (a necessary fungal cell membrane component). Loss of ergosterol production increases the cell membrane permeability, leading to cell death [16]. A major problem associated with the use of azoles is the emergence of resistance, mainly through point mutations affecting the gene encoding the target enzyme or by overexpression of drug efflux pumps [17]. However, azoles remain a mainstay to treat systemic mycosis in humans, and are widely used in agriculture.

Echinocandins

The final and most recently developed class of antifungals, having only been used since the new millennium, is the echinocandins which are semisynthetic lipopeptides. They act by blocking glucan synthase inhibiting 1,3- β -D-glucan synthesis [18]. 1,3- β -D-glucan is key structural component of the fungal cell wall that is not present in mammalian (host) cells. This makes echinocandins the first class of antifungals that target a fungal specific component; thus giving them an excellent safety profile [19]. Caspofungin was the first of the echinocandins to be introduced in 2001. Currently there are 3 total available echinocandins, namely caspofungin, anidulafungin and micafungin approved for human use by the FDA. All of them have a broad spectrum of activity against fungi. Despite their recent introduction, there has been a report of resistance to these antifungal agents mainly through the mutations in the gene encoding the target enzyme glucan synthase [20].

Other ergosterol biosynthesis inhibitors

In addition to azoles, other types of antifungal agents inhibit the ergosterol biosynthesis in fungi. The allylamine and thiocarbamates, such as terbinafine and tolnaftate, both inhibit the enzyme squalene epoxidase encoded by *ERG1* [21]. Likewise, the morpholines, such as amorolfine exert inhibitory effects on fungi by inhibiting two different enzymes of the biosynthetic pathway, $\Delta^7, 8$ -isomerase (encoded by *ERG24*) and the C14-reductase (encoded by *ERG2*) [22]. Due to their numerous side effects, their therapeutic regimens are limited to treat dermatophytosis and onychomycosis.

Syringomycin

Syringomycins are a family of small cyclic lipodepsinonapeptides that are produced as secondary metabolites by the plant bacterium *Pseudomonas syringae* pv. *syringae*. The best studied, syringomycin E (SRE), exhibits broad-spectrum antifungal activities without inhibiting bacteria. It has been reported that SRE tends to be more effective against yeast than against filamentous fungi [23].

Among these lipodepsinonapeptides, SRE is a broadly investigated peptide in terms of its structure and the fungicidal mechanism of action. Due to the presence of hydrophobic lipid moiety and the hydrophilic peptide portion, SRE acts as an amphipathic molecule with the ability to interact with the fungal plasma membrane as the primary site of action [24]. Upon binding to plasma membrane, SRE forms voltage dependent pores that facilitate the movement of intracellular ions such as K^+ and Ca^{2+} from fungal cells, leading to the cell death [25, 26, 27, and 28].

Molecular genetic analysis of yeast strains in response to SRE was conducted that allowed identification of the yeast genes necessary for SRE action [29, 30]. The majority of genes that are responsible for SRE action are sphingolipid biosynthetic genes such as *SYR2*, *FAH1*, *ELO2*, *ELO3*, *CSG1*, *CSG2*, and *IPT1*. One ergosterol biosynthetic gene, *SYR1/ERG3*, was also found to be involved in SRE action [29, 30, 31]. Mutant strains lacking function in any one of the above genes showed resistance to SRE whereas wild type strain was sensitive to SRE [32].

ANTIFUNGAL DRUG COMBINATION THERAPY

Antifungal therapies that are currently available show limited clinical efficacy to some invasive fungal infections, such as aspergillosis and fusariosis. The problem of frequent opportunist fungal infections and the resistance to available antifungal drugs promoted researchers to explore new strategies for treatment of fungal infections. Drug combination therapy offers unique advantages as the drugs can concurrently target different processes to enhance the potency of drug activity, overcome the problem of drug resistance, and reduce the effect of drug toxicity [33].

When two drugs or agents are combined for treatment, there can be three types of interaction between drugs or agents: synergistic, indifference and antagonistic. Synergistic interaction means that the effect of two chemicals taken together is greater than the sum of their separate effects at the same doses. Indifference interaction means the combined effect of two chemicals is simply the effect of the most active drug alone. Antagonistic interaction means that the combined effect of two chemicals is less than when two drugs are tested separately.

During past decades, several drug combinations that have been tested *in vitro* and *in vivo* have shown greater effectiveness in combination to treat invasive fungal infections compared to each drug alone. For example, amphotericin B acts synergistically with fluorocytosine to treat candidiasis both *in vitro* and *in vivo* [34, 35]. No synergy was observed between amphotericin B and fluconazole *in vitro*, but interestingly, in animal models this combination has been associated with improved survival rates and decreased

tissue burden of *C. albicans* [36, 37, 38]. It has been reported that the success rate of treating candidaemia with fluconazole-amphotericin B combination was 69% in combination therapy compared to 59% for those receiving monotherapy [39]. Similarly, azole-terbinafine combinations seem promising *in vitro* and in animal models [40]. Fluconazole acts synergistically with cyclosporine to reduce yeast burden in kidneys compared to the results seen with either agent alone in a rat model of endocarditis [41]. Similarly, amphotericin B-fluorocytosine combination therapy against *Candida* prosthetic hip infections [42] and meningitis [43, 44] were found to be very effective and successful. However, fluconazole- echinocandin combinations have not been successful *in vitro*. Combinations of fluconazole with antibacterial agents such as ciprofloxacin and trovafloxacin raised survival rates of mice in a model of systemic candidiasis [45].

Although investigation of antifungal drug combinations is still in the early stages, there have been documented examples of success of combination therapy improving survival rates in animal models against various fungal infections. Drug combination therapy may lead to the discovery of new clinically applicable antimicrobial therapies.

AMINOGLYCOSIDES

Aminoglycosides are highly potent, broad spectrum antibiotics that are used as therapeutics mostly to treat serious bacterial infections such as septicaemia, nosocomial respiratory tract infections, urinary tract infections (UTIs) and intra-abdominal infections caused by aerobic Gram negative bacilli in humans [46]. Aminoglycosides such as

streptomycin and gentamicin are also used to treat bacterial diseases in plants, such as the fire blight of apples and pears caused by species of *Erwinia*, *Pseudomonas*, and *Xanthomonas* [47]. Most of the aminoglycosides are naturally occurring antibiotics and are readily produced by actinomycetes of either genus *Streptomyces* or *Micromonospora* [48]. The era of aminoglycoside antibiotic therapy was initiated with the discovery of first antituberculosis agent, streptomycin, by Waksman in 1944. Since then a series of aminoglycosides including neomycin (1949), kanamycin(1957), paromomycin (1959), gentamicin (1963), tobramycin (1967), sisomicin (1970), butirosin (1971), lividomycin (1971),and others have been discovered and introduced to treat bacterial infections caused by Gram-negative and Gram-positive bacteria [49, 50].

Aminoglycosidemode of action

Aminoglycosides are hydrophilic sugars that consist of several amino and hydroxyl functionalities. They are also considered polycationic compounds as the amine moieties are mostly protonated at biologically significant pH. They show high affinities for RNAs, especially the prokaryotic rRNA [51, 52, 53] where they primarily bind to the aminoacyl site (A-site) of the 16S ribosomal RNA (rRNA) within the 30S ribosomal subunit of bacteria, inducing misreading of the genetic code and production of aberrant proteins [51]. Aberrant proteins may be inserted into the cell membrane, leading to the loss of membrane integrity and increased permeability for antibiotics [52]. As a result, aminoglycosides accumulate rapidly in the cytoplasm and saturate all ribosomes, resulting in cell death.

A majority of aminoglycosides are composed of 2-deoxystraptmaine (2-DOS) which are decorated by aminosugars at the C4, C5, and C6 positions. The 2-DOS moiety plays a critical role in the biological function of this class of antibiotics and has been shown to interact directly with the 16S ribosomal RNA [51, 53]. Kanamycins represent 4, 6 disubstituted 2-DOS-containing aminoglycosides that contain two aminosugars such as neosamine and kanasamine attached at 4- and 6-positions of the DOS ring respectively (Figure 1-1). They are one of the most commercially successful aminoglycoside antibiotics, produced by *Streptomyces kanamyceticus* against bacteria [54].

Despite being potent antibiotics, aminoglycosides were found to cause nephro- and ototoxic reactions in humans, affecting on an average 8-30% of treated patients [55]. There are also growing resistant against aminoglycosides that has been detected among bacterial species such as methicillin-resistant *Staphylococcus aureus* (MRSA). The major mechanism of aminoglycoside resistance by bacteria is due to enzymatic modification of the amino or the hydroxyl groups of these antibiotics by aminoglycoside-modifying enzymes (AMEs) such as aminoglycoside acetyltransferase, aminoglycoside phosphotransferase, aminoglycoside adenylyltransferase in the bacterial periplasma. There are more than 50 aminoglycoside deactivating enzymes known today [56, 57]. Although this has limited their uses as therapeutics, aminoglycosides still remain valuable drugs for the treatment of infections and for prophylaxis in special situations.

Thus, there is still a huge motivation to synthesize novel derivatives from aminoglycosides either to improve their efficacy or to seek new applications. This strategy has resulted in the development of new effective semisynthetic aminoglycoside derivatives, such as netilmicin, amikacin, and isepamicin [58, 59, 60]. In the past, efforts have also been made to design novel aminoglycosides that induce a dual action towards both protein synthesis and bacterial membranes. The latter are targeted by the addition of lipophilic tails [61], linear lipidic acyl groups [62, 63] and lipid chains, polyguanidinylated head groups [64], or hydrophobic residues in the form of polycarbamate and polyethers [65] to the backbone of aminoglycoside. All the synthesized derivatives have exhibited a strong activity against Gram-positive bacteria, including methicillin-resistant *Staphylococcus aureus* (MRSA) and vancomycin-resistant enterococci (VRE), but they have failed to show activity against Gram-negative bacteria [61, 62]. However, Ouberai et al. (2011) showed that the novel aminoglycoside naphthylmethylneamine derivatives inhibit the gram negative bacterium *P. aeruginosa* by targeting its cell membrane [66]. But for the first time, Chang et al. 2010 showed a novel neamine aminoglycoside analog, FG08—with a linear C8 alkyl chain as a major structural feature—is antifungal, in contrast to its prototype analog kanamycin B that is predominantly antibacterial. This strategy is an example of reviving a clinically important aminoglycoside by simple chemical modification to yield a new application [67].

Aminoglycosides as antifungal agents

The aminoglycosides are predominantly antibacterial. However, it has been reported that some aminoglycosides, such as validamycins are useful as a crop protectant against plant pathogenic fungi that attack roots and are also effective in protecting seedling and clone cuttings against fungal damping-off disease [68]. It has been noted that some unusual bicyclic ring-containing aminoglycosides are active against yeasts [69]. Additionally, a recent report revealed inhibition of plant pathogenic oomycetes *Phytophthora* spp. And *Pythium* spp. by neomycin, paramomycin, ribostamycin and streptomycin, although they showed comparatively little activity against several other fungal genera [70]. The exact mode of action of these aminoglycosides against fungi is still unknown. Recently, FG08 and K20, both novel aminoglycosides, have been reported to inhibit fungi but not bacteria. FG08 and K20 differ from most aminoglycosides by the addition of a C8 alkyl chain. FG08 and K20 appear to act by the disrupting fungal cell membrane but it is not clearly understood whether FG08 effects on membranes are direct or indirect [67]. Like syringomycin E, the amphipathic properties of these novel aminoglycosides may promote their interaction with the plasma membrane as a primary site of action.

Although potentially useful as crop protectants, the application of currently available aminoglycosides to prevent crop diseases is not advisable as such practices are anticipated to cause bacterial resistance to medically used antibiotics. It would be desirable to have a new antimicrobial agent that shows selective activity against either

bacteria or fungi so the treatment for one of either bacterial or fungal diseases does not promote the development of antimicrobial resistance in the other. Thus, the best aminoglycoside-based fungicides could be those like FG08 or K20 that show potent fungicidal activities, but completely lack their antibacterial capabilities.

JUSTIFICATION AND OBJECTIVES FOR THE PRESENT RESEARCH

Invasive fungal infections are on the rise as the number of patients with compromised immune systems continues to increase. Crops are threatened by emerging fungal diseases that pose serious threats to crop health and to the entire agriculture industry. Currently, there are few classes of antifungal agents available to fight against fungal infections in medicine and agriculture. These antifungal agents have a narrow spectrum of molecular targets. The therapeutic regimens of current antifungal agents are far from satisfactory and many fungi are evolving resistance to current antifungal agents. Further, declining efficacy of current antifungals due to resistance, concerns with animal and human toxicity, environmental impacts and costs also continue to challenge their uses as therapeutics. Thus, discovery of novel antifungals that exhibit broad-spectrum activities, selective toxicity, low incidences of resistance, and varied mechanisms of action is warranted. Some strategies, such as modifying the chemical structure of existing antibiotics or exploring the synergistic combination of two or more agents, may lead to the discovery of additional antimicrobials for therapies.

The overall goal of this research is to investigate the bioactive properties of novel aminoglycoside analogs, FG08 and K20—their bioactive properties, mechanism of action, and synergistic interactions with therapeutic antifungal azoles. FG08 and K20 are derived from kanamycin B and kanamycin A, respectively. They exhibit promising antifungal activities without inhibition of bacteria. As the spectrum of one antimicrobial can vary largely from others, it is essential to explore the bioactivity spectrum of these analogs for their specificity. For example, fungi share many biochemical targets with eukaryotic cells, so agents that interact with fungal targets may also attack similar targets present in animals and plants, making them unsuitable for treating fungal infections. As the fungicidal mechanism of action of these compounds is likely to be unique among aminoglycosides, studies of the fungicidal inhibitory action of these analogs are of major interest. Azoles are currently commercially available and widely used antifungal agents to treat fungal infections in agriculture and medicine. Since azoles are fungistatic, they may more likely lead to the development of fungal resistance. One of the possible strategies to prevent this problem is by using combination therapy. If synergy is observed between K20 and azoles, today's most widely used antifungal agents, it could have broad and important implications in agriculture and medicine to combat important fungal diseases. In the present study, the bioactive properties, mechanism of action of FG08 and K20, and their synergistic antifungal interactions with azoles were studied.

In addition to this, chemoenzymatic synthesis of novel aminoglycoside analog, FG08 (Appendix A), the effect of K20 on the dimorphic transition of *C. albicans*

3. Fisher MC, Henk DA, Briggs CJ, Brownstein JS, Madoff LC, et al. (2012) Emerging fungal threats to animal, plant and ecosystem health. *Nature* 484:186-194.
4. Nucci M, Marr KA (2005) Emerging fungal diseases. *Clin Infect Dis* 41:521-526.
5. Zhai B, Zhou H, Yang L, Zhang J, Jung K, et al. (2010) Polymyxin B, in combination with fluconazole, exerts a potent fungicidal effect. *J Antimicrob Chemother* 65:931-938.
6. Hewitt HG (1998) *Fungicides in crop protection*, CAB International, ISBN 0-85199-164-5, Wallingford, UK.
7. United States Environmental Protection Agency, Office of Pesticide Programs. 1999. Pesticide industry sales and usage. Retrieved from <http://www.epa.gov/oppbead1/pestsales/> [accessed 8 August 2002].
8. Dutcher JD (1968) The discovery and development of amphotericin B. *Br J Dis Chest* 54:40-42.
9. Baginski M, Resat H, Borowski E (2002) Comparative molecular dynamics simulations of amphotericin B-cholesterol/ergosterol membrane channels. *Biochim Biophys Acta* 1567:63-67.
10. Holeman CW Jr, Einstein H (1963). The toxic effects of amphotericin B in man *Calif Med* 99:90-93.
11. Duschinsky R, Plevin E, and Oberhansli W (1960) Synthesis of 5-fluoropyrimidine metabolites. *Acta Unio Int Contra Canc* 16:599-604.

12. Grunberg E, Titsworth E, Bennett M (1963) Chemotherapeutic activity of 5-fluorocytosine. *Antimicrob Agents Chemother* 161:566–568.
13. Polak A (1977) 5-Fluorocytosine—current status with special references to mode of action and drug resistance. *Contrib Microbiol Immunol* 4:158-167.
14. Woolley DW (1944) Some biological effects produced by benzimidazole and their reversal by purines. *J Biol Chem* 152:225-232.
15. Morton V, Staub T (2008) A short history of fungicides. Online, APSnet Features.doi: 10.1094/APSnetFeature-2008-0308.
16. Hitchcock C, Dickinson K, Brown SB, Evans EG, Adams DJ (1990) Interaction of azole antifungal antibiotics with cytochrome P450-dependent 14- α -sterol demethylase purified from *Candida albicans*. *J Biochem* 266:475-480.
17. Lupetti A, Danesi R, Campa M, Tacca MD, Kelly S (2002) Molecular basis of resistance to azole antifungals. *Trends Mol Med* 8:76-81.
18. Douglas CM, Marrinan JA, Li W, Kurtz MB (1994b) A *Saccharomyces cerevisiae* mutant with echinocandin-resistant 1, 3-beta-D-glucan synthase. *J Bacteriol* 176:5686-5696.
19. Ullmann AJ (2003) Review of the safety, tolerability, and drug interactions of the new antifungal agents caspofungin and voriconazole. *Curr Med Res Opin* 19:263-271.

20. Balasho, SV, Park S, Perlin DS (2006) Assessing resistance to the echinocandin antifungal drug caspofungin in *Candida albicans* by profiling mutations in FKS1. *Antimicrob Agents Chemother* 50:2058-2063.
21. Ryder N, Favre B (1997) Antifungal activity and mechanism of action of terbinafine. *Rev Contemp Pharmacother* 8:275-287.
22. Polak A (1992) Preclinical data and mode of action of amorolfine. *Dermatol* 1:3-7.
23. Takemoto JY, Brand JG, Kaulin YA, Malev VV, Schagina, LV, et al. (2003) The syringomycins: lipodepsipeptide pore formers from plant bacterium *Pseudomonas syringae*. In *Pore Forming Peptides and Protein Toxins* (Menestrina , G, Dalla Serra, M, Lazarovici, P, eds), p.266-271. Taylor and Francis, London.
24. Bender CL, Alarcon-Chaidez F, and Gross DC (1999) *Pseudomonas syringae* phytotoxins: mode of action, regulation, and biosynthesis by peptide and polyketide synthetases. *Microbiol Mol Biol Rev* 63:266-292.
25. Zhang L, Takemoto JY (1989) Syringomycin stimulation of potassium efflux by yeast cells. *Biochim Biophys Acta* 987:171-175.
26. Feigin AM, Takemoto JY, Wangspa R, Teeter JH, Brand JG (1996) Properties of voltage-gated ion channels formed by syringomycin E in planar lipid bilayers. *J Membr Biol* 149:41-47.
27. Kaulin YA, Schagina LV, Bezrukov SM, Malev VV, Feigin AM, et al. (1998) Cluster organization of ion channels formed by the antibiotic syringomycin E in bilayer lipid membranes. *Biophys J* 74:2918-2925.

28. Malev VV, Schagina LV, Gurnev PA, Takemoto JY, Nestorovich EM, et al. (2002) Syringomycin E channel: a lipidic pore stabilized by lipopeptide? *Biophys J* 82:1985-1994.
29. Takemoto JY, Zhang L, Taguchi N, Tachikawa T, and Miyakawa T (1991) Mechanism of action of the phytotoxin, syringomycin: a resistant mutant of *Saccharomyces cerevisiae* reveals an involvement of Ca²⁺ transport. *J Gen Microbiol* 137:653-659.
30. Stock SD, Hama H, Radding JA, Young DA, Takemoto JY (2000) Syringomycin E inhibition of *Saccharomyces cerevisiae*: requirement for biosynthesis of sphingolipids with very-long-chain fatty acids and mannose- and phosphoinositol-containing head groups. *Antimicrob Agents Chemother* 44:1174-1180.
31. Cliften P, Wang Y, Mochizuki D, Miyakawa T, Wangspa R, et al. (1996) *SYR2*, a gene necessary for syringomycin growth inhibition of *Saccharomyces cerevisiae*. *Microbiol* 142:477-484.
32. Takemoto JY, Yaxin Y, Stock SD, Miyakawa T (1993) Yeast genes involved in growth inhibition by *Pseudomonas syringae* pv. *syringae* syringomycin family lipodepsipeptides. *FEMS Microbiol Lett* 114:339-342.
33. Polak A (1990) Combination therapy in systemic mycoses. *J Chemother* 2:211-217.
34. Montgomerie JZ, Edwards JE Jr, Guze LB (1975) Synergism of amphotericin B and 5-fluorocytosine for *Candida* species. *J Infect Dis* 132:82-86.

35. Lewis RE, Kontoyiannis DP, Darouiche RO, Raad II, Prince RA (2002) Antifungal activity of amphotericin B, fluconazole, and voriconazole in an *in vitro* model of *Candida* catheter-related bloodstream infection. *Antimicrob Agents Chemother* 46:3499-3505.
36. Sanati H, Ramos CF, Bayer AS, Ghannoum MA (1997) Combination therapy with amphotericin B and fluconazole against invasive candidiasis in neutropenic-mouse and infective-endocarditis rabbit models. *Antimicrob Agents Chemother* 41:1345-1348.
37. Louie A, Banerjee P, Drusano GL, Shayegani M, Miller MH (1999) Interaction between fluconazole and amphotericin B in mice with systemic infection due to fluconazole-susceptible or -resistant strains of *Candida albicans*. *Antimicrob Agents Chemother* 43:2841-2847.
38. Sugar AM, Hitchcock CA, Troke PF, Picard M (1995) Combination therapy of murine invasive candidiasis with fluconazole and amphotericin B. *Antimicrob Agents Chemother* 39:598-601.
39. Rex JH, Pappas PG, Karchmer AW, Sobel J, Edwards JE, et al. (2003) A randomized and blinded multicenter trial of high-dose fluconazole plus placebo versus fluconazole plus amphotericin B as therapy for candidemia and its consequences in non-neutropenic subjects. *Clin Infect Dis* 36:1221-1228.
40. Barchiesi F, Di Francesco LF, Compagnucci P, Arzeni D, Giacometti A, et al. (1998) *In vitro* interaction of terbinafine with amphotericin B, fluconazole and

- itraconazole against clinical isolates of *Candida albicans*. J Antimicrob Chemother 41:59-65.
41. Marchetti O, Entenza JM, Sanglard D, Bille J, Glauser MP, et al. (2000) Fluconazole plus cyclosporine: a fungicidal combination effective against experimental endocarditis due to *Candida albicans*. Antimicrob Agents Chemother 44:2932-2938.
 42. Ramamohan N, Zeineh N, Grigoris P, Butcher I (2001) *Candida glabrata* infection after total hip arthroplasty. J Infect 42:74-76.
 43. Smego RA Jr, Perfect JR, Durack DT (1984) Combined therapy with amphotericin B and 5-fluorocytosine for *Candida meningitis*. Rev Infect Dis 6:791-801.
 44. Casado JL, Quereda C, Oliva J, Navas E, Moreno A, et al.(1997) *Candidal meningitis* in HIV-infected patients: analysis of 14 cases. Clin Infect Dis 25:673-676.
 45. Sugar AM, Liu XP, Chen RJ (1997) Effectiveness of quinolone antibiotics in modulating the effects of antifungal drugs. Antimicrob Agents Chemother 41:2518-2521.
 46. Durante-Mangoni E, Grammatikos A, Utili R, Falagas ME (2009) Do we still need the aminoglycosides? Int. J Antimicrob Agents 33:201-205.
 47. McManus PS, Stockwell VO, Sundin GW, and Jones AL (2003) Antibiotic use in plant agriculture. Ann Rev Phytopathol 40:443-465.

48. Zembower TR, Noskin GA, Postelnick MJ, Nguyen C, Peterson LR (1998) The utility of aminoglycosides in an era of emerging drug resistance. *Int. J Antimicrob Agents* 10:95-105.
49. Mingeot-Leclercq MP, Glupczynsky Y, Tulkens PM (1999) Aminoglycosides : activity and resistance. *Antimicrob Agents Chemother* 43:727-737.
50. Begg EJ, Barkclay ML (1995) Aminoglycosides-50 years on. *Br J Clin Pharmac* 39:597-603.
51. Fourmy D, Recht MI, Blanchard SC, Puglisi JD (1996) Structure of the A-site of *Escherichia coli* 16S ribosomal RNA complexed with an aminoglycoside antibiotic. *Science* 274:1367-1371.
52. Busse HJ, Wostmann C, Bakker EP (1992) The bactericidal action of streptomycin membrane permeabilization caused by the insertion of mistranslated proteins into the cytoplasmic membrane of *Escherichia coli* and subsequent caging of the antibiotics inside the cells degradation of these proteins. *J Gen Microbiol* 138:551-561.
53. Recht MI, Fourmy D, Blanchard SC, Dahlquist KD, Puglisi JD (1996) RNA sequence determinants for aminoglycoside binding to an A-site rRNA model oligonucleotide. *J Mol Biol* 262:421-436.
54. Umezawa H, Ueda M, Maeda K, Yagishita K, Kondo S, et al. (1957) Production and isolation of a new antibiotic, kanamycin. *J Antibiot* 10:181-188.

55. Kahlmeter G, Dahlager JI (1984) Aminoglycoside toxicity – a review of clinical studies published between 1975 and 1982. *J Antimicrob Chemother* 13:9-22.
56. Vakulenko SB, Mobashery S (2003) Versatility of aminoglycosides and prospects for their future. *Clin Microbiol Rev* 16:430-450.
57. Kotra LP, Haddad, J, Mobashery S (2000) Aminoglycosides: Perspectives on mechanisms of action and resistance and strategies to counter resistance. *Antimicrob Agents Chemother* 44:3249-3256.
58. Matsuno T, Yoneta T, Fukatsu S, Umemura E (1982) An improved synthesis of 3',4'-dideoxykanamycin B. *Carbohydr Res* 109:271-275.
59. Kondo S, Iinuma K, Yamamoto H, Ikeda Y, Maeda K (1973) Letter: Synthesis of (S)-4-amino-2-hydroxybutyryl derivatives of 3',4'-dideoxykanamycin B and their antibacterial activities. *J Antibiot* 26:705-707.
60. Kawaguchi H, Naito T, Nakagawa S, Fujisawa KI (1972) BB-K 8, a new semisynthetic aminoglycoside antibiotic. *J Antibiot* 25:695-708.
61. Bera S, Zhanel GG, Schweizer F (2008) Design, synthesis, and antibacterial activities of neomycin-lipid conjugates: polycationic lipids with potent gram-positive activity. *J Med Chem* 51:6160-6164.
62. Zhang J, Keller K, Takemoto JY, Bensaci MF, Litke A, et al. (2009) Synthesis and combinational antibacterial study of 5''-modified neomycin. *J Antibiot* 62:539-544.

63. Zhang J, Chiang FI, Wu L, Czyryca PG, Li D, et al. (2008) Surprising alteration of antibacterial activity of 5"-modified neomycin against resistant bacteria, *J Med Chem* 51:7563-7573.
64. Bera S, Zhanel GG, Schweizer F (2010) Antibacterial activity of guanidinylated neomycin B- and kanamycin A-derived amphiphilic lipid conjugates, *J Antimicrob Chemother* 65:1224-1227
65. Bera S, Zhanel GG, and Schweizer F (2010) Antibacterial activities of aminoglycoside antibiotics-derived cationic amphiphiles. Polyol-modified neomycin B-, kanamycin A-, amikacin-, and neamine-based amphiphiles with potent broad spectrum antibacterial activity, *J Med Chem* 53:3626-3631.
66. Ouberai M, El Garch F, Bussiere A, Riou M, Alsteens D, et al. (2011) The *Pseudomonas aeruginosa* membranes: a target for a new amphiphilicaminoglycoside derivative? *Biochim Biophys Acta* 1808:1716-1727.
67. Chang C-WT, Fosso M, Kawasaki Y, Shrestha S, Bensaci MF, et al. (2010) Antibacterial to antifungal conversion of neamine aminoglycosides through alkyl modification. Strategy for reviving old drugs into agrofungicides. *J Antibiot* 63:667-672.
68. Robson GD, Kuhn PJ, Trinci AP (1988) Effects of validamycin A on the morphology, growth and sporulation of *Rhizoctonia cerealis*, *Fusarium culmorum* and other fungi. *J Gen Microbiol* 134:3187-3194.

69. McGaha SM, Champney WS (2007) Hygromycin B inhibition of protein synthesis and ribosome biogenesis in *Escherichia coli*. *Antimicrob Agents Chemother* 51:591-596.
70. Lee HB, Kim Y, Kim JC, Choi GJ, Park SH, et al. (2005) Activity of some aminoglycoside antibiotics against true fungi, *Phytophthora* and *Pythium* species. *J Appl Microbiol* 99:836-843.

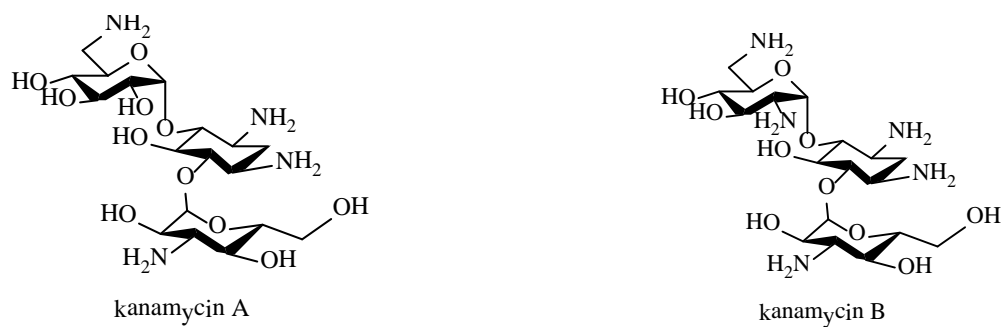


Figure 1-1: Structures of kanamycin A and B

CHAPTER 2

MEMBRANE LIPID-MODULATED MECHANISM OF ACTION AND NON-CYTOTOXICITY OF NOVEL FUNGICIDE AMINOGLYCOSIDE FG08

ABSTRACT

A novel aminoglycoside, FG08, derived from kanamycin B by substitution of a C8 alkyl chain at the 4''-O position, was previously reported. Unlike kanamycin B, FG08 shows broad-spectrum fungicidal but not anti-bacterial activities. To understand its specificity for fungi, the mechanism of action of FG08 was studied using intact cells of the yeast *Saccharomyces cerevisiae* and small unilamellar membrane vesicles. With exposure to FG08 ($30 \mu\text{g mL}^{-1}$), 8-fold more cells were stained with fluorescein isothiocyanate, cells had 4- to 6- fold higher K^+ efflux rates, and 18-fold more cells were stained with SYTOX Green in comparison to exposure to kanamycin B ($30 \mu\text{g mL}^{-1}$). Yeast mutants with aberrant membrane sphingolipids (no sphingoid base C4 hydroxyl group, truncated very long fatty acid chain, or lacking the terminal phosphorylinositol group of mannosyl-diinositolphosphorylphytoceramide) were 4 to 8-fold less susceptible to growth inhibition with FG08 and showed 2 to 10-fold lower SYTOX Green dye uptake rates than did the isogenic wild-type strain. FG08 caused leakage of pre-loaded calcein from 50% of small unilamellar vesicles with glycerophospholipid and sterol compositions that mimic the compositions of fungal plasma membranes. Less than 5 and 10% of vesicles with glycerophospholipid and sterol compositions that mimic bacterial and mammalian cell plasma membranes, respectively, showed calcein leakage. In tetrazolium

dye cytotoxicity tests, mammalian cell lines NIH3T3 and C8161.9 showed FG08 toxicity at concentrations that were 10 to 20-fold higher than fungicidal minimal inhibitory concentrations. It is concluded that FG08's growth inhibitory specificity for fungi lies in plasma membrane permeability changes involving mechanisms that are modulated by membrane lipid composition.

INTRODUCTION

Aminoglycosides are compounds having two or more amino sugars bound to an aminoacyclitol ring via glycosidic bonds. Many are used therapeutically against bacterial infections of humans and animals. Among them, kanamycin B (Figure 2-1), produced by the soil microbe *Streptomyces kanamyceticus*, is one of the most successful [1, 2, 3]. Kanamycin B is structurally based on sugar rings I and II of neamine with an attached ring III of *O*-6-linked kanosamine. The aminoglycosides are generally viewed to act against bacteria [3]. Most bind directly to the prokaryotic 16S rRNA in the decoding region A site, leading to the formation of defective cell proteins. Despite being mainly antibacterial, certain classical aminoglycosides are also found to inhibit crop pathogenic fungal oomycetes [4], and certain structurally unusual ones inhibit yeasts and protozoans [5, 6].

Recently, we reported a novel aminoglycoside, FG08 (Figure 1), with broad spectrum fungicidal activity [7]. FG08 is derived from kanamycin B by substitution of a C8 alkyl chain at the 4''-*O* position of ring III. It, however, lacks the antibacterial properties characteristic of kanamycin B and is fungicidal to a variety of yeasts,

oomycetes, and true fungi with *in vitro* minimal inhibitory concentrations (MICs) ranging between 3.9 and 31.3 $\mu\text{g mL}^{-1}$ [7]. The addition, the C8 alkyl chain, imparts an amphipathic character that suggests the possibility for interaction with cell membranes. Increased SYTOX Green dye uptake by FG08-treated *Fusarium graminearum* and *Candida albicans* indicate effects on the plasma membrane [7]. As a consequence, among antimicrobial aminoglycosides, FG08 appears to interact preferentially with membranes rather than ribosomes. What follows are questions about the mechanism of action on membranes and whether such a mechanism accounts for the fungicidal effects. To address these questions, it is important to determine FG08's initial molecular target, e.g. lipid or protein or both. FG08's structure, composed of a hydroxyl and multiple amino groups, suggests possible interactions with lipids or proteins with high-densities of hydrogen and ionic bonding sites exposed on the membrane external surface. Also, the molecular target(s) will need to account for FG08's preferential inhibition of fungi over bacteria and mammalian cells.

In this study, we investigated FG08's fungicidal mechanism of action on the plasma membrane of the yeast *S. cerevisiae*. We employed membrane-impermeable fluorescence-capable dyes and the cellular efflux of K^+ to measure FG08 membrane pore-forming capabilities. Comparisons between wild-type and gene deletion mutants with structural or compositional defects in anionic sphingolipids were investigated to determine the influence of these lipids in FG08 action. Small unilamellar vesicles (SUVs) with glycerophospholipid and sterol compositions that mimic the lipid compositions of fungal, bacterial and mammalian cell plasma membranes were examined to determine the

influence of these lipids on FG08 membrane interaction and specificity. Finally, the cell permeability and cytotoxic effects of FG08 on mammalian cells were evaluated. The results suggest that FG08's fungicidal mechanism of action involves interaction with and perturbation of the fungal plasma membrane and that its specificity for fungal vs. mammalian and bacterial cells is influenced by membrane lipid composition.

MATERIALS AND METHODS

FG08

FG08 was synthesized from kanamycin B as previously described [7]. A 10 mg mL⁻¹ stock solution was prepared in twice distilled water and stored at 5°C.

Yeast strains and growth medium

S. cerevisiae strains used in this study were W303C (*MAT α ade2 his3 leu2 trp1 ura3*) and isogenic sphingolipid biosynthesis mutant strains W303- Δ *syr2* (*MAT α ade2 his3 leu2 trp1 ura3 syr2 (sur2)::URA3*), W303- Δ *elo2* (*MAT α ade2 his3 leu2 trp1 ura3 elo2::HIS3*), W303- Δ *elo3* (*MAT α ade2 his3 leu2 trp1 ura3 elo2::HIS3*), and W303- Δ *syr4* (*ipt1*) (*MAT α ade2 his3 leu2 trp1 ura3 syr4 (ipt1)::URA3*) [8,9]. The mutants are single gene disruptants isogenic with parental strain W303C. They all have defective sphingolipids that either lack the C4-hydroxyl group of the phytosphingosine backbone (W303- Δ *syr2*), have truncated very long fatty acyl chains (W303- Δ *elo2* and W303- Δ *elo3*), or, because of the inability to add a terminal phosphoinositol group to MIPC, lack the most complex and abundant yeast sphingolipid, mannosyl-diinositolphosphorylphytoceramide (MIP₂C) (W303- Δ *syr4* (*ipt1*)). Phenotypically, these

mutants lack sensitivity to the antifungal syringomycin E - a membrane lipidic pore forming cyclic lipodespsipeptide [9]. Yeast cells were grown in YPD medium (1% yeast extract, 2% peptone, and 2% glucose).

Fluorescent dye staining

Yeast cells were grown for 18 h in YPD medium, and the cell density was adjusted to 1×10^7 cells mL^{-1} . Aliquots (500 μL) were taken and centrifuged for 2 min at 10,000g. The cell pellet was suspended in 10 mM HEPES, pH 7.4, centrifuged again, and suspended in 500 μL of distilled water [7]. For fluorescein isothiocyanate (FITC) staining, FG08 was added to 100 μL of the cell suspension to give final FG08 concentrations of 30, 62.5 and 125 $\mu\text{g mL}^{-1}$ (1, 2 and 4x the FG08 MIC, respectively) and incubated for 1 h at 28°C with continuous agitation. The cell suspensions were mixed with 6 $\mu\text{g mL}^{-1}$ FITC (Sigma Aldrich) (10 mg mL^{-1} stock solution in acetone) for 10 min following published procedures [10]. At least 400 imaged cells were scored for fluorescence per experiment. Staining with the cationic and fluorescent nucleic acid binding dye SYTOX Green (Molecular Probes) was performed as previously described [7, 11]. SYTOX Green was added (final concentration, 0.2 μM) to 100 μL of yeast cell suspensions and allowed to stand for 10 min before addition of FG08 (30 $\mu\text{g mL}^{-1}$) or kanamycin B (30 $\mu\text{g mL}^{-1}$). Negative (water) and positive (Triton X-100[®], 1%, vol vol⁻¹) treatment controls were also prepared. Glass slides were prepared with 10 μL of each cell suspension-FITC or SYTOX Green mixture and observed in bright field and fluorescence modes using an Olympus IX81 fluorescence microscope and an Olympus MWIB filter with excitation and emission wavelengths of 488 and 512 nm, respectively. Images and

data were obtained from at least two independent experiments each performed in duplicate. The percentages of stained cells were determined by comparing paired bright-field and fluorescence images.

K⁺ efflux

Previously described K⁺ efflux measurement methods [12] were used with modification. An overnight culture of *S. cerevisiae* W303C grown in YPD medium was centrifuged at 1200 g for 5 min at room temperature. The cell pellet was washed twice with sterile deionized water. After the second wash step, the cells were suspended in sterile 10mM HEPES-NaOH buffer, pH 6.5 with 25 mM glucose. Washed cells were used to inoculate 10 mL of sterile buffer solution to make final cell density of 1×10^7 CFU mL⁻¹ in a sterile 50mL capacity polyethylene tube (Corning). The cell suspension was incubated with 30 μg mL⁻¹ of FG08 for 1.0, 5.0, 10, 20 and 60 min in a MaxQ 6000 incubator (Thermo Fisher Scientific) at 30⁰C with agitation at 200 rpm. Cell-free filtrates were obtained by individually filtering each suspension with syringe filters (0.2 μm, Nalgene). The filtrates were subjected to atomic emission spectrometry using a Varian AA240 FS atomic absorption spectrometer at 766.5 nm to determine the extracellular K⁺ concentrations using a standard calibration curve based on KCl solutions. Boiled (20 min) cell suspensions were used to estimate total cellular K⁺. Untreated cells were used as negative controls. K⁺ efflux was calculated as percentage of total cellular K⁺ using the formula: $K^+ \text{ efflux (\%)} = ((\text{extracellular } K^+ - \text{extracellular } K^+ \text{ in negative control}) / (\text{total cellular } K^+)) \times 100$.

Calcein release from small unilamellar vesicles (SUVs)

Phosphatidylcholine (PC) from *Glycine max*, L- α -phosphatidylethanolamine (PE) from *Escherichia coli*, L- α -phosphatidylglycerol (PG) (sodium salt) from egg yolk lecithin, L- α -phosphatidylinositol (PI) (sodium salt) from *G. max*, ergosterol and cholesterol were purchased from Sigma-Aldrich. SUVs were prepared by dissolving the lipids (either singly or as mixtures) in chloroform/methanol (2:1, by vol). The mixtures were PC, PE, PI and ergosterol (5:4:1:2 by wt), PC and PG (7:3 by wt), and PC and cholesterol (10:1 by wt) that mimic the lipid compositions of fungal [11], bacterial [13], and mammalian cell plasma membranes, respectively [11]. The organic solvent was evaporated under a stream of nitrogen and the lipid mixture was allowed to dry under vacuum overnight. The dried lipid films were rehydrated in HEPES buffer (10 mM HEPES, 150 mM NaCl, pH 7.4) and 60 mM calcein (self-quenching concentration) and the suspensions were sonicated for 5 min using a bath sonicator (SonicatorTM Heat System, W-220F, Ultrasonic, Inc.) to generate SUVs with lipid concentrations at 10 mg mL⁻¹ [14]. The free calcein was removed by gel filtration through a Sephadex G-50 column. FG08 at 5, 20, and 50 $\mu\text{g mL}^{-1}$ were added to the calcein-loaded SUV suspensions (FG08:lipid molar ratios of 1.5:1, 6:1, and 14.5:1, respectively) and calcein leakage was followed by measuring fluorescence using a Synergy HT microplate reader at an excitation wavelength of 488 nm and emission wavelength of 520 nm. Complete (100%) dye release was obtained by addition of 1% (vol vol⁻¹) Triton X100[®]. The dye-leakage percentage was calculated as: %dye leakage = $100 \times (F - F_0) / (F_t - F_0)$, where F represents the fluorescence intensity 2 min after FG08 addition, and F_0 and F_t represent

the fluorescence intensity without FG08 and with 1% (vol vol⁻¹) Triton X-100®, respectively [14].

FG08 susceptibility testing of wild type and sphingolipid biosynthesis mutants

Microbroth dilution assays for determination of minimal inhibitory concentrations (MICs) were conducted using the protocols of the Clinical and Laboratory Standards Institute [15]. Yeast inocula were adjusted to a final concentration of 5×10^5 CFU mL⁻¹. Drug dilutions were prepared in YPD medium broth ranging between 0.97 and 250 µg mL⁻¹. For disk diffusion growth inhibitory assays, cultures were spread on YPD medium agar plate surfaces. Paper disks (0.5 cm diameter) were placed on the surfaces, and 10 µL aliquots of 1 mg mL⁻¹ of FG08 solution was applied to the disks. Clear zones of inhibition were observed after incubation at 28° C for 48 h. Each test was performed in triplicate.

Animal cell cytotoxicity

A C8161.9 melanoma cell line was a gift from Dr. Danny R. Welch, University of Kansas, Lawrence, KS (USA). The cells were grown in Dulbecco's Modified Eagle Medium (DMEM)/Ham's F12 (1:1) containing 10% fetal bovine serum [16]. NIH3T3 cells (ATCC® CRL-1658™, American Type Culture Collection, Manassas, VA, USA.) were grown in DMEM (high glucose) media containing 10%, vol vol⁻¹ fetal bovine serum in Corning Cell Bind flasks. The confluent cells were then trypsinized with 0.25% wt vol⁻¹ trypsin and resuspended in fresh medium (DMEM). The cells were transferred into 96-well plates at a density of 2×10^5 cells mL⁻¹. They were mixed with FG08 at final

concentrations of 10, 20, 50, 100 or 250 $\mu\text{g mL}^{-1}$ or an equivalent volume of sterile double distilled water (negative control). The cells were incubated for 24 h at 37°C with 5% CO₂ in a humidified incubator. To evaluate cell survival each well was treated with 10 μL of 3-(4, 5-dimethylthiazol-2-yl)-2, 5-diphenyltetrazolium bromide (MTT) (Sigma-Aldrich) for 4 h. In living cells, mitochondrial reductases convert the MTT tetrazolium to formazan which precipitates. Formazan was dissolved using acidified NaDodSO₄ (10 mM HCl) and quantified at A₅₇₀ using a Synergy 4 Gen 5 spectrophotometer (BioTek). Triton X-100[®] (1%, vol vol⁻¹) gave complete loss of cell viability and was used as the positive control. Percent cell survival was calculated as: (control value – test value) \times 100/control value, where control value represents cells + MTT – drug, and test value represents cells + MTT + drug.

RESULTS

Fluorescent dye uptake and K⁺ efflux by *S. cerevisiae* strain W303C

With exposure to FG08 at its MIC (30 $\mu\text{g mL}^{-1}$), 40% of the strain W303C cells were stained with FITC. In contrast, 8-fold fewer cells (5%) were stained when exposed to kanamycin B (30 $\mu\text{g mL}^{-1}$). Unexposed cells were negligibly stained (2%) (Figure 2-2, 1A- C). The FG08 effect was dose-dependent with complete (100%) staining achieved with 125 $\mu\text{g mL}^{-1}$ (Figure 2-2, D1).

Seventy percent of the cells of strain W303C in suspension showed accumulation of SYTOX Green after a 10 min exposure to FG08 at 30 $\mu\text{g mL}^{-1}$ (Figure 2-3, A1-A2). Six percent of cells were stained by SYTOX Green after exposure to kanamycin B (30 μg

mL⁻¹) (data not shown). When observed by phase contrast microscopy and in the absence of fluorescent dye, intact cells exposed for 10 min to FG08 (30 µg mL⁻¹) showed granular cytoplasmic contents not seen with untreated cells (Figure. 2-4).

Increased K⁺ efflux by yeast cells is observed with plasma membrane perturbation by pore forming agents [12, 13]. A rapid (half-maximum rate < 1 min) efflux of K⁺ was observed when strain W303C cells were exposed to FG08 at 20 to 100 µg mL⁻¹ concentrations (Figure 2-5). Extracellular K⁺ levels approached 90% (within 5 min) of the maximum (100%) level achieved with Triton X-100® (1%, vol vol⁻¹). Exposure to kanamycin B (50 µg mL⁻¹) caused rapid efflux up to 20% of maximum level, whereas untreated cells reached 10% of maximum level.

FG08-dependent calcein release by SUVs

In order to correlate FG08's membrane perturbation effects and its selective killing of fungi, calcein-loaded SUV model membranes representing fungal, bacterial and mammalian cell membranes were prepared and evaluated [11,13]. Within 30 min, FG08 (30 µg mL⁻¹) caused 50% calcein leakage from SUVs containing a mixture of PC, PE, PI, and ergosterol (5:4:1:2 by wt) (Figure 2-6). In contrast, at the same concentration of FG08, > 10 % leakage was observed from SUVs with PC and PG (7:3 by wt) and with PC and cholesterol (10:1 by wt) (Figure 2-6). SUV suspensions without added FG08 showed less than 2% leakage even after 2 h incubation.

FG08 susceptibility of mutants with sphingolipid biosynthesis defects

To determine the influence of sphingolipids on FG08's fungicidal activity, isogenic yeast mutant strains W303- Δ *syr2*, W303- Δ *elo2* and W303- Δ *elo3* and W303- Δ *syr4* (*ipt1*) with sphingolipid structural defects [8, 9] were examined. Strains W303- Δ *syr2*, W303- Δ *elo2*, W303- Δ *elo3* and W303- Δ *syr4* (*ipt1*) were all less susceptible to growth inhibition by FG08 compared to the isogenic wild-type strain W303C (Figure 2-7) with MICs that were 4 to 8-fold higher than for strain W303C (Table 2-1). With 10 min exposure to FG08 (30 μ g mL⁻¹), SYTOX Green stained 35%, 7%, 9.4% and 6.8% of the cells of strains W303- Δ *syr2*, W303- Δ *elo3*, W303- Δ *elo2*, and (W303- Δ *syr4* (*ipt1*), respectively, as compared to 70% of the strain W303C cells (Figure 2-3).

Animal cell cytotoxicity

FG08 concentrations needed to kill C8161.9 and NIH3T3 cells exceeded or equaled 250 μ g mL⁻¹, respectively (Figure 2-8). This is 10-20 fold higher than the antifungal MICs against wild type *S. cerevisiae* strain W303C. The membrane permeabilizing effect of FG08 was also measured on C6181.9 cells. Unlike its effect on *S. cerevisiae*, treatment of C6181.9 cells with 100 μ g mL⁻¹ of FG08 caused no influx of SYTOX Green dye over 30 min (Figure 2-9).

DISCUSSION

Multiple approaches were used to assess membrane-perturbation effects of FG08 on the yeast plasma membrane. The dye FITC traverses the cell surface if the plasma membrane is damaged or permeabilized by external agents and concentrates

intracellularly to impart green fluorescence [10]. Similarly SYTOX Green does not cross the plasma membrane of intact yeast cells unless its permeability is compromised [7, 11]. At antifungal MICs, FG08 elicited dye uptake by both FITC and SYTOX Green by strain W303C cells within 10 min and was 12-fold more effective than kanamycin B. Similar FG08 effects on SYTOX Green dye uptake by *Fusarium graminearum* and *Candida albicans* were previously observed [7]. In addition, rapid (< 5min) and massive (~95% of controls) effluxes of K⁺ with FG08 exposure suggest FG08 pore formation on the yeast plasma membrane. Finally, yeast cells showed granular cytoplasmic contents within 10 min of FG08 treatment with phase contrast microscopy (Figure. 2-4). The combined observations indicate that FG08's quick growth inhibitory effects are caused by membrane-perturbation effects that compromise normal ion and metabolite gradients across the cell surface.

To examine the influence of lipids on FG08 membrane perturbation effects and FG08's inhibitory preference for fungi, calcein leakage studies were conducted with model membrane SUVs. SUVs were produced with glycerophospholipid and sterol compositions that mimic those of fungal (PC, PE, PI, and ergosterol), bacterial (PC and PG), and mammalian (PC and cholesterol) plasma membranes [11, 13]. FG08 caused ~5 fold more calcein leakage with fungal plasma membrane-mimicking SUVs than with bacterial and mammalian plasma membrane-mimicking SUVs. These results further indicate the membrane perturbing action of FG08. They additionally suggest an influence of lipid composition on FG08 action that in turn contributes to FG08's growth inhibitory preference for fungi and yeasts. Compared to FG08's MICs that inhibit yeast growth,

however, about 2 times higher concentrations and longer incubation times (30 min) were needed to cause 80% leakage of calcein from fungal mimicking SUVs (Table 2-1 and Figure 2-6). These observations indicate that the studied SUV glycerophospholipid and sterol compositions influence but by themselves do not account for all of FG08's yeast growth inhibitory capabilities. Other factors including other lipids (e.g. sphingolipids, see below) or membrane components likely contribute. In addition, non-membrane cell components that facilitate membrane perturbation could have roles. For example, the antifungal action of the plant defensin NaD1 involves a specific interaction with the fungal cell wall, followed by membrane permeabilization [17].

Unique phosphorylinositol-containing sphingolipids occur predominantly in the yeast plasma membrane [18]. The 3 major yeast sphingolipids are inositol-phosphorylphytoceramide (IPC), mannosyl-inositol-phosphorylphytoceramide (MIPC), and M(IP)₂C with the latter two biosynthetically made by the sequential addition of mannosyl and phosphoinositol groups to IPC. All three sphingolipids possess high densities of hydrogen and ionic bonding sites for potential interaction with FG08. To determine possible influences of sphingolipids on yeast growth inhibition by FG08, biosynthetic mutants with aberrant sphingolipid structures or composition were screened against FG08. Strain W303- Δ *syr2* produces sphingolipids devoid of the phytosphingosine base C4 hydroxyl group. Strain W303- Δ *elo2* accumulates sphingolipids with truncated N-acylated C₂₂ very long fatty acids, whereas sphingolipids of strain W303- Δ *elo3* are devoid of the C₂₆ very long fatty acids. Strain W303- Δ *syr4* (*ipt1*) possesses IPC and MIPC but lacks M(IP)₂C [8,9]. All four mutant strains were less sensitive (4- to 8-fold)

to FG08 compared to the isogenic wild-type strain W303C (Figures 2-3 and 2-7) (Table 2-1). These differences in growth susceptibility to FG08 were further correlated with FG08 elicited cell permeability as determined by SYTOX Green uptake (Figure 2-7). These results indicate key roles for phosphoinositol sphingolipids in promoting FG08 action on the yeast plasma membrane. Similar roles for sphingolipids are known for the membrane pore-forming antifungal actions of *Pseudomonas syringae* lipodepsipeptide syringomycin E and plant defensin DmAMP1 [19, 20].

The influences of lipids on FG08 action could involve hydrogen and ionic bonding between FG08 and lipid head groups. FG08 has numerous hydroxyl and amino groups, and the yeast glycerophospholipid head groups and sphingolipid C4 hydroxyl and mannosyl and phosphorylinositol carbonyl and hydroxyl groups are all potential ionic and hydrogen bond donors and acceptors. While elongation of the sphingolipid very long fatty acid chain itself does not directly contribute to such interactions, it could do so indirectly by affecting the transverse position of the lipid in the membrane and therefore membrane surface accessibility of the sphingolipid head groups for bonding. Further research is needed to decipher such bonding and molecular interactions that should provide more insight into the membrane perturbation effects of FG08 and the reasons for the specific targeting of the fungal plasma membrane.

In a previous report, FG08 was not hemolytic to sheep erythrocytes even at concentrations that exceeded its antifungal MICs [7]. In the present report, we expand the descriptions of effects of FG08 on mammalian systems. It is shown that with animal cell lines NIH3T3 and C8161.9, FG08 shows low cytotoxicity and minimal membrane

perturbation effects at and even above FG08's antifungal MICs. Thus, FG08 appears to be relatively non-toxic to animals as compared to fungi.

CONCLUSIONS

FG08's growth inhibitory specificity for fungi is suggested to lie in its ability to increase plasma membrane permeability by mechanisms that are influenced by the lipid composition of the fungal plasma membrane. FG08 has broad-spectrum antifungal activities, no antibacterial activity that would promote antibiotic resistance, and low mammalian cell toxicities. It thus appears to be a useful lead compound for the development of novel antifungal agents.

REFERENCES

1. Umezawa H, Ueda M, Maeda K, Yagishita K, Kondo S, et al. (1957) Production and isolation of a new antibiotic: kanamycin. *J Antibiot* 10: 181–188.
2. Begg EJ, Barclay ML (1995) Aminoglycosides 50 years on. *Brit J Clin Pharmacol* 39: 597–603.
3. Vakulenko SB, Mobashery S (2003) Versatility of aminoglycosides and prospects for their future. *Clin Microbiol Rev* 16: 430-50.
4. Lee HB, Kim Y, Kim JC, Choi GJ, Park SH, et al. (2005) Activity of some aminoglycoside antibiotics against true fungi, *Phytophthora* and *Pythium* species. *J Appl Microbiol* 99: 836–843.

5. Wilhelm JM, Pettitt SE, Jessop JJ (1978) Aminoglycoside antibiotics and eukaryotic protein synthesis: structure—function relationships in the stimulation of misreading with a wheat embryo system. *Biochem* 17: 1143-1149.
6. Lynch SR, Puglisi JD (2001) Structural origins of aminoglycoside specificity for prokaryotic ribosomes. *J Mol Biol* 306: 1037-1058.
7. Chang C-WT, Fosso MY, Kawasaki Y, Shrestha S, Bensaci MF, et al. (2010) Antibacterial to antifungal conversion of neamine aminoglycosides through alkyl modification. Strategy for reviving old drugs into agrofungicides. *J Antibiot* 63: 667-672.
8. Grilley M, Stock SD, Dickson RC, Lester RL, Takemoto JY (1998) Syringomycin action gene SYR2 is essential for sphingolipid 4-hydroxylation in *Saccharomyces cerevisiae*. *J Biol Chem* 273: 11062-11068.
9. Stock SD, Hama H, Radding JA, Young DA, Takemoto JY (2000) Syringomycin E inhibition of *Saccharomyces cerevisiae*: requirement for biosynthesis of sphingolipids with very-long-chain fatty acids and mannose- and phosphoinositol-containing head groups. *Antimicrob Agents Chemother* 44: 1174-1180.
10. Mangoni ML, Papo N, Barra D, Simmaco M, Bozzi A, et al. (2004) Effect of the antimicrobial peptide temporin L on cell morphology, membrane permeability and viability of *Escherichia coli*. *Biochem J* 380(Pt 3): 859-865.
11. Makovitzki A, Avrahami D, Shai Y (2006) Ultrashort antibacterial and antifungal lipopeptides. *Proc Natl Acad Sci USA* 103: 15997-16002.

12. Zhang L, Takemoto JY (1989) Syringomycin stimulation of potassium efflux by yeast cells. *Biochim Biophys Acta* 987: 171-175.
13. Galanth C, Abbassi F, Lequin O, Sanmartin JA, Ladram A, et al. (2009) Mechanism of antibacterial action of dermaseptin B2: interplay between helix-hinge-helix structure and membrane curvature strain. *Biochem* 48: 313-327.
14. Zhang LJ, Rozek A, Hancock RWW (2001) Interaction of cationic antimicrobial peptides with model membranes. *J Biol Chem* 276: 35714-35722.
15. National Committee for Clinical Laboratory Standards. (2000) Reference Method for Broth Dilution Antifungal Susceptibility Testing of Yeasts—Second Edition: Approved Standard M27-A2. Wayne, PA, USA: NCCLS.
16. Nash KT, Phadke PA, Navenot J-M, Hurst DR, Accavitti-Loper MA, et al. (2007) Requirement of KISS1 secretion for multiple organ metastasis suppression and maintenance of tumor dormancy. *J Natl Cancer Inst* 99: 309-321.
17. van der Weerden N, Lay FT, Anderson A (2008) The plant defensin, NaD1, enters the cytoplasm of *Fusarium oxysporum* hyphae. *J Biol Chem* 283: 14445-14452.
18. Dickson, R. C (2010) Roles for sphingolipids in *saccharomyces cerevisiae*. *Adv Exp Med Biol* 688: 217–231.
19. Takemoto JY, Brand JG, Kaulin YA, Malev VV, Schagina LV, et al. (2003) The syringomycins: lipodepsipeptide pore formers from plant bacterium, *Pseudomonas syringae*. In: Pore forming peptides and protein toxins. (Menestrina G, Serra MD, Lazarovici P, eds.), p.260-271. Taylor and Francis London.

20. Thevissen K, François IE, Takemoto JY, Ferket KK, Meert EM, et al. (2003)

DmAMP1, an antifungal plant defensin from dahlia (*Dahlia merckii*), interacts with sphingolipids from *Saccharomyces cerevisiae*. FEMS Microbiol Lett 226: 169-173.

Table 2-1. Growth susceptibilities of yeast sphingolipid biosynthetic mutants to FG08

Strain	MIC ($\mu\text{g mL}^{-1}$)
W303C (WT)	15.6 - 31.3
W303- Δ <i>syr2</i> (<i>sur2</i>)	>125
W303- Δ <i>elo2</i>	>250
W303- Δ <i>elo3</i>	250
W303- Δ <i>syr4</i> (<i>itp1</i>)	250

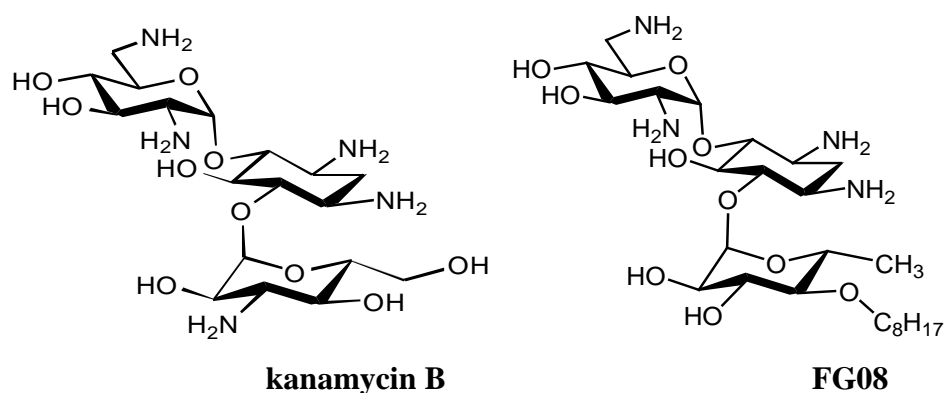


Figure 2-1. Structures of aminoglycosides kanamycin B and FG08.

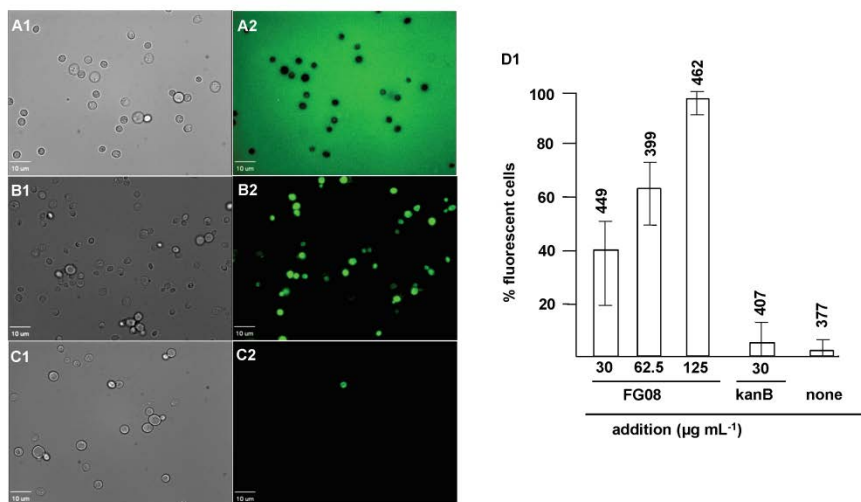


Figure 2-2. Membrane perturbation effects of FG08 on intact cells of *S. cerevisiae* strain W303C. FITC dye uptake without (A1, A2) and with FG08 ($30 \mu\text{g mL}^{-1}$) (B1, B2) or kanamycin B ($30 \mu\text{g mL}^{-1}$) (C1, C2) exposure for 10 min. Bright-field images (A1, B1 and C1) are compared with fluorescence images (A2, B2, and C2) to calculate % fluorescent cells that are stained with FITC. Image A2 (no FG08 and no kanamycin B) shows no fluorescent cells against a fluorescent background. Bar length is $10\mu\text{m}$. Panel D1 shows dose-dependent effects of FG08 on FITC dye uptake and effects of kanamycin B and no treatment. Triton X-100[®] (1%, vol vol⁻¹) gave 100% dye influx (data not shown). The range bars show variations in % fluorescent cells from analyses of 10 separate microscopic image fields randomly selected from at least two separate experiments. Numbers above the range bars indicate the number of cells analyzed.

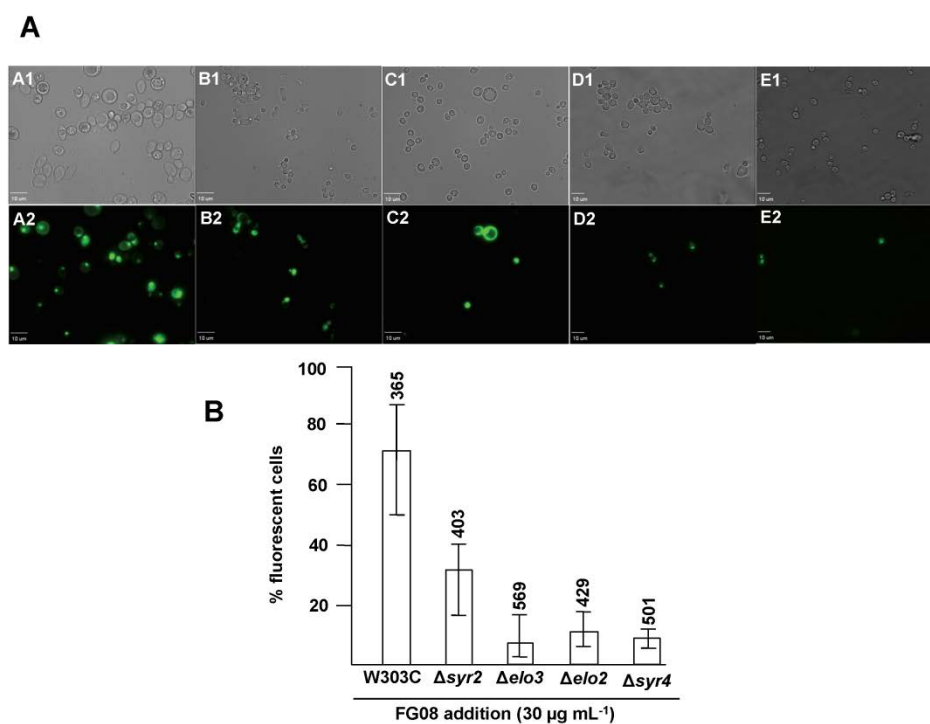


Figure 2-3. Effect of FG08 on SYTOX Green dye staining of *S. cerevisiae* strain W303C and isogenic sphingolipid biosynthetic mutants. Strain W303C (A1, A2), and isogenic mutants W303- Δ syr2(*sur2*) (B1, B2), W303- Δ elo3 (C1, C2), W303- Δ elo2 (D1, D2) and W303- Δ syr4 (*ipt1*) (E1, E2) were exposed to FG08 ($30 \mu\text{g mL}^{-1}$) for 10 min A) Each cell observed in bright-field mode (A1- E1) was also observed for fluorescence (A2- E2), B) The % of fluorescent cells in each microscopic field that stained with SYTOX Green was calculated. The range bars show variations in % fluorescent cells from analyses of 10 separate microscopic image fields randomly selected from at least two separate experiments. The numbers above the range bars indicate the total number of cells analyzed. Untreated yeast cells showed less than 3% staining. Distance bar length shows $10 \mu\text{m}$.

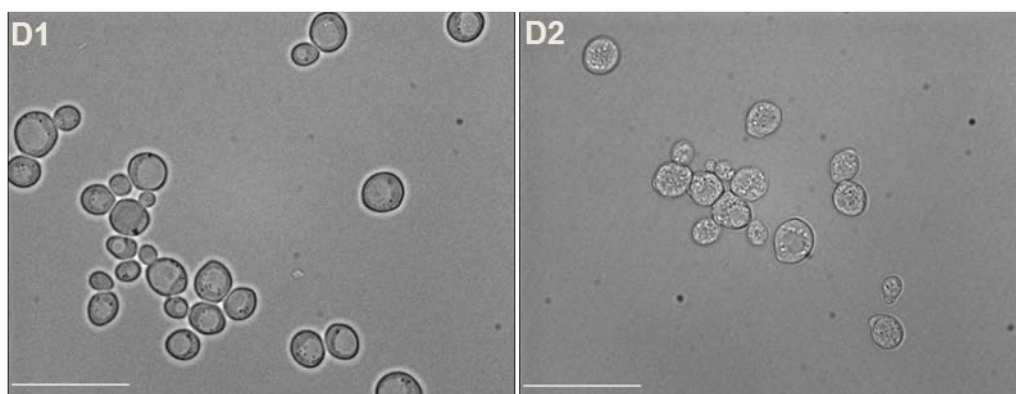


Figure 2-4. Phase contrast microscope images of FG08 effects on the cell internal structure of *S. cerevisiae* strain W303C. Cells were not treated (A) or treated (B) with FG08 ($30 \mu\text{g mL}^{-1}$) for 10 min before visualization by phase contrast microscopy.

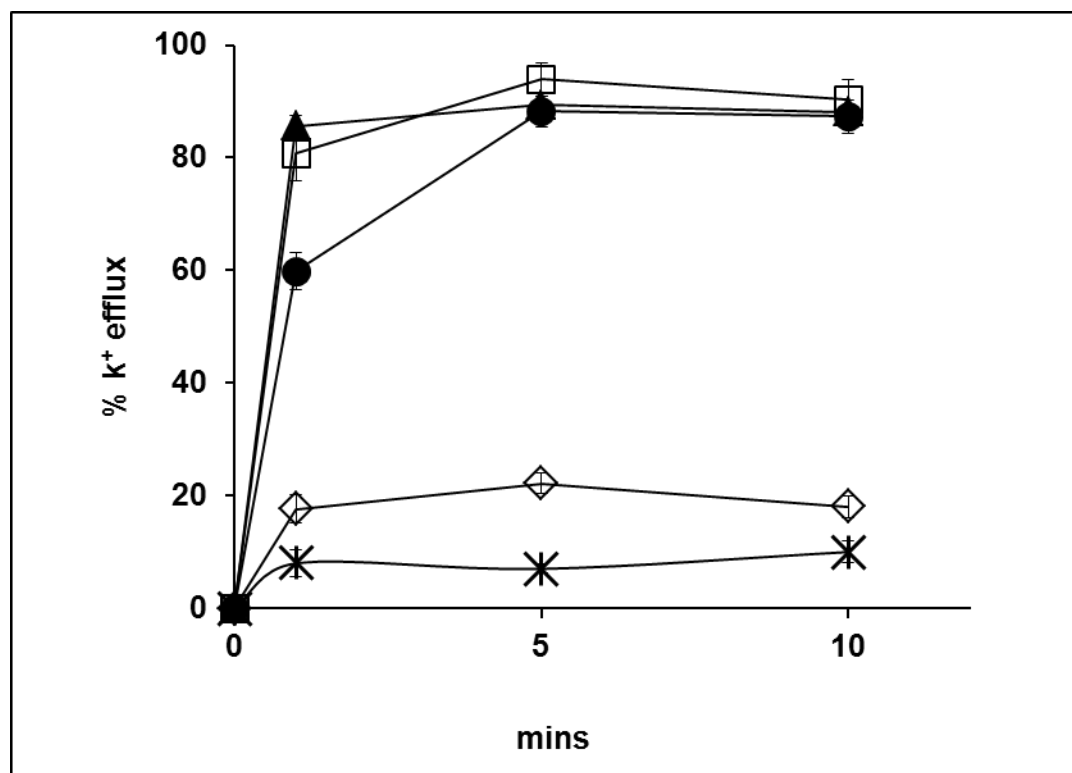


Figure 2-5. Dose-dependent effect of FG08 on cellular K⁺ efflux by *S. cerevisiae* strain W303 Cells growing in YPD medium were washed and suspended in 10 mM HEPES-NaOH buffer, pH 6.5, 25 mM glucose with FG08 at concentrations of 20 (●), 50 (□) or 100 (▲) µg mL⁻¹ or kanamycin B at 50 µg mL⁻¹ (◇). Controls (×) were not treated with FG08 or kanamycin B. Error bars represent data compiled from three separate experiments.

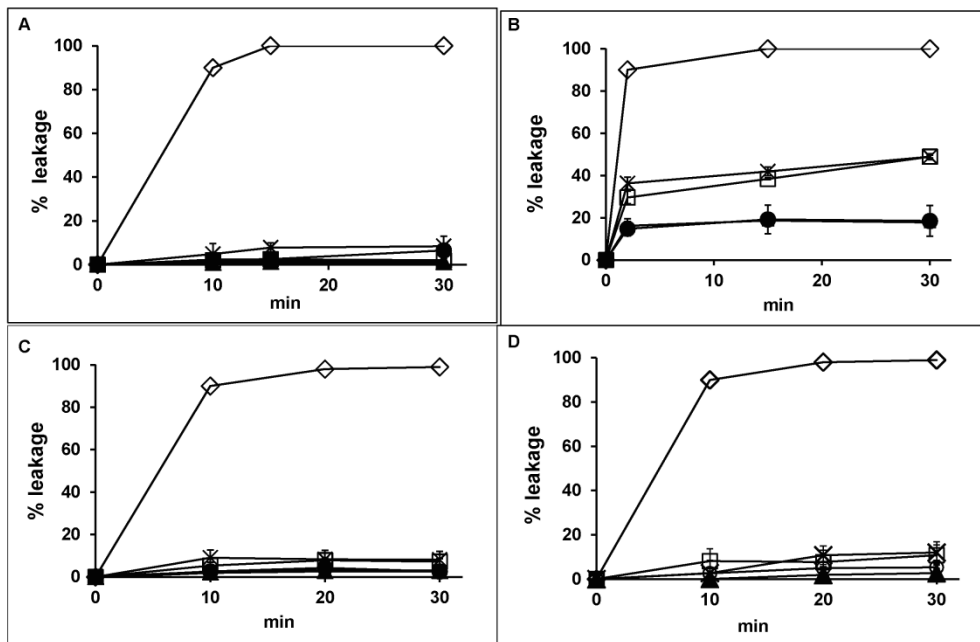


Figure 2-6. Effect of FG08 on calcein release from SUVs that mimic glycerophospholipid and sterol compositions of fungal, bacterial, and mammalian cell plasma membranes. Calcein-loaded SUVs made with PC alone (A), or with glycerophospholipid and sterol compositions that mimic fungal (PC/PE/PI/ergosterol [5:4:1:2]) (B), bacterial (PC/PG [7:3]) (C) or mammalian cell (PC/cholesterol [10:1]) (D) plasma membranes [12, 14] were exposed to FG08 at 5 (▲), 30 (□), and 62.5 (×) $\mu\text{g mL}^{-1}$, kanamycin B (62.5 $\mu\text{g mL}^{-1}$) (●) and Triton-X 100 (1%) (◇). Error bars represent data compiled from three separate experiments.

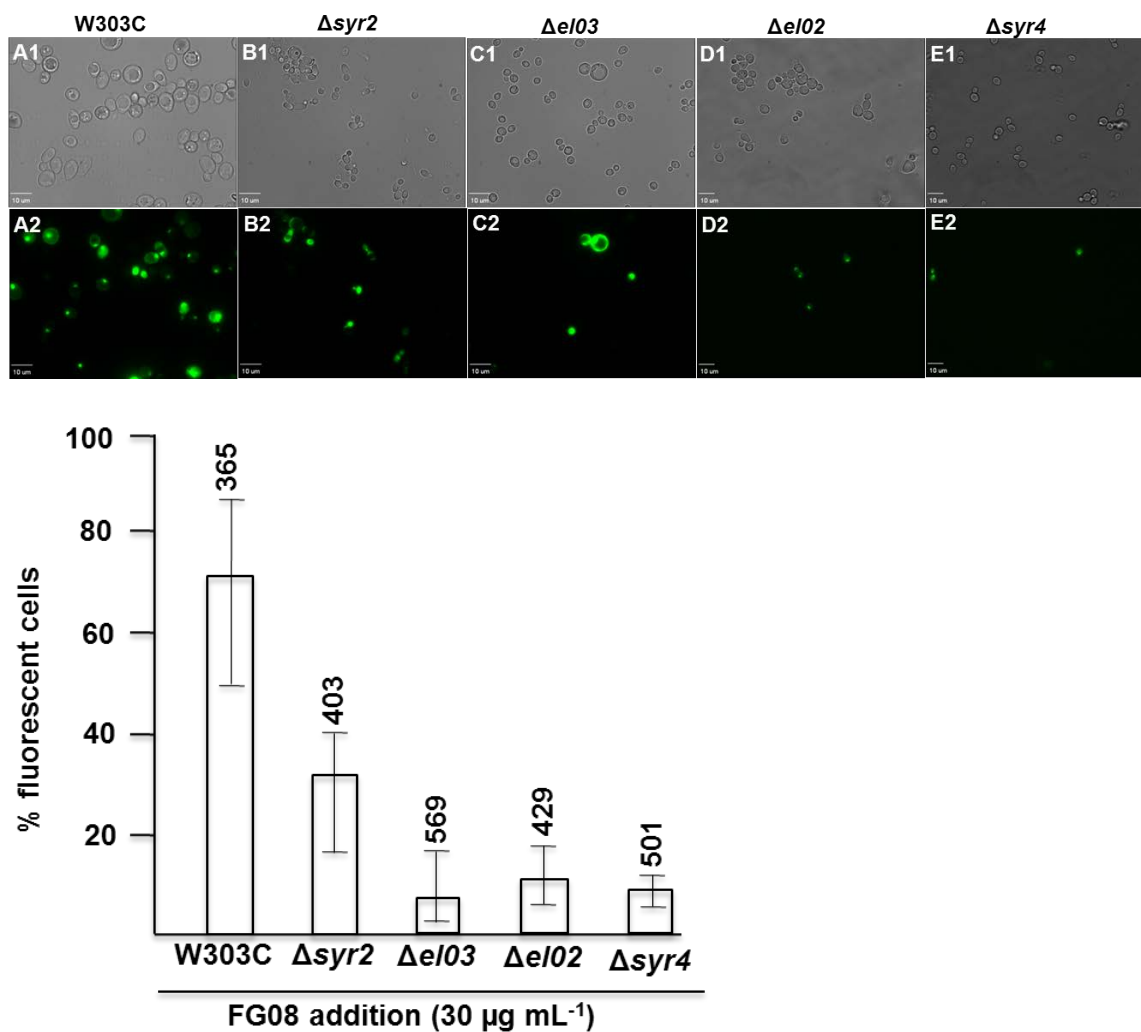


Figure 2-7. Disk-diffusion antifungal assays of FG08 against *S. cerevisiae* W303C and sphingolipid biosynthetic mutants. Ten μL aliquots of 1 mg mL^{-1} solutions of FG08 were applied to paper disks placed on YPD medium agar surfaces spread-plated with YPD medium-grown cells of *S. cerevisiae* strain W303C (A), W303- Δ syr2 (*sur2*) (B), W303- Δ elo2 (C), W303- Δ elo3 (D) and W303- Δ syr4 (*itp1*) (E). The plates were incubated for 48 h at 28°C .

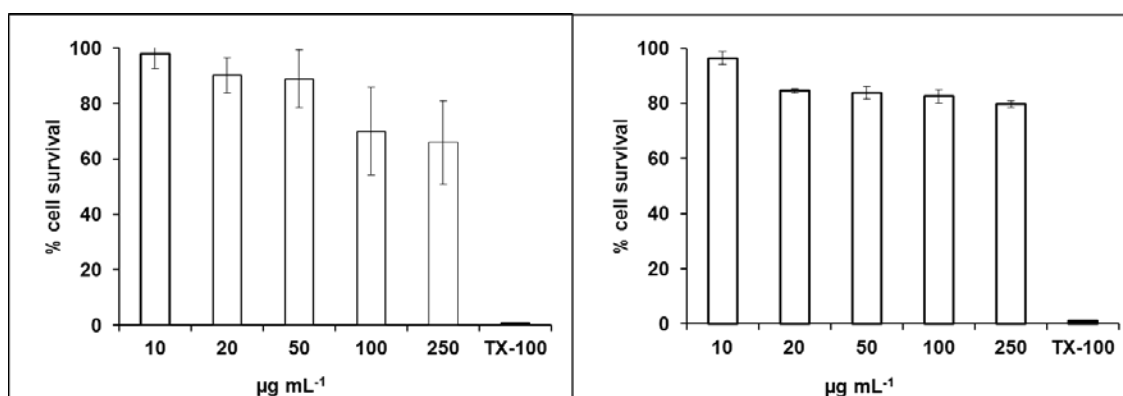


Figure 2-8. Mammalian cell cytotoxicities of FG08. MTT-based cytotoxicity assays were performed with NIH3T3 mouse fibroblast (A) and C8161.9 melanoma (B) cells with 24 h exposure to FG08 at various concentrations. The positive control (100% cytotoxicity = no cell survival) was provided by treatment with Triton X-100 (1% vol vol⁻¹) (filled bar). Error bars represent data combined from three separate experiments.

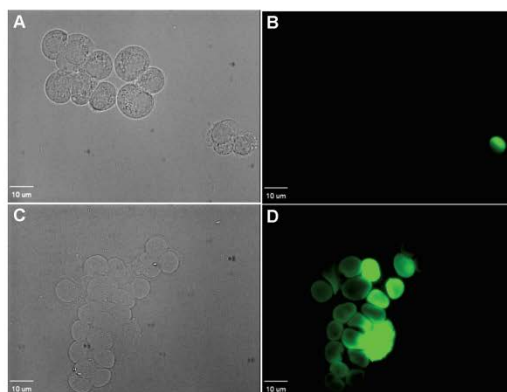


Figure 2-9. Effect of FG08 on SYTOX Green dye staining of C8161.9 cells. Cultured C6181.9 cells were exposed to $100 \mu\text{g mL}^{-1}$ FG08 and SYTOX Green and viewed microscopically in bright-field (A) and fluorescence (B) modes. Cells treated with Triton X-100[®] ($1\% \text{ vol vol}^{-1}$) and SYTOX Green was also viewed by bright-field (C) and fluorescence (D) microscopy. Bar length is $10 \mu\text{m}$.

CHAPTER 3

NOVEL AMINOGLYCOSIDE K20: ANTIFUNGAL PROPERTIES, MECHANISM OF ACTION, AND SUPPRESSION OF MURINE PULMONARY *CRYPTOCOCCUS NEOFORMANS* INFECTION**ABSTRACT**

This study investigated the *in vitro* antimicrobial activities, cytotoxicity, and mechanism of action of K20 and determined its efficacy to suppress pulmonary cryptococcosis.

Antimicrobial susceptibility testing was determined as minimal inhibitory concentrations (MICs) using microbroth dilutions assays and with time kill curves. Cytotoxicity activities of K20 were evaluated using sheep erythrocytes and mammalian cell lines. Mechanisms of action of K20 were studied using intact fungal cells and small unilamellar lipid vesicles. Efficacy of K20 to suppress pulmonary cryptococcal infection was studied in a murine model.

K20 exhibited broad-spectrum *in vitro* antifungal activities but did not inhibit common bacteria such as *Escherichia coli*, *Staphylococcus aureus*, and *Micrococcus luteus*. Hemolysis of sheep erythrocytes and half-maximal cytotoxicities of mammalian cells occurred at K20 concentrations that ranged from 10- to 32-fold higher than fungicidal MICs. With fluorescein isothiocyanate, 20 to 25 mg/L K20 caused staining of >95% of *Cryptococcus neoformans* and *Fusarium graminearum* cultures. Within 2 min, K20 caused leakage of 50% of calcein from preloaded small unilamellar lipid vesicles. In

a murine model for pulmonary cryptococcosis, K20 treatment reduced lung infection rates by 4-fold compared to untreated mice.

K20 is a broad-spectrum fungicide that exhibits minimal animal cell cytotoxicity and suppresses pulmonary infection by *C. neoformans*. The fungicidal mechanism of action of K20 is due to pore formation in the fungal plasma membrane. K20 is a novel and attractive lead compound for development of a new class of therapeutic antifungals.

INTRODUCTION

The frequency of invasive fungal infections has increased due to the rising number of immunocompromised individuals resulting largely from AIDS, cancer chemotherapies, and bone marrow and organ transplantations.^{1,2} For example, *C. neoformans* is a major fungal pathogen that causes life threatening fungal infections such as meningitis and pneumonia in immunocompromised patients. Globally, more than 600,000 people are killed by cryptococcal meningitis, mostly in areas with high HIV rates, such as sub-Saharan Africa.³ Pulmonary cryptococcosis is seen in 25 to 55% of patients with AIDs and cryptococcal meningitis.⁴ The route of cryptococcal infection occurs via inhalation of basidiospores into the lungs that later spread to the central nervous system. Currently, a limited number of antifungal drugs such as amphotericin B, fluorocytosine and azoles are used to treat invasive cryptococcosis in humans.⁵ Growing fungal resistance and host side effects limit their therapeutic efficacy. There is therefore a growing need to develop novel antifungal drugs to combat cryptococcosis as well as other fungal diseases.

Aminoglycosides are compounds having two or more amino sugars bound to an aminoacyclitol ring via glycosidic bonds. Many are used therapeutically against bacterial infections of humans and animals. Among them, kanamycin A, produced by the soil microbe *Streptomyces kanamyceticus*, is one of the most successful.^{6,7,8} Kanamycin A is structurally based on sugar rings I and II of neamine with an attached ring III of *O*-6-linked kanosamine. The aminoglycosides are generally viewed to act against bacteria.⁸ Most bind directly to the prokaryotic 16S rRNA in the decoding region A site, leading to the formation of defective cell proteins. Despite being mainly antibacterial, certain classical aminoglycosides are also found to inhibit crop pathogenic fungal oomycetes,⁹ and certain structurally unusual ones inhibit yeasts and protozoans.¹⁰ Previously, we reported a novel aminoglycoside FG08 with broad-spectrum antifungal properties that did not inhibit tested bacterial and mammalian cells. FG08 differs from kanamycin B by substitution of a C8 alkyl chain at the 4''-*O* position of ring III.¹¹ Despite these properties, FG08's development as a lead antifungal agent is limited. Incorporation of the C8 alkyl chain at the kanamycin B 4''-*O* position is difficult and the product yield is low. These shortcomings prompted the search for structurally similar aminoglycosides using alternative synthetic approaches. Here, we describe aminoglycoside K20 (Figure 3-1) that is structurally similar to FG08 and also possesses broad-spectrum antifungal activities. K20 is derived from kanamycin A by substitution of an octanesulfonyl chain at 6''-*O* position of ring III and is amenable to scalable production.¹²

In this study, we report activities of K20 against fungal species that include several animal and plant pathogens, and we evaluate its cytotoxicity to erythrocytes and

mammalian cells. We investigated K20's antifungal mechanism using intact fungal cells and with model lipid bilayer membranes (also called SUVs). Finally, the efficacy of K20 to prevent the establishment of pulmonary cryptococcosis infection was determined in a mouse model. In summary, K20 exhibits antifungal activity against a broad range of fungal species, increases membrane permeability as its mechanism of action, is relatively non-toxic to mammalian cells, and shows therapeutic efficacy against pulmonary cryptococcosis infection.

MATERIALS AND METHODS

K20

Aminoglycoside K20 was synthesized from kanamycin A as previously described.¹² A 10 g/L stock solution was prepared in twice distilled water and stored at 5°C.

Organisms and culture conditions

F. graminearum strain B-4-5A was obtained from the Small Grain Pathology Program, University of Minnesota, Minneapolis MN, USA. *E. coli* TGI, *S. aureus* ATCC6538, *M. luteus*, *R. pilimanae* ATCC9449, *C. albicans* ATCC10231, *C. albicans* ATCC64124 and *C. albicans* ATCC MYA-2876 were obtained from the American Type Culture Collection (Manassas, VA, USA). *Saccharomyces cerevisiae* W303C was previously described.¹³ *C. neoformans* H99 was obtained from Dr. J. Perfect (Duke University Medical Center, Durham, NC, USA), *C. neoformans* 94-2586, *C. neoformans* 90-26, *C. tropicalis* 95-41, *C. pseudotropicalis* YOGI, and *C. lusitaniae* were obtained

from Dr. J. Takemoto (Utah State University, Logan, UT, USA). *Aspergillus flavus*, *A. niger*, *Rhizopus stolonifer*, *F. oxysporum*, *Ulocladium* spp., *F. culmorum*, *Microdochium nivale*, *Verticillium* spp., *Mucor haemalis* and *Cladosporium cladosporioides* were obtained from Dr. B. Kropp (Utah State University, Logan, Utah, USA). Filamentous fungi and yeasts were cultivated in potato dextrose broth (PDB) (Difco, BD, Franklin Lakes, NJ, USA) at 28-30°C. *S. cerevisiae* W303C was grown in YPD (1% yeast extract, 2% peptone, and 2% glucose) medium. Bacterial strains were grown at 37°C for 24 h on Luria-Bertani medium¹⁴ except *S. aureus* ATCC6538, which was grown on Mueller-Hinton medium (Difco, BD, Franklin Lakes, NJ, USA).

Yeast growth inhibition assays

The *in vitro* effects of K20 on the growth of yeast strains *C. neoformans* H99, *C. neoformans* 94-2586, *C. neoformans* 90-26, *R. pilimanae* 9449, *C. albicans* 10231, *C. albicans* 62124, *C. albicans* MYA-2876, *C. tropicalis* 95-41, *C. pseudotropicalis* YOGI and *C. lusitaniae* 95-767 were assayed in microtiter plates as described in the reference methods on antifungal susceptibility testing of the Clinical and Laboratory Standards Institute (CLSI) (formerly the National Committee for Clinical Laboratory Standards).¹⁵ Cells were grown in PDB for 48 h, counted using a hemocytometer and diluted to a concentration of 5×10^4 CFU/mL in fresh PDB. Cell suspensions (100 μ L) containing 0.48 - 250 mg/L of K20 were added to the wells of a 96-well microtiter plate (uncoated polystyrene, Corning Costar, Corning, NY, USA) and incubated for 48 h at 30°C. Each test was performed in triplicate.

Fungal growth inhibition assays

In vitro antifungal activity against *F. graminearum*, *F. oxysporum*, *F. culmorum*, *C. cladosporioides*, *R. stolonifer*, *Ulocladium* spp., *M. nivale*, *Pencillium* spp., *A. flavus* and *M. haemalis* was assessed as described in Lay *et al.* 2003.¹⁶ Spores were isolated from sporulating cultures growing in PDB medium by filtration through sterile glass wool. Microbroth dilution assays for determination of minimal inhibitory concentrations (MICs) were conducted using the protocols of the CSLI.¹⁷ Serial dilutions of K20 were made in sterile 96-well plates in the range of 250 - 0.48 mg/L and spore suspensions were added to make a final concentration of 5×10^5 CFU/mL. The plates were incubated at 25°C for 48 h. Each test was performed in triplicate.

Bacterial growth inhibition assays

The *in vitro* effects of K20 on the growth of bacterial species *E. coli*, *M. luteus* and *S. aureus* were assayed in microtiter plates and MICs were determined using CLSI protocols.¹⁸ Cells were grown overnight in Luria-Bertani medium and diluted to a concentration of 1×10^4 CFU/mL. Ten μ L of the diluted overnight culture were then added to 190 μ L of Luria-Bertani medium containing K20 at concentrations ranging between 0.48 and 250 mg/L. The plates were incubated at 37°C without shaking for 16 h before determination of MICs. Experiments were performed in triplicate.

Time kill curve studies

Time kill curve studies were performed as described previously.¹⁹ Colonies from 24 to 48 h cultures were suspended in 9 mL sterile water and adjusted to 1×10^8

CFU/mL. One mL of the adjusted fungal suspension was then added to either growth medium alone (control) or a solution of PDB plus an appropriate amount of K20 stock solution. These procedures resulted in a starting inoculum of approximately 1×10^5 CFU/mL and a K20 concentration of 2,4 or 8 mg/L. Test solutions were incubated in a water bath shaker (Model G76, New Brunswick Scientific, New Jersey, USA) with agitation at 30°C. At 0, 4, 9, 24 and 48 h, 100 µL aliquots were removed from each solution and serially diluted 10-fold in sterile water. One hundred µL volumes of each dilution were spread on agar surfaces of potato dextrose agar [PDB containing agar (2%, w/v)] plates to allow growth. Colony counts were determined after incubation for 48 h. The experiment was performed in triplicate. The lower limit for accurate and reproducible quantification was 50 CFU/mL.¹⁹

Hemolytic activity

Hemolytic activity was determined using methods described by Dartois *et al.* 2005²⁰ with modification. Sheep erythrocytes were obtained by centrifuging sheep whole blood at $1,000 \times g$, washing four times with phosphate-buffered saline (PBS), and resuspending in PBS to a final concentration of 10^8 erythrocytes mL⁻¹. The erythrocyte suspension (80 µL) was added to wells of a 96-well polystyrene microtiter plate containing 20 µL of serially diluted K20 in water. The plate was incubated at 37°C for 60 min. Wells with added deionized water and Triton X-100 (1% v/v) served as negative (blank) and positive controls, respectively. Percent hemolysis was calculated using the following equation: % hemolysis = [(absorbance of sample) – (absorbance of blank)]

$\times 100 /$ (absorbance of positive control). Fifty percent hemolysis (HC_{50}) values were calculated as K20 concentrations required to lyse 50% of the erythrocytes.

Animal cell cytotoxicity assay

C6181.9 (melanoma) cells were grown in DMEM/Ham's F12 (1:1) containing 10% fetal bovine serum (FBS). NIH3T3 cells were grown in DMEM (high glucose) medium containing 10% FBS in Corning Cell Bind flasks. The confluent cells were then trypsinized with 0.25%, w/v trypsin and resuspended in fresh medium (DMEM). The cells were transferred into 96-well microtiter plates at a density of 2×10^5 cells/mL. They were mixed with K20 at final concentrations of 10, 20, 50, 100 and 250 mg/L or an equivalent volume of sterile double distilled water (positive control). The cells were incubated for 24 h at 37°C with 5% CO₂ in a humidified incubator. To evaluate cell survival, each well was treated with 10 μ L of 3-(4,5-dimethylthiazol-2-yl)-2,5-diphenyltetrazolium bromide (MTT) (Sigma-Aldrich) for 4 h. In living cells, mitochondrial reductases convert the MTT tetrazolium to formazan, which precipitates. Formazan was dissolved using acidified sodium dodecyl sulfate (NaDodSO₄) (0.01 M HCl) and quantified at A₅₇₀ using a Synergy 4 Gen 5 spectrophotometer (BioTek Instruments Inc, Winooski, VT, USA). Triton X-100[®] (1%, v/v) gave complete loss of cell viability and was used as the positive control. Percent cell survival was calculated as: $(\text{control value} - \text{test value}) \times 100 / \text{control value}$, where control value represents cells + MTT – drug, and test value represents cells + MTT + drug.

Membrane permeabilization assay

C. neoformans H99 (5×10^5 CFU/mL) or *F. graminearum* (5×10^5 conidia/mL) were grown for 18 h in PDB with continuous agitation. Aliquots (500 μ L) were taken and centrifuged for 2 min at $10,000 \times g$. The fungal pellet was suspended in 10 mM HEPES, pH 7.4, centrifuged again, and suspended in 500 μ L distilled water.¹¹ Treatment with K20 was 1 h at 28°C with continuous agitation at 1/2, 1 and 2 times the MIC value for the tested organism; 4, 8 and 25 mg/L K20 for *C. neoformans* cells and 7.8, 15.6 and 32 mg/L K20 for *F. graminearum* hyphae. The K20 treated fungi were assessed 10 min after addition of fluorescein isothiocyanate (FITC) (10 g/L stock in acetone) (Sigma-Aldrich, St. Louis, MO, USA) to 6 mg/L as previously described²¹ with slight modification. Negative (water) and positive (Triton X-100[®] 1%, v/v) treatment controls were also prepared. Glass slides were prepared with 10 μ L of each mixture and observed in dark-field and fluorescence (using an Olympus MWIB filter, excitation and emission wavelength 488-512 nm) modes with an Olympus IX81 fluorescence microscope (Olympus, Center Valley, PA, USA). Data was obtained from at least three independent experiments.

Small unilamellar vesicles (SUVs)

Lipids used were phosphatidylcholine from *Glycine max* (PC), L- α -phosphatidylethanolamine from *E. coli* (PE), L- α -phosphatidylinositol sodium salt from *G. max* (PI), and ergosterol. The lipids were purchased from Sigma-Aldrich. SUVs were prepared by dissolving mixtures of lipids in chloroform/methanol (2:1, v/v). The mixtures chosen, PC, PE, PI, and ergosterol (5:4:1:2 ratios by weight) and PC and ergosterol (10:1

ratio by weight), mimic the lipid compositions of fungal plasma membranes.^{21, 22} The organic solvent was evaporated under a stream of nitrogen and the lipid mixture was allowed to dry under vacuum overnight. The dried lipid films were rehydrated in HEPES buffer (10 mM HEPES, 150 mM NaCl, pH 7.4) to generate SUVs with lipid concentrations at 10 g/L.

Calcein release from SUVs

Lipid films were prepared as described above and were suspended in 10 mM HEPES, 150 mM NaCl, pH 7.4, containing 60 mM calcein (self-quenching concentration).²¹ Liposome suspensions were sonicated for 2 min using a sonicator (Sonicator™ Heat System, W-220F, Ultrasonics, New York). The free calcein was removed by gel filtration through a Sephadex G-50 column. K20 at 31.3, 62.2, and 125 mg/L was added to the calcein-loaded SUV suspensions (lipid concentration of 6-10 μM) and calcein leakage was followed by measuring fluorescence using a Synergy HT microplate reader at an excitation wavelength of 488 nm and emission wavelength of 520 nm. Complete (100%) dye release was obtained by addition of Triton X-100® (1%, v/v). The dye-leakage percentage was calculated as follows: % dye leakage = $100 \times (F - F_0) / (F_t - F_0)$, where F represents the fluorescence intensity 2 min after K20 addition, and F_0 and F_t represent the fluorescence intensity without K20 and with Triton X-100® (1%, v/v), respectively.²³

In vivo efficacy of K20 in treatment of mice pulmonary cryptococcosis

RAG^{-/-} mice lacking both T and B cells due to a defect in the recombination antigen gene were obtained from Jackson Laboratories (Bar Harbour, ME, USA) and maintained at the Montana State University Animal Resource Center (Bozeman, MT, USA). Cryptococcosis infection was induced in RAG^{-/-} mice by methods as described previously.²⁴ Three groups of mice were compared and each group consisted of 5 mice per therapy. Group A received one dose of 100 μ L of 200 mg/L K20 in phosphate buffered saline (PBS, 10 mM phosphate, 2.7 mM KCl and 137 mM NaCl, pH 7) by intratracheal instillation alone, group B received 100 μ L of 200 mg/L K20 mixed with 3×10^5 *Cryptococcus* yeast cells/mL, and group C received *Cryptococcus* cells mixed in PBS only. Mice were monitored for signs of distress and their weight recorded daily over the course of infection. Weight loss or gain was plotted as percent of weight change. Mice were euthanized if weight loss exceeded 25%. At day 15 post-infection, lungs were removed, and homogenized in 5 mL PBS. Lung cryptococcal burden was assessed by plating 100 μ L of the homogenized suspension onto YPD agar plates at 1:10, 1:100, and 1:1000 dilutions in PBS, incubated for 3 days, and colonies counted.

RESULTS

In vitro antifungal activities

The MICs of K20 against an array of agriculturally and clinically important fungi and bacteria are given in Table 3-1. K20 MICs against Gram-positive and Gram-negative bacteria were 65- to 125-fold higher than shown by kanamycin A (Table 3-1). In contrast,

K20 inhibited a variety of fungi, with MICs ranging between 8-128 mg/L for yeasts and 7.8-62.5 mg/L for filamentous fungi (Figure 3-2). Among the yeasts tested, *C. neoformans* strains were consistently the most susceptible to inhibition by K20.

Time kill curves

The time kill curves for K20 and *C. neoformans* H99, showed that an MIC level of K20 (4 mg/L) reduced the CFU/mL by $\geq 2 \log_{10}$ units (Figure 3-3). However, a $2 \times$ MIC level (8 mg/L) of K20 was required to achieve a fungicidal effect (100% killing). At 4 mg/L ($1 \times$ MIC), K20 exhibited a fungistatic effect after 10 h incubation.

Sheep erythrocyte hemolysis

K20 lysed less than 40% of sheep erythrocytes at 500 mg/L (Figure 3-4) which is >50 -fold higher concentration than the antifungal MIC against *C. neoformans* H99. The HC_{50} value of K20 was determined to be 1g/L. Kanamycin A did not show hemolytic activity against sheep erythrocytes (data not shown).

Animal cell cytotoxicity

K20 did not show toxicity against C8161.9 and NIH3T3 cells at concentrations of up to 250 mg/L (Figure 3-5). The 50% inhibitory concentrations (IC_{50} s) of K20 for both C8161.9 and NIH3T3 cells were greater than 250 mg/L (Figure 3-5), and at least 31-fold higher than the antifungal MIC against *C. neoformans* H99 (Table 3-1).

Fluorescent dye uptake

FITC dye was used to assess the membrane-perturbation effects of K20 on the plasma membrane of *C. neoformans*H99 and *F. graminearum*. FITC traverses cell surface membranes damaged or permeabilized by external agents and concentrates intracellularly to impart green fluorescence.^{25, 26} At antifungal MICs of 8 mg/L for *C. neoformans* H99 (Figure 3-6) and 15.6 mg/L for *F. graminearum* (Figure 3-7), K20 caused 64% and 90% FITC cell staining, respectively. In contrast, < 5% of yeast cells and nearly no hyphae were stained when exposed to kanamycin A (50 mg/L). Unexposed cells were negligibly stained (< 2%) (Figures 3-8 and 3-9). K20 caused dose-dependent FITC staining of hyphae and yeast cells with complete (100%) staining achieved with 25 and 32 mg/L, respectively (Figures 3-6 and 3-7).

SUV calcein release assays

To further study the fungal membrane action of K20, SUV model membranes representing fungal cell membranes were prepared and evaluated. K20 showed dose-dependent effects on release of calcein from the SUVs. Within 2 min, K20 (30 mg/L) caused 50% calcein leakage from SUVs composed of PC, PE, PI, and ergosterol (5:4:1:2 by weight) and of PC and ergosterol (7:3 by weight) (Figure 3-10). At 62.5 mg/L, K20 caused >80% leakage from both types of SUVs within 2 min (Figure.3-8). SUVs without added K20 or treated with Triton X-100® showed < 10% or 100% calcein leakage, respectively.

In vivo efficacy of K20 against mice pulmonary cryptococcosis infection

Both *C. neoformans* H99-infected and non-infected mice treated intratracheally with K20 maintained their body weights over a 15 day infection time course. In contrast, non-treated but infected mice showed weight losses starting at day 10 post-infection (Figure 3-9). In K20-treated infected mice, lung fungal burdens were decreased 4-fold ($p = <0.01$) in comparison to untreated infected mice (Figure 3-9A). Stained images of lung homogenates also showed decreased fungal burdens in infected mice treated with K20 as compared to non-treated mice (Figure 3-10B-C).

DISCUSSION

Recently we reported a novel aminoglycoside analog of kanamycin B, FG08, possessing broad spectrum antifungal activities.^{11, 26} FG08 differs from kanamycin B by the attachment of a C8 alkyl chain at the 4''-O position of ring III and greatly diminished antibacterial properties.¹¹ Structure/bioactivity studies identified FG08 from among a set of kanamycin B analogs with varied lengths and positions of the alkyl chain as exhibiting the greatest antifungal properties.¹¹ However, the synthesis of FG08 is technically difficult. It requires numerous chemical synthesis steps and has a low overall yield. In contrast, production of K20, derived from kanamycin A by the substitution of an octanesulfonyl chain at the 6''-O position of ring II, requires only three chemical synthesis steps and has a high overall yield. Like FG08, the structurally related K20 displays broad-spectrum antifungal activities but not antibacterial activities (Table 3-1). It thus appears that the fungicidal activity of K20 is due to the incorporation of an

octanesulfonyl chain to the 6''-O position of III ring of kanamycin A. Interestingly, K20 is slightly more active against filamentous fungi (except for *A. flavus*) than against yeasts. Exceptions are *C. neoformans* strains with susceptibilities to K20 at relatively low MICs (Table 3-1). K20 exhibited dose-dependent fungicidal activity against *C. neoformans* H99 that completely suppressed the growth of H99 strain at 8 mg/L after 10 h (Figure 3-3).

In order to distinguish between selective antimicrobial activity and non-selective lytic activity, we measured the toxicity of K20 against sheep erythrocytes and living mammalian cells. At and above antifungal MICs, K20 did not lyse sheep erythrocytes (Figure 3-3) and did not inhibit the proliferation of NIH3T3 and C6181.9 cells (Figure 3-4). These results confirm the selective killing of K20 against fungi.

Due to the octanesulfonyl chain at the 6''- O position, K20 assumes an amphipathic character that suggests interaction with cell membranes. To study the possibility for a membrane-targeted antifungal mechanism of action by K20, its effects on the cellular uptake of excess FITC dye were measured with *C. neoformans* H99 and *F. graminearum*. FITC uptake only occurs when the plasma membrane is damaged or permeabilized. Once FITC enters a cell, it binds to cellular proteins and can be visualized as a green fluorescence.^{25, 26} At antifungal MICs, K20 caused rapid FITC dye uptake by *C. neoformans* H99 cells and *F. graminearum* hyphae within 10 min of incubation. K20 was >12-fold more effective than kanamycin A. Similar effects on FITC dye uptake by *S. cerevisiae* W303C with exposure to FG08 were previously observed.²⁶ To further study membrane perturbation effects of K20, calcein leakage studies were conducted with model lipid bilayer membranes, SUVs. SUVs were produced with glycerophospholipid

and sterol compositions that mimic those of fungal plasma membranes.^{22, 23} At MICs shown for yeasts, K20 caused the rapid release of calcein from SUVs. The rapidity of dye influx by cells (10 min) and calcein leakage (2 min) from SUVs suggests that K20's growth inhibitory effect is due to direct and rapid effects on plasma membrane permeability. The results also show that K20, in contrast to its parent molecule kanamycin A, is altered not only in the group of organisms it targets, but it also has an altered mode of action. Kanamycin A targets protein translation, whereas K20 acts through membrane perturbation.

An *in vivo* efficacy study of K20 was conducted in a mouse model to determine its capabilities for preventing the establishment of pulmonary cryptococcosis. K20 significantly prevented the establishment of pulmonary cryptococcus infection in mice when *C. neoformans* H99 was administered intratracheally, showing that even a single initial treatment of K20 made a significant difference ($p = <0.01$) in the propagation of the fungal pathogen. Animal toxicity effects of K20 were not evident as both infected and non-infected mice treated with K20 (at 10-fold MIC) maintained their weight for 15 days post-infection. Untreated, infected mice showed weight losses starting at day 10 post-infection.

In conclusion, a novel aminoglycoside analog of kanamycin A, K20, with an octanesulfonyl chain as a major structural feature, is a broad spectrum fungicide and is not antibacterial. K20 is not hemolytic and showed low mammalian cell toxicities. The *in vivo* efficacy of K20 to prevent the establishment of pulmonary cryptococcosis in mice

suggests the therapeutic application of K20 in medicine in addition to its potential as a crop protectant in agriculture.

REFERENCES

1. Fisher MC, Henk DA, Briggs CJ *et al.* Emerging fungal threats to animal, plant and ecosystem health. *Nature* 2012; **484**:186-194.
2. Zhai B, Zhou H, Yang L *et al.* Polymyxin B, in combination with fluconazole, exerts a potent fungicidal effect. *J Antimicrob Chemother* 2010; **65**: 931-938.
3. Rajasingham R, Rolfes MA, Birkenkamp KE *et al.* Cryptococcal meningitis treatment strategies in resource-limited settings: A cost-effectiveness analysis. *PLoS Med* 2012; **9**: e1001316. doi:10.1371/journal.pmed.1001316.
4. Shirley RM, Baddley JW. Cryptococcal lung disease. *Curr Opin Pulm Med* 2009; **15**: 254-260.
5. Jarvis JN, Harrison, TS. Pulmonary cryptococcosis. *Semin Respir Crit Care Med* 2008; **29**: 141-150.
6. Umezawa H, Ueda M, Maeda K *et al.* Production and isolation of a new antibiotic: kanamycin. *J Antibiot* 1957; **10**: 181-188.
7. Begg EJ, Barclay ML. Aminoglycosides 50 years on. *Brit J Clin Pharmacol* 1995; **39**: 597-603.
8. Vakulenko SB, Mobashery S. Versatility of aminoglycosides and prospects for their future. *Clin Microbiol Rev* 2003; **16**: 430-50.

9. Lee HB, Kim Y, Kim JC *et al.* Activity of some aminoglycoside antibiotics against true fungi, *Phytophthora* and *Pythium* species. *J Appl Microbiol* 2005; **99**: 836-843.
10. Wilhelm JM, Pettitt SE, Jessop JJ. Aminoglycoside antibiotics and eukaryotic protein synthesis: structure-function relationships in the stimulation of misreading with a wheat embryo system. *Biochem* 1978; **17**: 1143-1149.
11. Chang C-WT, Fosso MY, Kawasaki Y *et al.* Antibacterial to antifungal conversion of neamine aminoglycosides through alkyl modification. Strategy for reviving old drugs into agrofungicides. *J Antibiot* 2010; **63**: 667-672.
12. Chang, C-WT, Takemoto JY. Aminoglycosides: synthesis and use as antifungals, Appl. No. 13/316,720, US 2012/0316125 A1, U.S. Patent and Trademark Office.
13. Grilley M, Stock SD, Dickson RC *et al.* Syringomycin action gene *SYR2* is essential for sphingolipid 4-hydroxylation in *Saccharomyces cerevisiae*. *J Biol Chem* 1998; **273**: 11062-11068.
14. Sambrook J, Fritsch EF, Maniatis T. Molecular cloning: a laboratory manual. Cold Spring Harbor Laboratory, cold spring harbor, New York, NY, USA, 1989.
15. National Committee for Clinical Laboratory Standards. *Reference Method for Broth Dilution Antifungal Susceptibility Testing of Yeasts—Second Edition: Approved Standard M27-A2*. NCCLS, Wayne, PA, USA, 2002.
16. Lay FT, Brugliera F, Anderson MA. Isolation and properties of floral defensins from ornamental tobacco and petunia. *Plant Physiol* 2003; **131**: 1283-1293.

17. National Committee for Clinical Laboratory Standards. *Reference Method for Broth Dilution Antifungal Susceptibility Testing of Filamentous Fungi—Second Edition: Approved Standard M38-A2*. NCCLS, Wayne, PA, USA, 2008.
18. National Committee for Clinical Laboratory Standards. *Methods for Dilution Antimicrobial Susceptibility Tests for Bacteria that Grow Aerobically—Third Edition: Approved Standard M7-A3*. NCCLS, Villanova, PA, USA, 1993.
19. Klepser ME, Malonel D, Lewis RE *et al*. Evaluation of voriconazole pharmacodynamics using time-kill methodology. *Antimicrob Agents Chemother* 2000; **40**: 1917-1920.
20. Dartois V, Sanchez-Quesada J, Cabezas E *et al*. Systemic antibacterial activity of novel synthetic cyclic peptides. *Antimicrob Agents Chemother* 2005; **49**: 3302-3310.
21. Makovitzki A, Avrahami D, Shai Y. Ultrashort antibacterial and antifungal lipopeptides. *Proc Natl Acad Sci USA* 2006; **103**: 15997-16002.
22. Lee J, Park C, Park SC *et al*. Cell selectivity membrane phospholipids relationship of the antimicrobial effects shown by pleurocidin enantiomeric peptides. *J Pept Sci* 2009; **15**: 601-606.
23. Zhang LJ, Rozek A, Hancock RWW. Interaction of cationic antimicrobial peptides with model membranes. *J Biol Chem* 2001; **276**: 35714-35722.
24. Searles S, Gauss K, Wilkison M *et al*. Modulation of inflammasome-mediated pulmonary immune activation by type I IFNs protects bone marrow homeostasis during systemic responses to pneumocystis lung infection. *J Immunol* 2013; **191**: 3884-3895.

25. Mangoni ML, Papo N, Barra D, Simmaco M *et al.* Effect of the antimicrobial peptide temporin L on cell morphology, membrane permeability and viability of *Escherichia coli*. *Biochem J* 2004; **380**: 859-865.
26. Shrestha S, Grilley M, Fosso MY *et al.* Membrane lipid-modulated mechanism of action and non-cytotoxicity of novel fungicide aminoglycoside FG08. *PLoS ONE* 2013; **8**(9): e73843. doi:10.1371/journal.pone.0073843

Table 3-1. Minimal inhibitory concentrations (MICs) of K20 and kanamycin A against bacteria and fungi

Organism	^a MIC (mg/L)	
	K20	kanamycin A
Yeasts		
<i>Cryptococcus neoformans</i> H99	4-8	>125
<i>Cryptococcus neoformans</i> 94-2586	4-8	>125
<i>Cryptococcus neoformans</i> 90-26	15.6	nd
<i>Candida pseudotropicalis</i> YOGI	31	. nd
<i>Candida lusitaniae</i> 95-767	31.5	. nd
<i>Candida rugosa</i> 95-967	62.5	.nd
<i>Candida tropicalis</i> 95-41	31	. nd
<i>Candida albicans</i> 10231	31.3-128	>250
<i>Candida albicans</i> 62124	300	>500
<i>Rhodotorula pilimanae</i> 9449	15.6	>250
<i>Saccharomyces cerevisiae</i> W303C	15.6-31.3	>250
Filamentous fungi		
<i>Fusarium graminearum</i> B-4-5A	15.6	>125
<i>Fusarium oxysporum</i>	31.3	>250
<i>Fusarium culmorum</i>	7.8	.. ^b nd
<i>Microdochium nivale</i>	3.9	nd
<i>Mucor haemalis</i>	15.6	>125
<i>Ulocladium</i> spp.	15.6	>125
<i>Penicillium</i> spp	31.3	nd
<i>Rhizopus stolonifer</i>	15.6	>250
<i>Cladosporium cladosporioides</i>	31.3	nd
<i>Aspergillus flavus</i>	>500	nd
<i>Aspergillus niger</i>	500	nd
Bacteria		
<i>Escherichia coli</i> TG1	125-250	1.95
<i>Staphylococcus aureus</i> ATCC 25923	250	<0.98
<i>Micrococcus luteus</i>	62.5	1.95

^aMicrobroth dilution assays were performed at least twice, and each in triplicate.

^b not determined

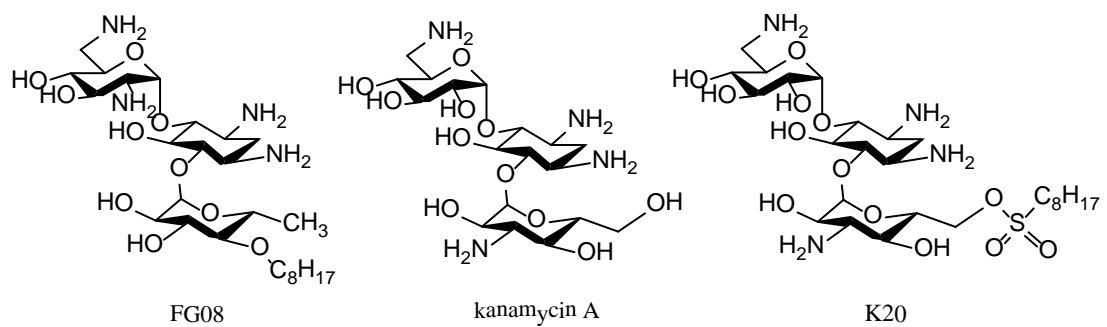


Figure 3-1. Structures of aminoglycosides FG08, kanamycin A, and K20.

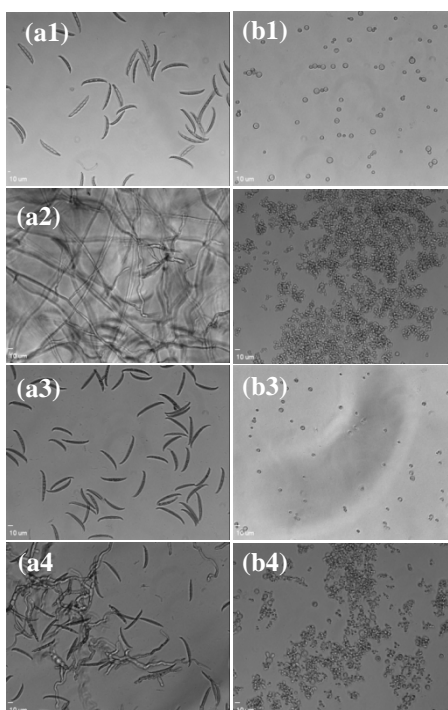


Figure 3-2. Microscopic images of *F. graminearum* and *C. neoformans* H99 suspended and incubated in PDB in microtiter plate wells of MIC microbroth dilution assays. Shown are *F. graminearum* macroconidia at 0 h (a1), after 24 h (a2), after 24 h with 15.6 mg/L K20 (a3), and after 48 h with 62.5 mg/L kanamycin A (a4) and *C. neoformans* H99 cells (5×10^{-4} CFU/mL) at 0 h (b1), after 24 h (b2), after 24 h with 8 mg/L K20 (b3), and after 48 h with 62.5 mg/mL kanamycin A (62.5 mg/L) (b4).

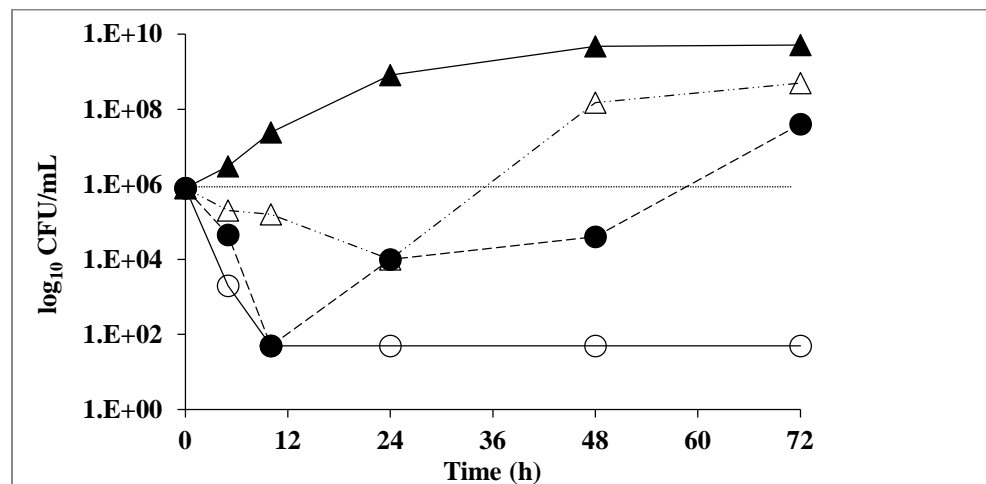


Figure 3-3. Time kill curves for *C. neoformans* H99 at different concentrations of K20: control (no drug) (filled triangles), 2 mg/L (open triangles), 4 mg/L (filled circles), and 8 mg/L (open circles).

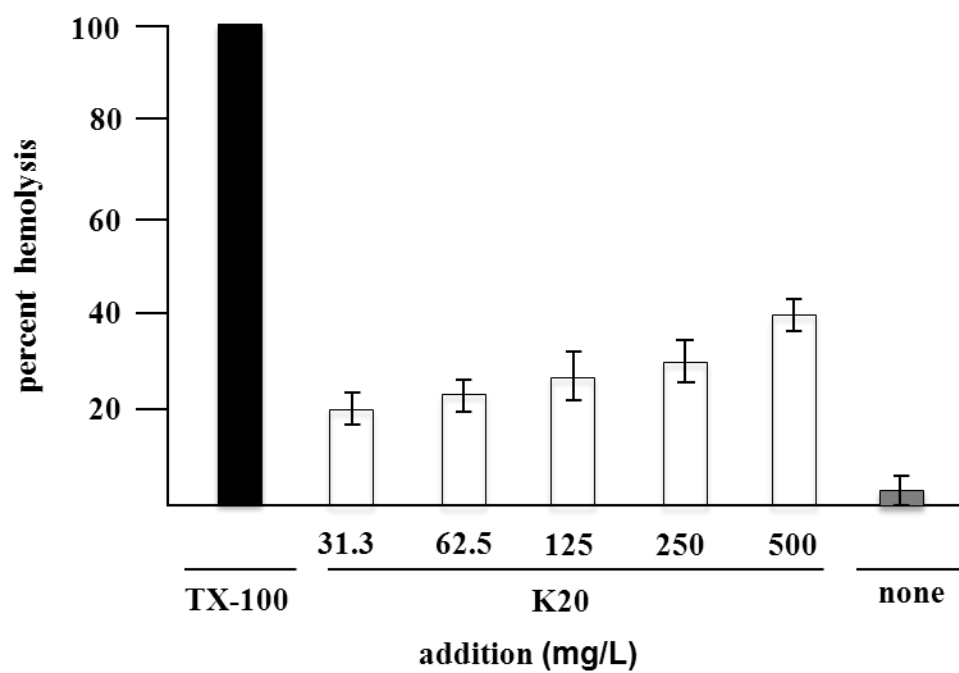


Figure 3-4. Hemolytic activity of K20 (white bars) against sheep erythrocytes after 1 h exposure at 37°C. Positive control (100% hemolysis) was provided by treatment with Triton X100® (1%, v/v) (black bar). Negative control (grey bar) without drug.

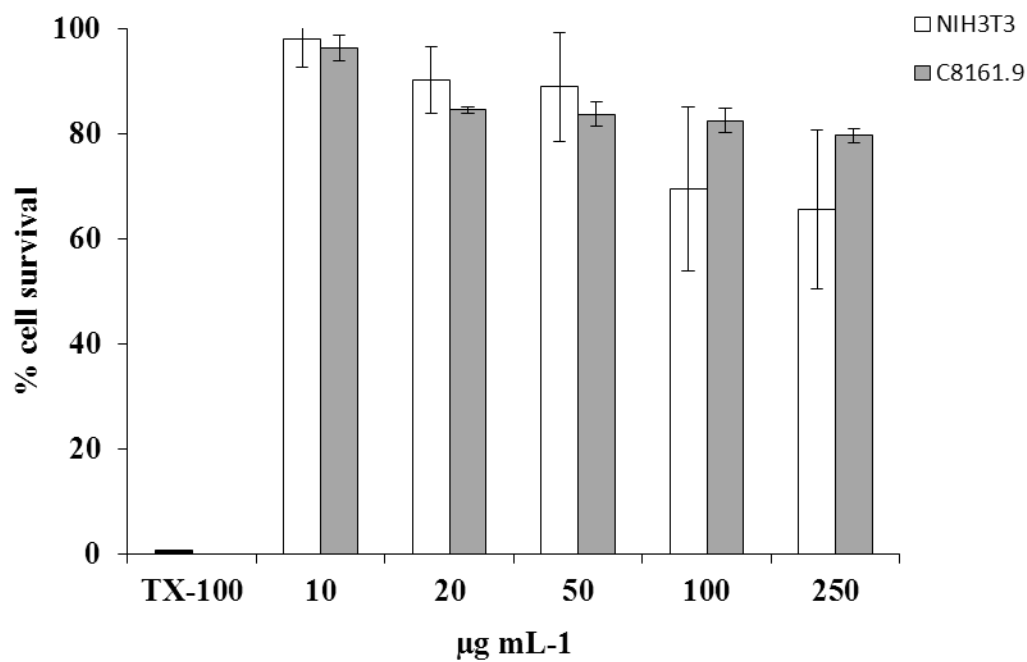


Figure 3-5. Mammalian cell cytotoxicities of K20. MTT cytotoxicities of NIH3T3 mouse fibroblast cells (white bars) and C8161.9 melanoma cells (grey bars) with 24 h exposure to K20 at various concentrations. Positive control (0% cell survival) was provided by treatment with Triton X100[®] (1%, v/v) (black bar).

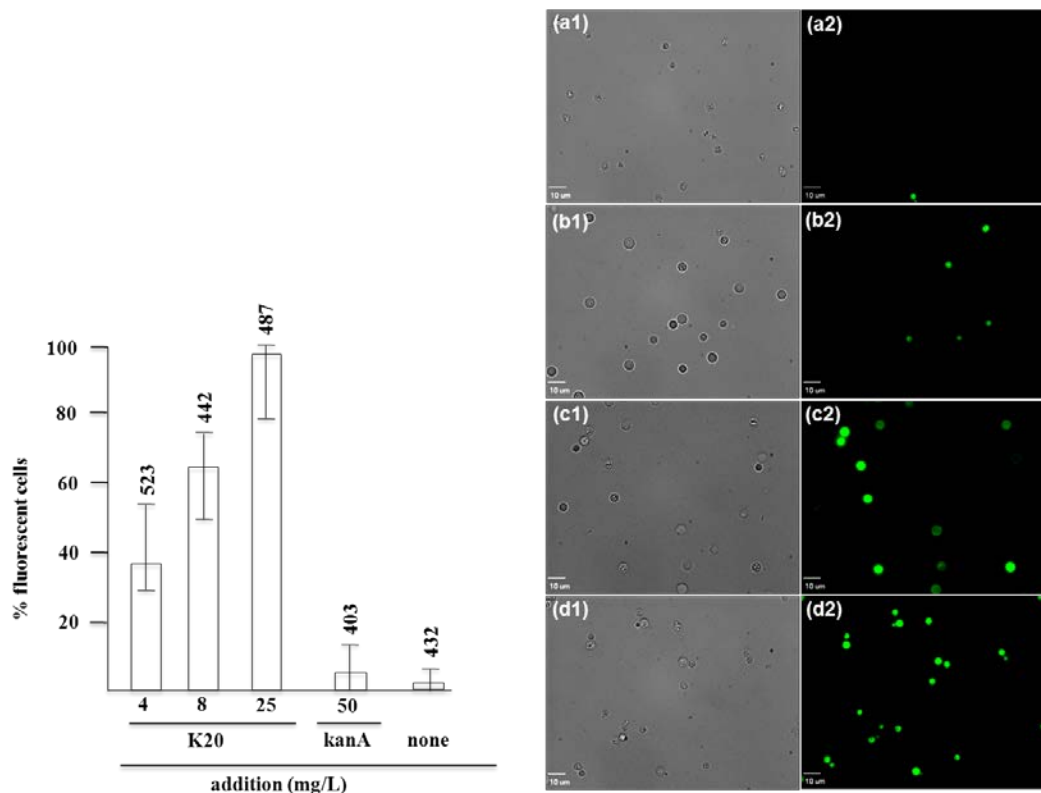


Figure 3-6. Dose-dependent membrane perturbation effects of K20 on *C. neoformans* H99. FITC dye uptake without (a1, a2) and with K20 (4 mg/L) (b1, b2), (8 mg/L) (c1, c2) and (25 mg/L) (d1, d2) exposure for 10 min. Bright-field images (a1, b1, c1 and d1) are compared with fluorescence images (a2, b2, c2 and d2). Bar length is 10 μ m. Panel (e1) shows dose-dependent effects of K20 on FITC dye uptake and effects of kanamycin A and no treatment Triton X-100[®] (1%,v/v) gave 100% dye influx (data not shown). The error bars show SD from analyses of 10 separate microscopic image fields randomly selected from at least two separate experiments. Numbers above the range bars indicate the number of cells analyzed.

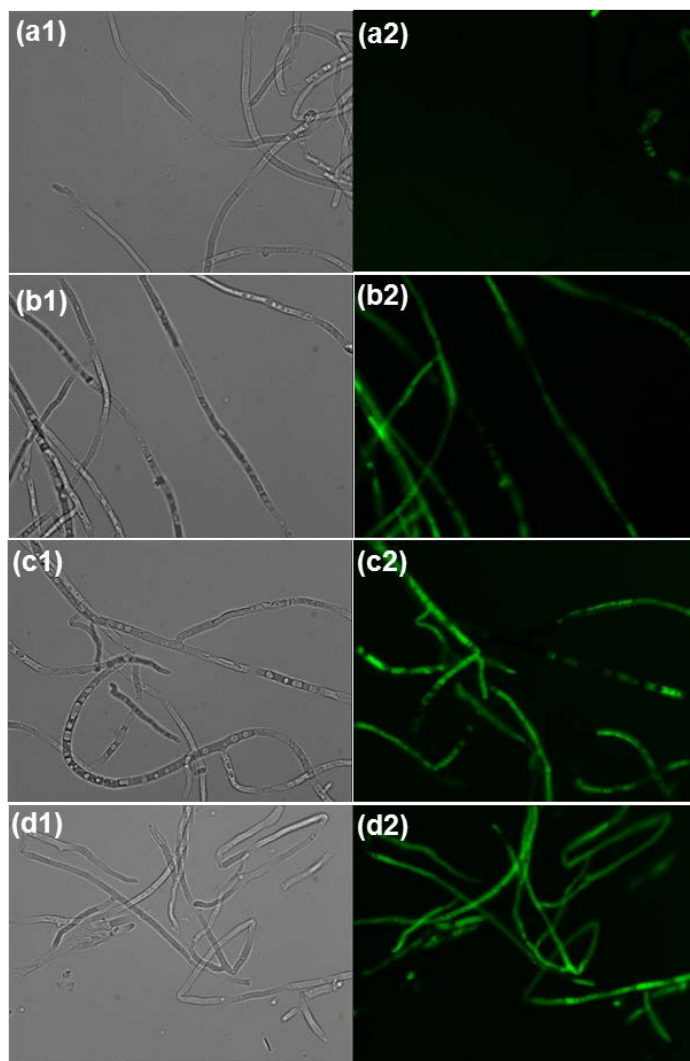


Figure 3-7. Dose-dependent membrane perturbation effects of K20 on *F. graminearum*. FITC dye uptake without (a1, a2) and with K20 (7.8 mg/L) (b1, b2), (15.6 mg/L) (c1, c2) and (32 mg/L) (d1, d2) exposure for 10 min. Bright-field images (a1, b1, c1 and d1) and fluorescence images (a2, b2, c2 and d2). Image a2 (no FG08 and no kanamycin A) shows no fluorescent cells against a fluorescent background. Bar length is 10 μ m. Triton X-100[®] (1%, v/v) gave 100% dye influx (data not shown).

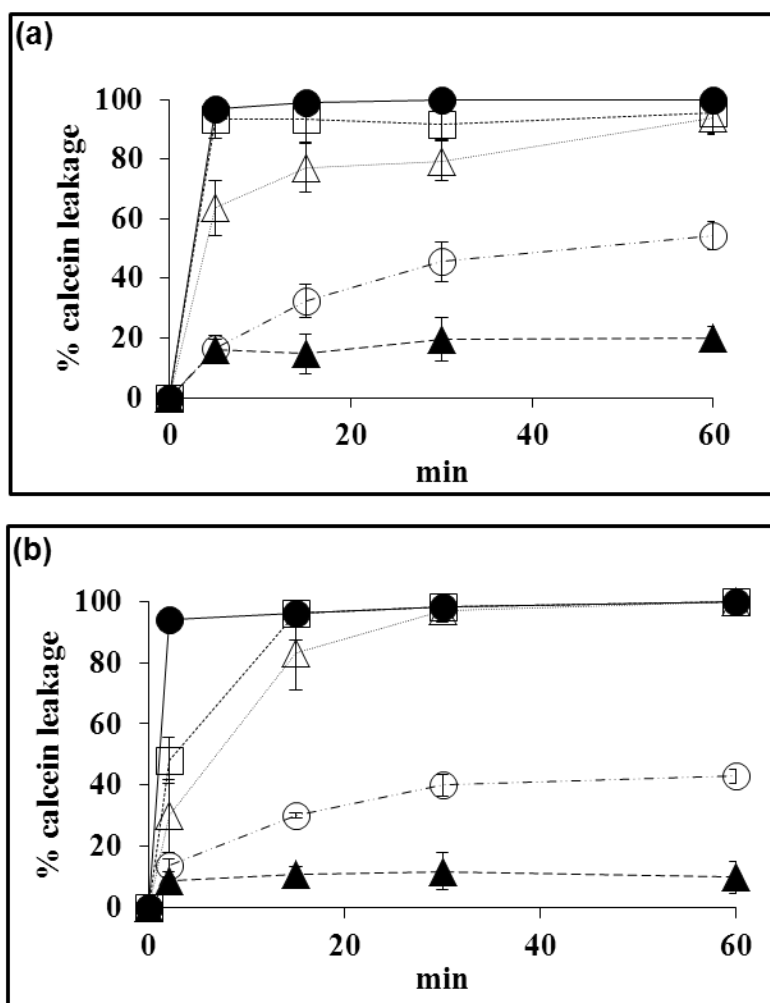


Figure 3-8. Effect of K20 on calcein release from SUVs that mimic fungal plasma membranes. Calcein released from SUVs made with PC/PE/PI/ergosterol (5:4:1:2) (a) and PC/ergosterol (7:3) (b) were exposed to 30 (open circles), 62.5 (open triangles), and 125 (open squares) mg/L K20, kanamycin A (62.5 mg/L) (filled triangles) and Triton X-100[®] (1%) (filled circles). Data compiled from three separate experiments.

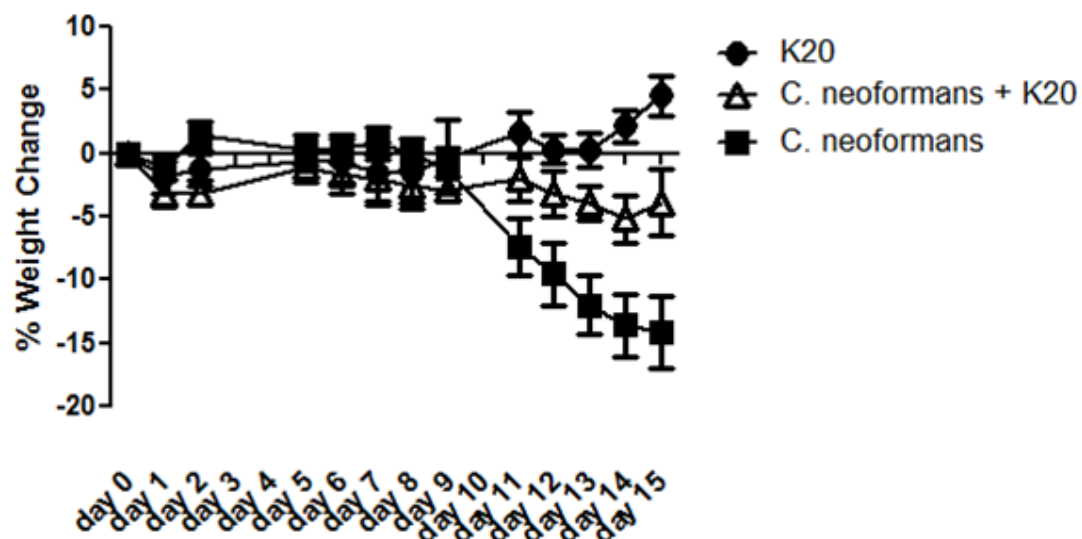


Figure 3-9. Mean percent weight change in groups of mice receiving treatments of K20 (filled circles), infected with *C. neoformans* H99 and treated with K20 (open triangles), and infected with *C. neoformans* H99 and with no K20 treatment (filled squares).

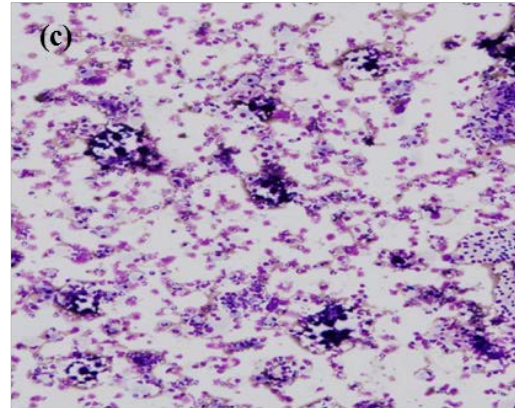
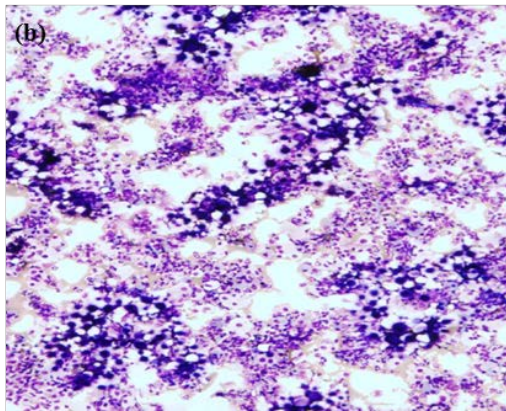
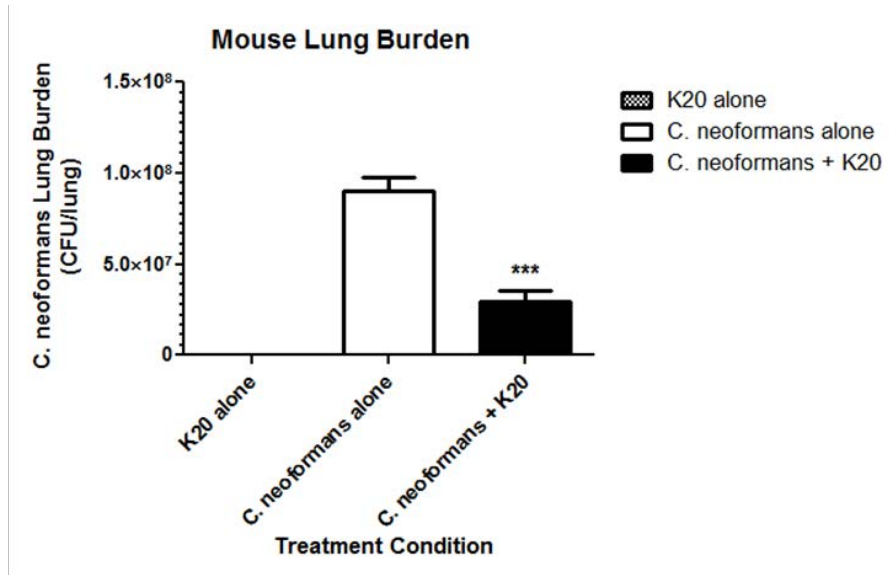


Figure 3-10. (a) Mouse pulmonary fungal burden at day 15 post-*C. neoformans* infection as assessed by plating for CFU. Grey bar, K20 alone; white bar, no K20 treatment; black bar, K20 treated infected mice. (b) Image of lung homogenate prepared from non-treated mice and (c) K20-treated mice 15 days after *C. neoformans* infection.

CHAPTER 4

ANTIFUNGAL SYNERGISM BETWEEN AMINOGLYCOSIDE K20 AND AZOLE
ANTIFUNGALS**ABSTRACT**

Opportunistic invasive fungal infections are a major cause of morbidity and mortality in immunocompromised patients. *Candida*, *Cryptococcus* and *Aspergillus* are three major opportunistic human pathogens that cause an increasing number of systemic fungal infections in critically-ill patients. Azoles are widely used antifungals to treat these infections. But the increasing frequency of cross-resistance against azoles requires improved therapeutic strategies. Recently, a novel aminoglycoside, K20, derived from kanamycin A, was shown to be inhibitory to filamentous fungi, yeasts and oomycetes, but not to bacteria. In this study, combinations of K20 and six azoles were investigated to establish whether antifungal synergy exists against *Candida* and *Aspergillus*.

Checkerboard microdilution methods and time-kill curves were used to assess synergistic, indifferent and antagonistic effects, with K20 used in combination with fluconazole, itraconazole, voriconazole, clotrimazole, ketoconazole, and posaconazole. The interactions were assessed by calculation of fractional inhibitory concentration indices. Time kill curve and disk diffusion assays were performed to confirm the synergistic interaction between these drugs.

All six azoles showed antifungal synergy in combination with K20 against two azole-resistant *Candida albicans* strains, 10231 and 64124, and one azole sensitive strain,

MYA 2876, with mean fractional inhibitory concentration indices ranging from 0.09 - 0.37. However, only itraconazole, and posaconazole were synergistic with K20 against *Aspergillus flavus*, with mean fractional inhibitory concentration indices ranging from 0.22 - 0.37. A time kill curve performed by colony counting confirmed the synergistic interactions of K20 and azoles, with a $\geq 2 \log_{10}$ decrease in CFU/mL compared with the corresponding azoles alone.

K20 showed potent antifungal synergism when combined with each of six well-known azoles against *C. albicans* strains and with two azoles against *A. flavus*. These results suggest that combination therapies of K20 and azoles may represent a new and effective strategy to combat invasive fungal infection caused by azole-resistant *C. albicans* and *A. flavus*.

INTRODUCTION

The frequency of invasive fungal infections has increased due to the rising number of immunocompromised individuals resulting largely from AIDS, cancer chemotherapies, and bone marrow and organ transplantations (1, 2). *Candida albicans*, *Cryptococcus neoformans* and *Aspergillus fumigatus* are the major human fungal pathogen associated with unacceptably high mortality rates of 20-40 % (3), 20-70 % (4), and 50-90 % (3), respectively, in immunocompromised patients. Several studies have also estimated that 6-11 % of all positive nosocomial bloodstream infections could be attributed to *Candida* spp. (5, 6).

Currently, azoles have emerged as the first-line drugs used to treat various fungal infections including candidal infections in critically ill patients (7). However, the major weakness of azoles as an antifungal agent is that they are fungistatic. Their efficacy depends on the degree of host immunity and is thus lacking in immunocompromised patients (7). In addition, the fungistatic properties of azoles are predicted to promote development of fungal resistance that further complicates the management of fungal disease (8). Therefore, new strategies for the treatment of invasive fungal infections are warranted. Previously, promising results were observed by combining azoles with different compounds such as tacrolimus (FK506), cyclosporine A, amiodarone, and retigeric acid B against *C. albicans* strains (9, 10, 11, and 12). The combination therapy of azoles with other antifungal or non-antifungal agents may lead to new antimicrobial therapies.

Aminoglycosides are compounds having two or more amino sugars bound to an aminoacyclitol ring via glycosidic bonds. Many are used therapeutically against bacterial infections of humans and animals. Among them, kanamycin A, produced by the soil microbe *Streptomyces kanamyceticus*, is one of the most successful (13, 14, 15). Kanamycin A is structurally based on sugar rings I and II of neamine with an attached ring III of *O*-6-linked kanosamine. The aminoglycosides are generally viewed to act against bacteria (15). Most bind directly to the prokaryotic 16S rRNA in the decoding region A site, leading to the formation of defective cell proteins. Despite being mainly antibacterial, certain classical aminoglycosides are also found to inhibit crop pathogenic fungal oomycetes (16), and certain structurally unusual aminoglycosides inhibit yeasts

and protozoans (17). Recently, we reported a novel aminoglycoside K20 that is derived from kanamycin A by substitution of an octanesulfonyl chain at the 6''- *O* position of ring III (18). K20 exhibited broad-spectrum antifungal activity but did not inhibit tested bacterial and mammalian cells. Because of its broad-spectrum antifungal activity and feasibility for mass production, K20 may be a good candidate for therapeutic use in medicine. However, synergistic effectiveness of K20 and azoles on antifungal action has not been explored. In this study, we investigated the combined effects of six azoles and K20 against clinically important fungal isolates by the checkerboard microbroth dilution method, time kill curves and disk diffusion assays.

MATERIALS AND METHODS

Antifungal agents

Aminoglycoside K20 was synthesized from kanamycin A as previously described (18). A 10 g/L stock solution was prepared in twice distilled water and stored at 5°C. The antifungal agents fluconazole (FLC), ketoconazole (KTZ), and chlotrimazole (CTZ) (Sigma- Aldrich); voriconazole (VRC) and posaconazole (POS) (Selleck Chemical, Houston, Texas), itraconazole (ITC) (Cayman Chemical, Ann Arbor, MI); metconazole (BASF corporation) were from commercial sources. FLC was dissolved in distilled water at a final concentration of 2.5 mg/mL. KTZ, CTZ, ITC, VRC, and POS were dissolved in DMSO at final concentrations of 5 mg/mL for each.

Organisms and culture conditions

Azole-resistant (azole-R) strains *C. albicans* ATCC 64124 and *C. albicans* ATCC 10231 and azole-sensitive (azole-S) *C. albicans* ATCC MYA-2876 were obtained from the American Type Culture Collection (Manassas, VA, USA). *A. flavus* was obtained from Dr. B. Kropp (Utah State University, Logan, Utah, USA). Yeasts and filamentous fungi were cultivated in potato dextrose broth (PDB) (Difco, BD, Franklin Lakes, NJ, USA) at 30 – 35°C.

Inoculum preparation

All *C. albicans* strains were grown on potato dextrose agar medium (PDA) for 48 h at 35°C. A single colony of each isolate was then used to inoculate 5 mL of PDB and incubated for 24 h at 35°C. Similarly, *A. flavus* was grown in PDB for 7 days at 30°C. Spores were isolated from sporulating cultures growing in PDB medium by filtration through sterile glass wool. The cells were titrated using a hemocytometer to attain the inoculum size of 2×10^6 CFU/mL for both yeasts cells and fungal spores in PDB medium. Finally, the inoculum size was verified by plate colony count method on PDA.

Antifungal susceptibility testing

In order to choose the appropriate range of drug concentrations for the combination studies, the minimal inhibitory concentrations of K20 and azoles against yeast strains and filamentous fungi were assayed in 96 well microtiter plates as described in CLSI M-27-A2 (19) for yeasts and CLSI M-38-A for filamentous fungi (20). Two-fold serial dilutions of K20 and azoles were made in sterile 96-well plates (uncoated

polystyrene, Corning Costar, Corning, NY, USA) in the range of 0.48 - 250 mg/L for K20 and fluconazole and 0.048 - 25 mg/L for rest of the azoles. Cells or spores were added to each well except the sterility control well to achieve a final concentration of 1×10^5 CFU/mL. The plates were incubated at 35°C for 48 h (yeasts) or 72 h (filamentous fungi). The fungal growth was measured using a visual observation method that was further confirmed using a Zeiss Invertoskop 40C (Carl Zeiss Inc., Germany). For visual reading, MIC was defined as the lowest drug concentration showing 80% (or more) growth inhibition compared to drug-free control. Each test was performed in triplicate.

Checkerboard analysis

The combination studies between K20 and azoles against different fungal strains were performed using a microdilution checkerboard technique according to CLSI M27-A2 (19) guidelines for yeasts. Synergistic interactions were performed using 96-well flat-bottomed microtiter plates. The final concentration of yeast cells or fungal spores was at a viable cell density of 1×10^5 CFU/mL as determined by viable cell colony counting on agar plates. Similarly, the final concentrations of the drugs ranged from 0.04 to 3 µg/mL for ITC; 0.3 to 48 µg/mL for FLC; 0.01 to 1 µg/mL for VRC; 0.07 to 2.5 µg/mL for CTZ; 0.005 to 2 µg/mL for POS; 0.3 to 24 µg/mL for KTZ and 2 to 256 µg/mL for K20. Plates were incubated at 35°C for 48 - 72 h. The growth in each well was measured by visual observation that was confirmed using a Zeiss Invertoskop 40C (Carl Zeiss Inc., Germany) in the same manner as antifungal susceptibility testing. Each experiment was performed in triplicate.

Interaction model

A non-parametric model, the FICI model that is based on a no interaction theory Loewe additivity (LA) (21) was used to evaluate the interaction nature of K20 and azoles. The LA theory is based on the idea that a drug cannot interact with itself. In the LA-based model, concentrations of the drugs, alone or in combinations, which produce the same effect, are compared. According to LA theory, FICI can be defined as the sum of the MIC of each drug when used in combination divided by the MIC of the drug used alone. Drug interactions were classified as synergistic, indifferent, or antagonistic according to the fractional inhibitory concentration index (FICI). The interaction was defined as synergistic if the FICI was ≤ 0.5 , indifferent if $>0.5 - 4$, and antagonistic if >4 (21).

Time kill curves

Time kill curves were performed to study the activity of K20 with or without ITC or FLC against azole resistant *C. albicans* 10231. The strain *C. albicans* 10231 was prepared at the starting inoculum of 10^5 CFU/mL in PDB medium. A set of solutions was prepared a drug-free growth control, K20 alone (32 $\mu\text{g/mL}$), ITC alone (0.18 or 0.37), FLC alone (12 $\mu\text{g/mL}$), and combinations of K20 with each azole. All solutions were incubated at 35°C with continuous agitation (22). At various time points (0, 3, 6, 9, 24 and 48 h after incubation), a 100 μL aliquot was removed from each solution and serially diluted 10-fold in sterile water. A volume of 100 μL of each dilution was spread on the PDA plate to allow growth. Colony counts were determined after incubation for 48 h. The experiment was performed in triplicate. For antifungal interactions tested by time-kill methods, the following criteria are commonly followed: (i) synergy is defined as a ≥ 2

log₁₀ decrease in CFU/mL compared to the most active constituent; (ii) antagonism is defined as a ≥ 2 log₁₀ increase in CFU/mL compared to the least active agent (22).

Disk diffusion assay

C. albicans MYA-2876 (azole-S) and *C. albicans* 64124 (azole-R) yeast cells at a cell density of $\sim 5 \times 10^5$ were spread onto PDA medium. A sterile Whatman paper disk (7 mm) was placed on top of the PDA. For azole-S strain, either 10 μ L of water, ITC (0.5 μ g/mL), K20 (32 μ g/mL), or their combination (0.5 μ g/mL, ITC plus 32 μ g/mL, K20) were applied on the filter disks. Similarly, for azole-R strain, 10 μ L of water, ITC (800 μ g/mL), K20 (1000 μ g/mL), or their combination (800 μ g/mL, ITC plus μ g/mL, K20) were applied on the filter disks. The cells were incubated for 24-48 h at 30°C.

RESULTS

Antifungal susceptibility testing

K20 showed a weak inhibitory effect against azole-S *C. albicans* MYA2876, azole-R *C. albicans* 64124 and *A. flavus*, with MICs ranging between 128 μ g/mL, and 1250 μ g/mL (Table 4-1). Among azoles, POS had the strongest activity against all tested fungi with MICs ranging from 0.15 - 6 μ g/mL, followed by CLZ (0.5 - 6 μ g/mL). ITC and VRC were also active with all of the fungal strains except for *C. albicans* 64124, with MICs ranging between 0.37 - 48 μ g/mL (ITC) and 0.015-64 μ g/mL (VRC). Conversely, all of the tested fungal strains significantly less sensitive to KTZ (MICs ranging from 6 - 25 μ g/mL) and FLC (MICs ranging from 48 - 400 μ g/mL) (Table 4-1).

Interaction between K20 and azoles

The nature of the interaction between K20 and azoles was evaluated by the non-parametric FICI model. The MICs of K20 and azoles, alone and in combination against tested fungal strains, are summarized in Table 4-1. K20 exhibited strong synergy with all six azoles tested against azole resistant *C. albicans* strains 10231 and 64124, and one azole sensitive strain, MYA 2876, with mean fractional inhibitory concentration indices ranging from 0.09 - 0.37. However, only POS and ITC in combination with K20 showed synergy against *A. flavus*, with an FICI value of 0.37 for both azoles. The mean MICs of azoles in the presence of K20 and K20 in presence of azoles were reduced by 4-fold to 65-fold, and 8-fold to 32-fold, respectively, against tested fungal strains. For example, the MIC of FLC against azole-S strain *C. albicans* MYA 2876 decreased from 300 µg/mL when tested alone to 4.6 µg/mL in the presence of K20, a decrease of 65-fold (Table 4-1).

Time kill curves

The synergistic interaction of ITC and FLC in combination with K20 was confirmed by time kill curves against one chosen azole-R *C. albicans* 10231 (Figure 4-1). In the presence of 32 µg/mL K20, growth of *C. albicans* was comparable to the growth control. Likewise, at the concentrations used, ITC (0.37 µg/mL) and FLC (12 µg/mL) alone showed fungistatic effect after 24 h growth. However, ITC-K20 (0.37 - 32 µg/mL) and FLC-K20 (12 - 32 µg/mL) combination therapy yielded a ≥ 2 log₁₀ decrease in CFU/mL compared with each compound alone. The K20-azole combinations showed significant reduction in candidal growth at 3 h and 6 h and completely killed by 9 h of treatment.

Disk diffusion

To further reconfirm the synergistic interaction of K20 with azoles, the susceptibility of azole-R *C. albicans* 64124 and azole-S *C. albicans* MYA2876 strains to K20, ITC and POS alone and in combination was analyzed by disk diffusion assay. As shown in Figure 4-2, K20 alone at 500 and 1000 $\mu\text{g/mL}$ per disk did not show inhibition against azole-R *C. albicans* 64124. Interestingly, when combined with POS (100 $\mu\text{g/mL}$) or ITC (800 $\mu\text{g/mL}$), notable zones of inhibition were observed. Similarly, K20 alone at 32 $\mu\text{g/mL}$ per disk did not show inhibition against azole-S *C. albicans* MYA2526 but when combined with 0.5 $\mu\text{g/mL}$ of ITC or 2 $\mu\text{g/mL}$ of POS, zones of inhibition were observed (Figure 4-2).

DISCUSSION

Invasive fungal infections are on the rise as the number of patients with compromised immune systems continues to increase (1). The antifungal therapies that are currently available show limited clinical efficacy to some invasive fungal infections, such as candidiasis, aspergillosis and cryptococcosis. Currently, azoles are the first-line drugs that have been shown to be as effective as amphotericin B against various fungal infections. However, the major weakness of azoles as an antifungal agent is they are only fungistatic, and they also tend to promote fungal resistance. This has expanded the need for the discovery of novel antifungal agents or the new strategies to keep fungal infections at bay. The combination therapy of azoles with other antifungal or non-antifungal agents may lead to new antimicrobial therapies

A novel aminoglycoside analog K20, was shown to have promising antifungal activities against fungi (16), being slightly more active against filamentous fungi (except for *A. flavus*) than against yeasts (except for *C. neoformans* strains). In this study, K20 exhibited high MICs against *C. albicans* strains and *A. flavus* which were consistent with the previous results of K20 on antifungal susceptibility testing. Similarly, ITC, POS, CLZ, and VRC showed good sensitivity to all tested fungal strains (except for *C. albicans* 64124) with the MICs ranging from 0.015 - 3 $\mu\text{g/mL}$ (Table 4-1). Interestingly, all of the candidal strains were resistant to FLC and moderately resistant to KTZ, with MICs ranging from 48 - 400 $\mu\text{g/mL}$ and 6 - 25 $\mu\text{g/mL}$, respectively.

Checkerboard microdilution technique was performed to understand interaction of K20 and azoles against three strains of *C. albicans* and one strain of *A. flavus in vitro*. The nature of interactions between these two drugs was evaluated by an FICI model. To minimize the experimental error in determining FICI values, triplicate experiments performed for each strain for combination studies were considered as one outcome. The data showed promising synergy between K20 and all six azoles against tested fungi except for *A. flavus*, with FICI values >0.5 . Interestingly, only PSC-K20, and ITC-K20 combinations showed synergy against *A. flavus* (Table 4-1). Antagonism was not observed between K20 and azoles with any of the strains tested.

The synergistic interactions by checkerboard microdilution were confirmed by a time-kill test in this study. This method is widely used because this provides growth kinetic information and the effect of combination therapy on cell viability over time (20). ITC and FLC in combination with K20 against one chosen strain, *C. albicans* 10231,

showed a ≥ 2 log₁₀ decrease in CFU/mL compared with ITC, FLC or K20 alone after 3 h of incubation. These combination therapies also showed a fungicidal effect by 9 h. This is in contrast to the fungistic effect of azoles when used alone (Figure 4-2). Agreement was seen between the FICI method and the time-kill curves for all fungal strains tested.

Disk diffusion assay was further used to reconfirm the synergistic interaction between K20 and azoles. K20, ITC and POS alone at investigated concentrations did not produce clear zones of inhibition against azole-R and azole-S *C. albicans*. Interestingly, when ITC and PSC were combined with K20, they produced notable zones of inhibition against tested strains, suggesting the synergistic interaction between K20 and azoles does exist.

Azoles act by inhibition of 14- α -demethylase, the enzyme that converts lanosterol to ergosterol in fungi. This leads to the accumulation of 14-methylated sterol, which can cause disruption of the fungal membrane (23, 24). Previously, our study on the mechanism of action of K20 revealed that it acts on fungi by disrupting the fungal membrane. However, the exact molecular target for K20 is yet to be determined. It has been reported that novel aminoglycoside FG08 exhibits a membrane lipid-modulated mechanism of action against fungi (25). K20 is believed to have the similar mode of action against fungi. Although, the mechanism of synergistic interaction with azoles remains unclear at present, it could be presumed that both K20 and azoles target different molecular sites in the fungal plasma membrane. This may facilitate the swift destabilization of the fungal plasma membrane, thus augmenting the fungicidal activity. We have also previously reported the low cytotoxicity profile of K20 against animal cells *in vitro* and *in vivo*, thus, K20 is potentially a good candidate for use as a therapeutic

antifungal agent. The use of K20 in combination with azoles may provide further improvement in treating invasive fungal infections in medicine.

In conclusion, our study demonstrates the synergistic combination effects between K20 and six azoles against tested *C. albicans* strains. These synergistic interactions were further confirmed by time kill curves and disk diffusion assay. K20-azoles combination therapy might be mainly beneficial to treat invasive fungal infections like candidiasis and aspergillosis. However, rigorous animal model studies are required to validate the significance of K20-azole combination as a potential antifungal therapy and further studies with wide array of clinical isolates are needed.

REFERENCES

1. **Fisher, M. C., D. A. Henk, C. J. Briggs, J. S. Brownstein, L. C. Madoff, S. L. McCraw, and S. J. Gurr.** 2012. Emerging fungal threats to animal, plant and ecosystem health. *Nature* **484**:186-194.
2. **Zhai, B., H. Zhou, L. Yang, J. Zhang, K. Jung, C. Z. Giam, X. Xiang, and X. Lin.** 2010. Polymyxin B, in combination with fluconazole, exerts a potent fungicidal effect. *J. Antimicrob. Chemother.* **65**: 931-938.
3. **Lai, C. C., C. K. Tan, Y. T. Huang, P. L. Shao, and P. R. Hsueh.** 2008. Current challenges in the management of invasive fungal infections. *J. Infect. Chemother.* **14**: 77-85.
4. **Park, B. J., K. A. Wannemuehler, B. J. Marston, N. Govender, P. G. Pappas, and T. M. Chiller.** 2009. Estimation of the current global burden of

cryptococcal meningitis among persons living with HIV/AIDS. *AIDS* **23**: 525-530.

5. **Wisplinghoff, H., T. Bischoff, S. M. Tallent, H. Seifert, R. P. Wenzel, and M. B. Edmond.** 2004. Nosocomial bloodstream infections in US hospitals: analysis of 24,179 cases from a prospective nationwide surveillance study. *Clin. Infect. Dis.* **39**: 309-317.
6. **Pfaller, M. A., and D. J. Diekema.** 2007. Epidemiology of invasive candidiasis: a persistent public health problem. *Clin. Microbiol. Rev.* **20**:133-163.
7. **Masia Canuto, M., F. Gutierrez Rodero, V. Ortiz de la Tabla Ducasse, I. Hernández Aguado, C. Martín González, A. Sánchez Sevillano, and A. Martín Hidalgo.** 2000. Determinants for the development of oropharyngeal colonization or infection by fluconazole-resistant *Candida* strains in HIV-infected patients. *Eur. J. Clin. Microbiol. Infect. Dis.* **19**:593-601
8. **Denning, D. W., G. G. Baily, and S. V. Hood.** 1997. Azole resistance in *Candida*. *Eur. J. Clin. Microbiol. Infect. Dis.* **16**:261-280.
9. **Sun, S., Y. Li, Q. Guo, C. Shi, J. Yu J, and L. Ma.** 2008. *In vitro* interactions between tacrolimus and azoles against *Candida albicans* determined by different methods. *Antimicrob. Agents Chemother.* 2008. **52**:409-417.
10. **Marchetti, O., P. Moreillon, M. P. Glauser, B. Jacques, and S. Dominique.** 2000. Potent synergism of the combination of fluconazole and cyclosporine in *Candida albicans*. *Antimicrob. Agents Chemother.* **44**:2373-2381.

11. **Guo, Q., S. Sun, J. Yu, Y. Li, and L. Cao.** 2008. Synergistic activity of azoles with amiodarone against clinically resistant *Candida albicans* tested by checkerboard and time-kill methods. *J. Med. Microbiol.* **57**:457-462.
12. **Sun, L., S. Sun, A. Cheng, X. Wu, Y. Zhang, and H. Lou.** 2009. *In vitro* activities of retigeric acid B alone and in combination with azole antifungal agents against *Candida albicans*. *Antimicrob. Agents Chemother.* **53**: 1586-1591.
13. **Umezawa, H., M. Ueda, K. Maeda, K. Yagishita, S. Kondo, Y. Okami, R. Utahara, Y. Osato, K. Nitta, and T. Takeuchi.** 1957. Production and isolation of a new antibiotic: kanamycin. *J. Antibiot.* **10**:181-188.
14. **Begg, E. J., and M. L. Barclay.** 1995. Aminoglycosides 50 years on. *Brit. J. Clin. Pharmacol.* **39**:597-603.
15. **Vakulenko, S. B., and S. Mobashery.** 2003. Versatility of aminoglycosides and prospects for their future. *Clin. Microbiol. Rev.* **16**: 430-50.
16. **Lee, H. B., Y. Kim, J. C. Kim, G. J. Choi, S. H. Park, and H. S. Jung.** 2005. Activity of some aminoglycoside antibiotics against true fungi, *Phytophthora* and *Pythium* species. *J. Appl. Microbiol.* **99**:836-843.
17. **Wilhelm, J. M., S. E. Pettitt, and J. J. Jessop.** 1978. Aminoglycoside antibiotics and eukaryotic protein synthesis: structure—function relationships in the stimulation of misreading with a wheat embryo system. *Biochem.* **17**:1143-1149.

18. **Chang, C-W. T., and J. Y. Takemoto.** Aminoglycosides: synthesis and use as antifungals, Appl. No. 13/316,720, US 2012/0316125 A1, U.S. Patent and Trademark Office.
19. **NCCLS/CLSI.** 2002. Reference method for broth dilution antifungal susceptibility testing of yeasts. Approved standard. M27-A2, 2nd ed. National Committee for Clinical Laboratory Standards/Clinical Laboratory Standards Institute, Wayne, PA.
20. **NCCLS/CLSI.** 2008. Reference method for broth dilution antifungal susceptibility testing of filamentous fungi. Approved standard. M38-A2. National Committee for Clinical Laboratory Standards/Clinical Laboratory Standards Institute, Wayne, PA.
21. **Meletiadis, J., J. W. Mouton, J. F. Meis, and P. E. Verweij.** 2003. *In vitro* drug interaction modeling of combinations of azoles with terbinafine against clinical *Scedosporium prolificans* isolates. Antimicrob. Agents Chemother. **47**:106-117.
22. **Klepser. M. E., D. Malonel, R. E. Lewis, R. E, Michael, E. J. Ernst, and M. A. Pfaller.** 2000. Evaluation of voriconazole pharmacodynamics using time-kill methodology. Antimicrob Agents Chemother **40**:1917
23. **Ribeiro, M. A. and C. R. Paula.** 2007. Up-regulation of *ERG11* gene among fluconazole-resistant *Candida albicans* generated in vitro: is there any clinical implication? Diagn. Microbiol. Infect. Dis. **57**:71-75.

24. **Hitchcock, C., K. Dickinson, S. B. Brown, E. G. Evans, and D. J. Adams.**
1990. Interaction of azole antifungal antibiotics with cytochrome P450-dependent 14 α -sterol demethylase purified from *Candida albicans*. *J. Biochem.* **266**:475-480.
25. **Shrestha, S., M. Grilley, M. Y. Fosso, C-W. T. Chang, and J. T. Takemoto.**
2013. Membrane lipid-modulated mechanism of action and non-cytotoxicity of novel fungicide aminoglycoside FG08. *PLoS ONE* 8(9): e73843.
doi:10.1371/journal.pone.0073843.

Table 4-1. Suceptibility of fungal strains to K20 and azoles alone and in combination

Combination	Strains	Mean MIC ($\mu\text{g/mL}$)				FICI	Interpretation
		drug alone		drug in combination			
		azole	K20	azole	K20		
FLC+K20	<i>C. albicans</i> 64124	400	300	100	75	0.37	Synergy
	<i>C. albicans</i> 10231	>48	128	3	16	0.18	Synergy
	<i>C. albicans</i> MYA2876	300	128	4.6	8	0.09	Synergy
	<i>A. flavus</i>	nd	nd	nd	nd	nd	nd ^a
POS+K20	<i>C. albicans</i> 64124	6	300	0.37	37.5	0.18	Synergy
	<i>C. albicans</i> 10231	0.75	128	0.09	16	0.24	Synergy
	<i>C. albicans</i> MYA2876	nd	128	nd	nd	nd	nd
	<i>A. flavus</i>	0.15	1000	0.019	125	0.37	Synergy
ITC+K20	<i>C. albicans</i> 64124	48	300	6	75	0.37	Synergy
	<i>C. albicans</i> 10231	>3	128	0.18	32	0.31	Synergy
	<i>C. albicans</i> MYA2876	1	128	0.03	32	0.28	Synergy
	<i>A. flavus</i>	0.37	1250	0.04	156.2	0.22	Synergy
VRC+K20	<i>C. albicans</i> 64124	64	300	4	37.5	0.18	Synergy
	<i>C. albicans</i> 10231	1	128	0.125	4	0.15	Synergy
	<i>C. albicans</i> MYA2876	0.015	128	0.003	8	0.31	Synergy
	<i>A. flavus</i>	0.5	625	0.125	312.5	0.75	Indifference
CLZ+K20	<i>C. albicans</i> 64124	6	300	0.75	37.5	0.25	Synergy
	<i>C. albicans</i> 10231	1.25	128	0.15	8	0.18	Synergy
	<i>C. albicans</i> MYA2876	2	128	0.06	32	0.28	Synergy
	<i>A. flavus</i>	>2	1250	nd	nd	nd	nd
KTZ+K20	<i>C. albicans</i> 64124	25	150	6.25	18.7	0.37	Synergy
	<i>C. albicans</i> 10231	24	128	1.5	32	0.31	Synergy
	<i>C. albicans</i> MYA2876	12	128	1	32	0.33	Synergy
	<i>A. flavus</i>	6	1250	0.75	625	0.62	Indifference

^and, not determined

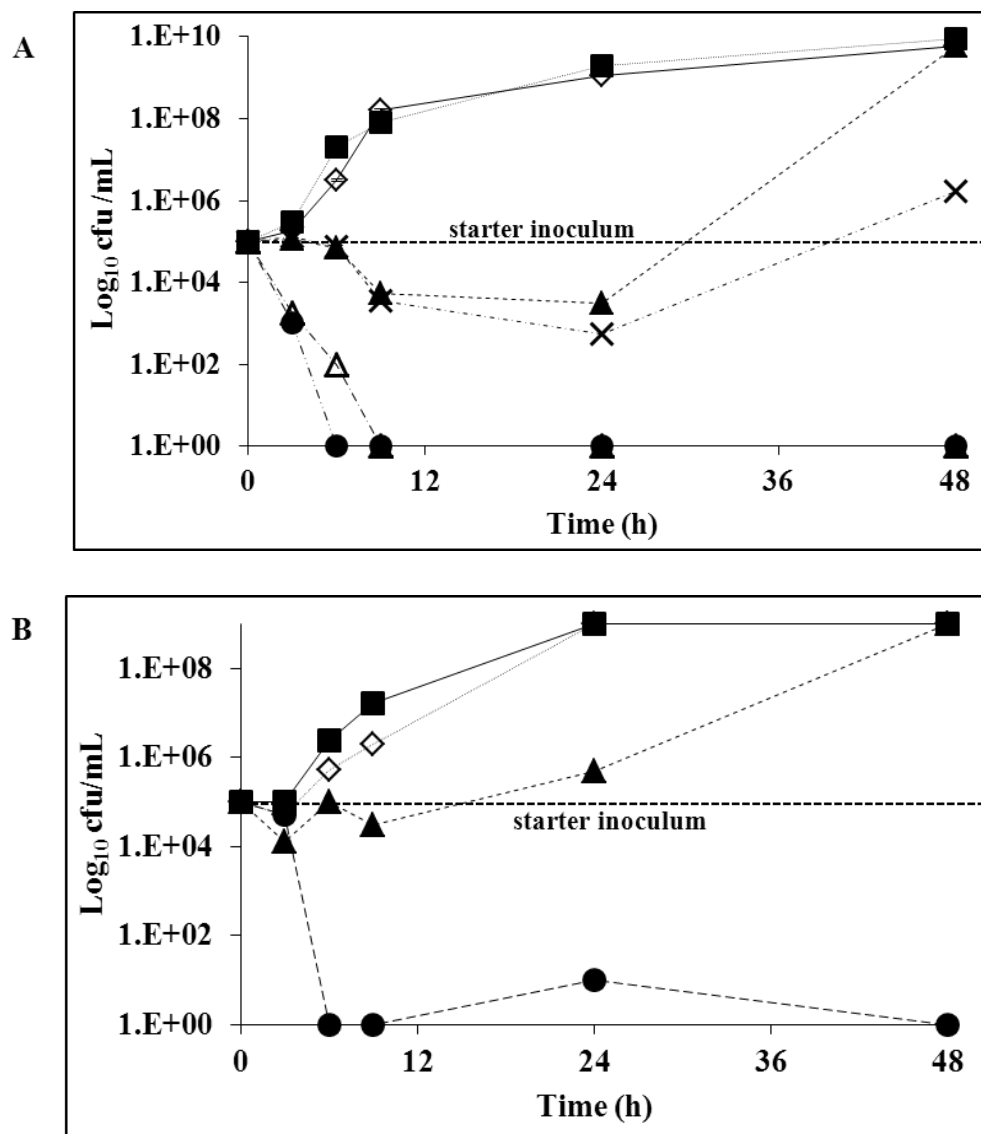


Figure 4-1. Time kill curves of ITC or FLC and K20 alone and in combination against azole-R *C. albicans* 10231. (A) *C. albicans* cells were exposed to K20 at $32 \mu\text{g/mL}$ (◇), ITC at $0.37 \mu\text{g/mL}$ (▲) or $0.18 \mu\text{g/mL}$ (×), K20 + ITC at $32 + 0.18 \mu\text{g/mL}$ (△) or at $32 + 0.37 \mu\text{g/mL}$ (●), and no drug (■). (B) Cells were exposed to K20 at $32 \mu\text{g/mL}$ (◇), FLC at $12 \mu\text{g/mL}$ (▲), K20 + FLC at $32 + 12 \mu\text{g/mL}$ (●), and no drug (■).

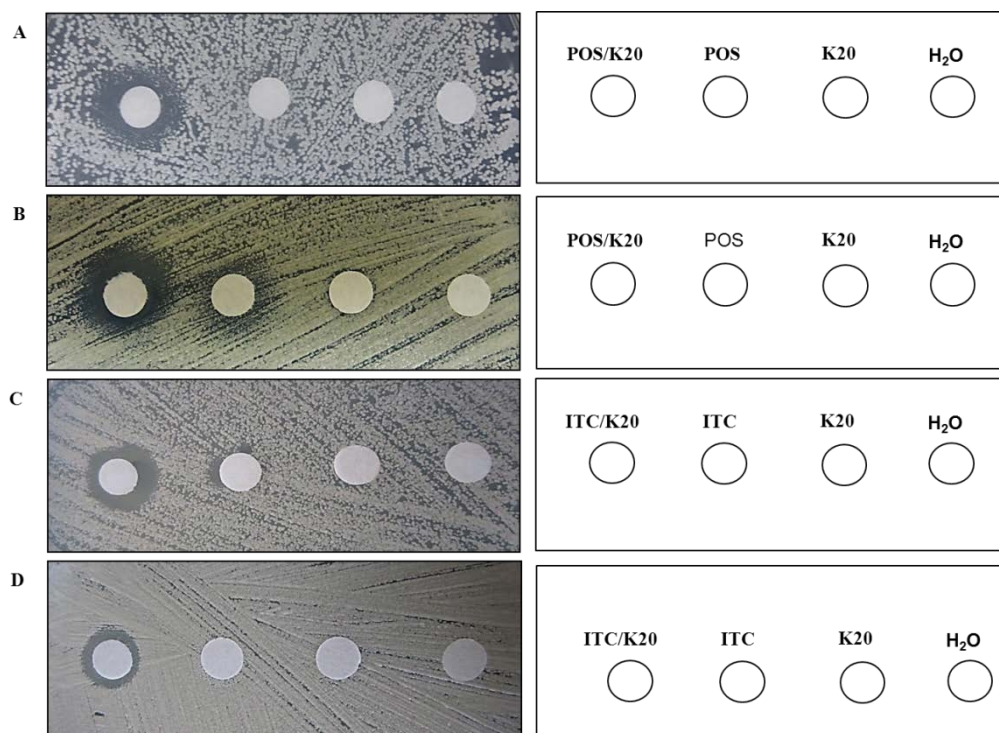


Figure 4-2. Disk diffusion assay showing synergistic interaction of K20 with POS or ITC against azole-R *C. albicans* 64124 and azole-S *C. albicans* MYA 2876. Disks containing water, K20, ITC or the drug combinations were dried and overlaid on a lawn of yeast cells derived from the strains indicated. Cells were incubated for 24 h to 48 h (A) POS (2 $\mu\text{g}/\text{mL}$) and K20 (32 $\mu\text{g}/\text{mL}$) against *C. albicans* strain MYA 2876; (B) POS(100 $\mu\text{g}/\text{mL}$) and K20 (500 $\mu\text{g}/\text{mL}$) against *C. albicans* strain 64124; (C) ITC (0.5 $\mu\text{g}/\text{mL}$) and K20 (32 $\mu\text{g}/\text{mL}$) against *C. albicans* strain MYA 2876 (D) ITC (800 $\mu\text{g}/\text{mL}$) and K20 (1000 $\mu\text{g}/\text{mL}$) against *C. albicans* strain 64124

CHAPTER 5

SUMMARY AND FUTURE DIRECTIONS

The main goals of this research were to investigate the bioactive properties and mechanism of action of FG08 and K20 and their synergistic interactions with azoles.

Previously, it was shown that novel aminoglycoside FG08 exhibits promising antifungal activities but does not inhibit bacteria (1). However, little was known about the broad-spectrum bioactivities of FG08. In this study, I explored the broad-spectrum bioactivities of FG08 and K20 against bacteria, oomycetes, yeasts, filamentous fungi and mammalian cells. The results show that FG08 and K20 are broad-spectrum antifungal agents that do not show activity against bacteria (1, 2). In particular, FG08 was shown to suppress Fusarium head blight of wheat, a crop disease caused by *F. graminearum* and that results in severe economic losses worldwide (1). K20 also showed lower MICs of 3.9-7.8 $\mu\text{g/mL}$ against *F. graminearum* *in vitro* and would expect to show similar effects against Fusarium head blight of wheat in the greenhouse as does FG08. The results indicate that FG08 and K20 may be considered promising lead compounds for novel fungicides in agriculture. Aminoglycosides are mainly antibacterial but some are reported to have mild antifungal properties (3). However, the application of aminoglycosides to combat bacterial or fungal diseases in agriculture is not recommended due to the reason that they may promote bacterial resistance. Here we show potentially new applications of novel aminoglycosides, FG08 and K20, as antifungal agents that inhibit fungi but not bacteria. Their application as fungicides in

agriculture, thus, seems attractive as they selectively kill fungi and will not promote the development of bacterial resistance.

Fungi share many biochemical targets with eukaryotic cells and antifungal agents may interact with targets may also be present in eukaryotic cells, making them unsuitable for therapeutic use. In order to distinguish between selective antimicrobial activity and non-selective lytic activity, I measured the toxicity of FG08 and K20 against sheep erythrocytes and living mammalian cells. At and above antifungal MICs, FG08 and K20 did not lyse sheep erythrocytes and did not inhibit the proliferation of NIH3T3 and C6181.9 cells. These results reveal that FG08 and K20 are not only broad-spectrum fungicides, but also appear to have an excellent safety profiles in terms of toxicity against mammalian cells. These data further expands the significance of FG08 and K20 for the application as antifungal agents for therapeutic use. However, the synthesis of FG08 is technically difficult. It requires numerous chemical synthesis steps and has a low overall yield. Because of this, it would not be cost effective to develop FG08 as an antifungal agent for commercial proposes. In contrast, production of K20 requires only three chemical synthesis steps and has a high overall yield. K20 exhibits broad-spectrum antifungal activities that are comparable to or sometimes show better activity than FG08. Thus, K20 appears more promising than FG08 as a lead compound for the development of novel antifungal agrochemicals or therapeutics. Because of this point, K20 became the major focus of my research. The *in vivo* efficacy of K20 was further explored in a murine model to determine its capabilities for preventing the establishment of pulmonary cryptococcosis. The results showed that K20 significantly prevented the establishment of

pulmonary cryptococcosis infection in the mouse model and did not exhibit side effects in the host at a high concentration of K20 (250 µg/mL). The combined observations from *in vitro* and *in vivo* results suggest that K20 shows promise as antifungal therapy for the clinical trials to treat invasive fungal infections such as pulmonary cryptococcosis.

The antifungal mechanisms of action of FG08 and K20 were investigated using intact fungal cells and model lipid bilayer membranes (SUVs). The combined observations of FITC / SYTOX Green dye permeation, K⁺ efflux, and calcein leakage from model membranes (SUVs) showed that the selective fungicidal action of FG08 against fungi is due to increasing membrane permeability that is modulated by the lipid composition of the fungal plasma membrane (4). In parallel, K20 has also shown inhibitory effects against fungi and is believed to have similar mode of action against fungi. Possibly, the amphipathic and polycationic features of FG08 and K20 may facilitate the interactions of these compounds with the fungal plasma membrane. The interactions could establish hydrogen and ionic bonding between these compounds and anionic lipid head groups such as sphingolipids, thus facilitating the fungal plasma membrane permeabilization. However, further research is desirable to elucidate such bonding and molecular interactions that should provide more understanding into the membrane perturbation effects of FG08 and the reasons for the specific targeting of the fungal plasma membrane (4). Perhaps, studying the effect of FG08 or K20 on planar lipid bilayer membranes consisting of different ratios of lipids, including sphingolipids, will help to define the interactions of these compounds with the plasma membrane and the effect of membrane composition on their antifungal activity (5).

Finally, I studied the synergistic antifungal interactions of K20 and azoles against *C. albicans* strains and *A. flavus*. K20 showed strong synergistic antifungal activities with azoles against investigated fungal strains. Currently, azoles are the principal and first-line drugs used to treat various fungal infections in humans. However, azoles are fungistatic rather than fungicidal, thus they are prone to develop resistance by fungi. Combining K20 and azoles has demonstrated remarkable fungicidal effects against azole-S and azole-R *C. albicans* strains and also has significantly reduced their antifungal MICs comparative to when they were used alone. The need for high doses of azoles to combat infections of resistant fungal strains can be lowered by combining K20 with azoles. Thus, the combination therapy appears promising to reduce side effects on hosts that may incur due to application of high doses of azoles to clear infections. This finding presents a new and potential avenue for the treatment option of systemic mycoses in medicine. The results of K20-azoles combination therapy have further encouraged us to think about the possible mechanism of synergistic antifungal action against fungi. Although, the mechanism of synergistic interaction with azoles remains unclear at present, it could be presumed that both K20 and azoles target different molecular sites in the fungal plasma membrane. This may facilitate the swift destabilization of the fungal plasma membrane, thus augmenting the fungicidal activity.

In conclusion, novel aminoglycosides FG08 and K20 are broad-spectrum antifungal agents that do not show activity against bacteria or mammalian cells. They appear to inhibit fungi by triggering plasma membrane permeability that leads to cell death. K20 demonstrated strong antifungal synergy with azoles against different fungal

strains. FG08 and K20 appear favorable for their applications as fungicides in agriculture and medicine. However, further studies, such as in animal models, are required to validate the significance of FG08, K20, and K20-azole combinations as potential antifungal therapies. Rigorous studies are warranted to test the efficacies of these drugs alone and in combination with azoles using a wide spectrum of clinical isolates of fungi. Furthermore, *in vivo* studies in pharmacodynamics and pharmacokinetics of FG08, K20 and K20-azole combinations can be performed to establish the rational dosing regimens, and identification of antifungal susceptibility breakpoints (6). Overall, these studies set an example by offering new approaches of using conventional aminoglycosides (antibacterial) in their new form as antifungal agents. Combining these novel antifungals with therapeutic antifungals such as azoles, polyenes, and echinocandins may lead to development of novel and effective antifungal therapy against fungal infections in agriculture and medicine.

REFERENCES

1. Chang C-WT, Fosso MY, Kawasaki Y, Shrestha S, Bensaci MF, et al. (2010) Antibacterial to antifungal conversion of neamine aminoglycosides through alkyl modification. Strategy for reviving old drugs into agrofungicides. *J Antibiot* 63: 667-672.
2. Chang C-WT, Takemoto JY. Aminoglycosides: synthesis and use as antifungals, Appl. No. 13/316,720, US 2012/0316125 A1, U.S. Patent and Trademark Office.

3. Lee HB, Kim Y, Kim JC, Choi GJ, Park SH, et al. (2005). Activity of some aminoglycoside antibiotics against true fungi, *Phytophthora* and *Pythium* species. *J Appl Microbiol* 99:836-843.
4. Shrestha S, Grilley M, Fosso MY, Chang C-WT, Takemoto JY. (2013). Membrane lipid-modulated mechanism of action and non-cytotoxicity of novel fungicide aminoglycoside FG08. *PLoS ONE* 8(9): e73843. doi:10.1371/journal.pone.0073843.
5. Bensaci MF, Gurnev PA, Bezrukov, SM, Takemoto JY. (2011) Fungicidal activities and mechanisms of action of *Pseudomonas syringae* pv. *syringae* lipodepsipeptide syringopeptins 22A and 25A. *Front. Microbiol.* 2:216.
6. Andes D. (2003). Pharmacokinetics and pharmacodynamics in the development of antifungal compounds. *Curr. Opin. Investig. Drugs* 4:991-998.

APPENDICES

APPENDIX A

Chemoenzymatic synthesis of novel aminoglycoside analog, FG08

FG08 is a novel aminoglycoside analog that is derived from well-known aminoglycoside kanamycin B by substitution of a C8 alkyl chain at the 4''- *O* position of ring III. It exhibits broad-spectrum of antifungal activities against a wide range of fungi including yeasts, oomycetes, and filamentous fungi but does not inhibit bacteria and mammalian cells. FG08 appears attractive for applications as a fungicide in agriculture and medicine. Despite these properties, FG08's development as an antifungal agent is limited. Incorporation of the C8 alkyl chain at the kanamycin B 4''- *O* position is difficult and the product yield is low. Since the production of FG08 via chemical synthesis is difficult, a chemo-biosynthetic strategy for its production was attempted. For this purpose, the glycosyltransferase gene, *KanE*, from *Streptomyces kanamyceticus* was cloned and expressed in *E. coli*. Purified enzyme was incubated with the substrates neamine (acceptor) and UDP-4-*O*-octyl glucoside (donor) to make FG08 or FG03. However, Kudo et al. 2009 showed a strict substrate specificity of enzyme KanE (also known as KanM2) that limited its use to make FG08 or FG03.

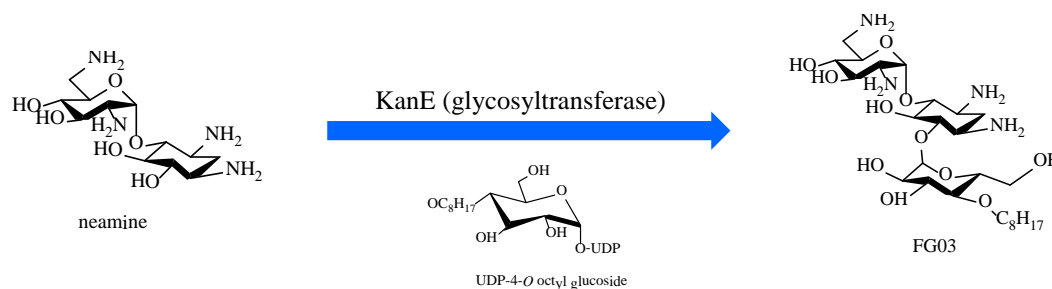


Figure A-1. Schematic diagram of chemo-enzymatic synthesis of FG03.

Bacterial strains, plasmids and culture condition:

Streptomyces kanamyceticus ATCC12853 was a gift from Dr. Jae Kyung Sohng at Department of Pharmaceutical Engineering, Institute of Biomolecule Reconstruction, Sun Moon University, Republic of Korea. It was cultured in LB medium at 28°C. The plasmid pRSET C (Invitrogen) was used for gene cloning and expression in *E. coli*. It was propagated and maintained in *E. coli* strain TOP10. Transformants were selected on LB plates containing 50-100 $\mu\text{g mL}^{-1}$ ampicillin. *E. coli* BL21(DE3) pLysS was used as a host for cloning and heterologous expression of protein. Transformants were selected on LB plates using 35 $\mu\text{g mL}^{-1}$ chloramphenicol and 50 $\mu\text{g mL}^{-1}$ ampicillin. Vector NTI software was used to design primers which was later ordered from Integrated DNA Technologies.

Cloning and DNA sequencing of *KanE* gene

DNA cloning, ligation, restriction enzyme digestion and other manipulations were carried out according to the methods described by Hopwood *et al.* 2003, Kieser *et al.* 2000, Sambrook and Russell, 2001. To obtain the chromosomal DNA, a *Streptomyces*

kanamyceticus culture was heat lysed at 100°C for 10 min in sterile water. One µL of cell suspension (chromosomal DNA) was used as a template source to amplify *kanE* gene by PCR. Two restriction sites, PstI and EcoRI (NEB), were introduced at 5' end and 3' end of *kanE* gene fragment using primers 5'-GCACTGCAGGGCATGCACCTGCTGGTGCG-3'(forward primer) and 5'-CAGGAATTCTCACAGCCCGATCTCCCGGT-3'(reverse primer), respectively. PCR was performed in a thermal cycler (Mastercycler gradient; Eppendorf, Hamburg, Germany). Each assay (100 µL) consisted of 200 ng chromosomal DNA, 0.5 µM of each primer, and 1x Phusion Master Mix with GC buffer (Phusion High Fidelity PCR Master Mix, BioLabs) and 3% DMSO to improve the denaturation of GC-rich template DNA. PCR was performed under following conditions; (Total cycles-30, denaturing, annealing and extension temperatures were 98°C for 10 sec, 62°C for 30 sec, and 72°C for 1 min with additional extension of 10 min). Amplified *kanE* was inserted into the corresponding sites of pRSET C (Invitrogen) to obtain pRSET C-*kanE* recombinant plasmid (Figure A-2). The recombinant plasmid was transformed into *E.coli* BL21(DE3)pLysS by a standard heat-shock transformation protocol (Invitrogen) for overexpression.

KanE gene was successfully isolated and cloned in pRSET C vector and was confirmed by sequencing.

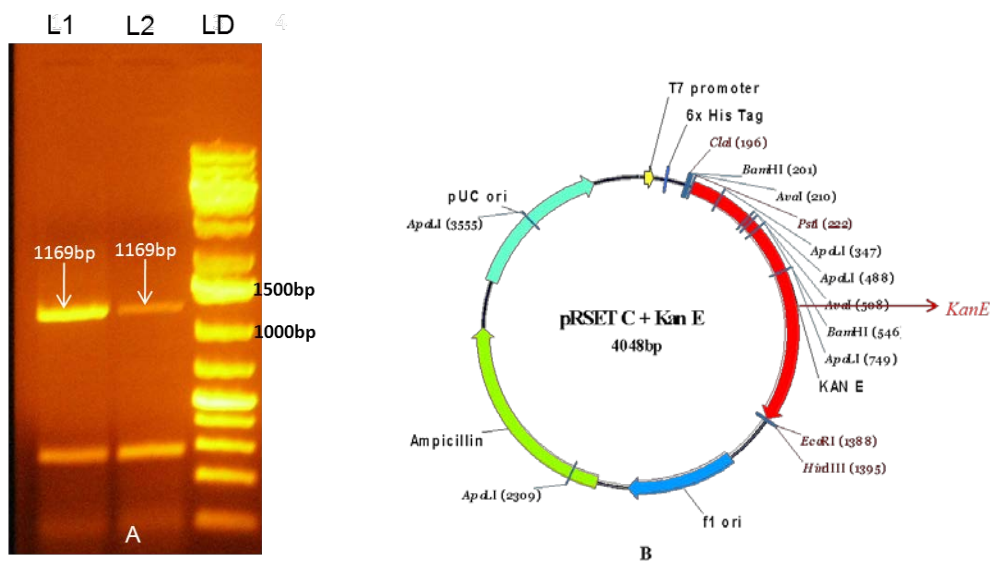


Figure A-2. (A) PCR amplified *kanE* gene and bands are shown by arrows lane 1 and lane 2). (B) Construction of recombinant plasmid pRSETC + KanE, for the expression of *kanE* in *E.coli*.

Heterologous expression of KanE in *E. coli* BL21 (DE3)pLysS

A single colony harboring pRSETC-*kanE* was grown overnight in 3 mL of super optimal broth (SOB, 2 % tryptone, 0.5 % yeast extract, 10 mM NaCl, 2.5mM KCl, 10 mM MgCl₂, 10 mM MgSO₄, and 20 mM glucose) containing ampicillin (50 µg mL⁻¹) and chloramphenicol (35 µg mL⁻¹) at 37°C in a shaker incubator 225 rpm. About 2 mL of pre-culture was used to inoculate 200 mL of fresh SOB medium and grown at 37°C with 225 rpm until OD₆₀₀ reached 0.5-1.0. T7 RNA polymerase was induced by the addition of 0.5 mM IPTG and grown continuously at 18°C for 15-18 h. Cells were harvested by

centrifugation at 8000 rpm for 15 min at 4°C. Cell pellets were washed twice by HEPES buffer (50 mM, pH 8 containing 10 % glycerol and 1 mM MgCl₂) and later resuspended in 20 mL HEPES buffer. The cell suspension was lysed by using French press at 4000-5000 psi. The process was repeated thrice to lyse the cells completely. PMFS (phenyl methyl sulfonyl fluoride) and DNase I were added before each passage through French press. The resulting cell extract was centrifuged at 10000 rpm for 30 min at 4°C. A portions of the supernatant obtained was fractionated on SDS-PAGE gel to confirm the desired protein expression. A protein band of the expected size was observed and a sample recovered to be was sent out for analysis by mass spectroscopy at Alphalyse (Alphalyse, Palo Alto, CA). The cell extract was loaded onto the Ni-NTA column for further purification.

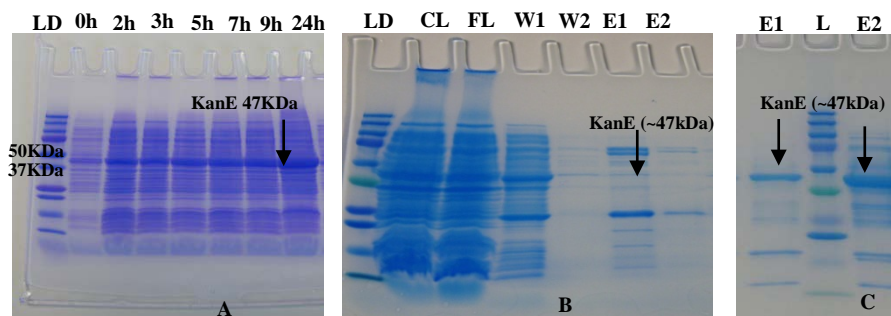


Figure A-3. SDS-PAGE analysis of KanE expressed in *E. coli* (A) KanE protein expression at different time points (0 h to 24 h). (B) Kan E protein purification from soluble fraction (C) KanE protein purification from insoluble fraction. A band for KanE was shown by arrow. LD, ladder; CL, cell lysate; FL, flow through; W1, wash 1; W2, Wash 2; E1, elution 1; E2, elution 2.

KanE glycosyltransferase enzyme was successfully expressed in *E.coli* and was confirmed by protein identification

Immunoblotting

SDS gels then were transferred to PVDF membranes. Membranes were incubate in Tris-buffered saline containing 0.05% Tween-20 and 5% fat free dry milk for 1 h at room temperature. Membranes were incubated with primary antibodies Anti His HRP (Invitrogen) overnight at 4°C. Signals were visualized using ECL (Pierce, Rockford, IL) following manufacturer's instructions.

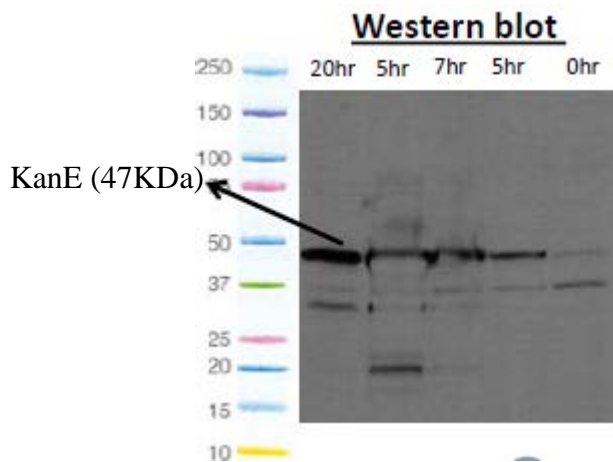


Figure A-4. Expression of KanE protein in *E. coli* detected by immunoblotting.

Enzymatic assay of KanE protein

KanE crude extract was reacted with 5 mM of acceptor (paromamine, neamine) and 5 mM of donor UDP-glucose in HEPES-NaOH buffer (50 mM, pH 8, 10 % glycerol, 1 mM MgCl₂). The reaction was continued overnight. The reaction mixture (50 µL) was treated with 25µL of 5 % 2,4-Dinitrofluorobenzene (DNFB) (Sigma-Aldrich) in methanol, 12.5 µL of DMSO and 2 M of NaOH at 60°C for 1 h. The dinitrophenyl derivative reaction products were extracted by addition of ethyl acetate (500 µL). The excess ethyl acetate reagent was removed by running the sample under a slow stream of N₂ gas. The residues obtained were dissolved in 100 µL methanol for HPLC analysis.

HPLC analysis was performed using a Waters Alliance HPLC (Waters, Manchester, UK) equipped with a Symmetry® C18 column (4.6 mm x 75 mm). A mobile phase system consists of solvent A: 99.9% and 0.1% trifluoroacetic acid and solvent B: 99.9 % acetonitrile and 0.1 % trifluoroacetic acid. The elution gradient program was: 100 % solvent A, 1min; 0-40 % solvent B, 5 min; 40-50 % solvent B, 2 min; 50 - 60 % solvent B, 8 min; 60-90 % solvent B, 2min; 90-100 %, 2 min; 100 % solvent B, 1 min. Each sample (20 µL) was injected into HPLC. Flow rate used was 1 mL/min. Column oven was 40°C and UV absorption at wavelength 350 nm was recorded.

APPENDIX B

The effect of K20 on the dimorphic transition of *C. albicans*

C. albicans 10231 cells were maintained by periodic subculturing in yeast extract dextrose broth (YPDB) medium. Cultures of yeast cells were maintained in YPDB at 32°C. To induce mycelial formation, cultures were directly supplemented with 20 % of fetal bovine serum (FBS). The dimorphic transition in *C. albicans* was investigated with cultures containing 32 $\mu\text{g mL}^{-1}$, 64 $\mu\text{g mL}^{-1}$ and 128 $\mu\text{g mL}^{-1}$ of K20; 128 $\mu\text{g mL}^{-1}$ of kanamycin B; supplemented with FBS (positive control) and without FBS (negative control) which were incubated for 48 h at 32°C (Jung et al., 2007; Sung et al. 2007). The dimorphic transition to the mycelial form was detected by phase contrast light microscopy (an Olympus IX81 fluorescence microscope using brightfield mode).

The dimorphic transition of *C. albicans* from yeast form to mycelial form is responsible for pathogenicity, with mycelial shapes being predominantly found during the invasion of host tissue. A mycelial form can be induced by temperature, pH, and serum (McLain et al., 2000). K20 significantly inhibited the serum-induced mycelial transition in comparison to the control and kanamycin A treated yeast cells (Figure B-1).

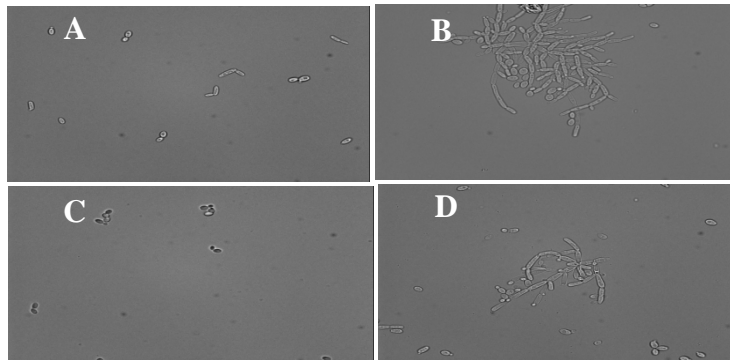


Figure B-1. The effect of K20 on the dimorphic transition in *C. albicans* 10231 (A) Yeast control without 20 % FBS and K20 (B) Cells treated with only 20 % FBS, (C) Cells treated with $16 \mu\text{g mL}^{-1}$ of K20 with FBS, and (D) Cells treated with $128 \mu\text{g mL}^{-1}$ of kanamycin A with FBS.

APPENDIX C

Bioactivity of novel aminoglycoside, FG03

Antifungal activity against *Fusarium graminearum*, *Verticillium* spp, *Botrytis cinerea*, *Microdochium nivale*, *Curvularia brachyspora* and *Pythium ultimum*, was assessed essentially as described in Lay et al. 2003. Spores were isolated from sporulating cultures growing in PDB medium at 25°C by filtration through sterile glass wool. Similarly, *Candida albicans* and *Rhodotorula pilimanae* were grown in PDA for 48 h at 35°C. A single colony of each isolate was then used to inoculate 5 mL of PDB and incubated for 24 h at 35°C. The cells were titrated using a hemocytometer to attain the inoculum size of 2×10^6 CFU mL⁻¹ for both yeasts cells and fungal spores in PDB medium. The minimal inhibitory concentrations of FG03 against yeasts and filamentous fungi were assayed in 96 well microtiter plates as described in CLSI M-38-A for filamentous fungi and CLSI M-27-A2 for yeast. Serial dilutions of FG03 was made in sterile 96 well plates (Corning Costar, Corning, NY) in the range of 250 - 0.48 µg mL⁻¹ and spore suspension was added to make final concentration of 5×10^5 CFU mL⁻¹. The plate was incubated at 35°C for 48-72 h. For disk diffusion assays, spores or cells were spread on agar plate. Sterile paper disks (0.5 cm diameter) were placed on the surface and 10 µL of FG03 solutions were applied to the disks. The plates were incubated for 24 to 48 h and zone of inhibition was measured.

The effect of FG03 on the growth of the bacterial strains *Escherichia coli*, and *Staphylococcus aureus* was assayed in microtiter plates. Cells were grown overnight in LB broth and diluted to a concentration of 1×10^4 CFU mL⁻¹. Ten microliters of the

diluted overnight culture was then added to 190 μL of LB containing 0.48 - 250 $\mu\text{g mL}^{-1}$ FG03. Plates were incubated at 37°C without shaking for 16 h. Each test was performed in triplicate.

Table.C-1. Antimicrobial activities of FG03 and kanamycin B.

Microorganisms	MIC ($\mu\text{g mL}^{-1}$)	
	FG03	kanamycin B
Bacteria		
<i>E. coli</i> ATCC25922	>250	1.95
<i>S. aureus</i>	>250	0.98
Filamentous fungi		
<i>Botrytis cinerea</i>	31.3	nd ^a
<i>Curvularia brachyspora</i>	31.3	nd
<i>Pythium ultimum</i>	31.3	nd
<i>Verticillium</i> spp.	15.2	nd
<i>Microdochium nivale</i>	7.8	nd
<i>F. graminearum</i>	7.8	>250
Yeasts		
<i>Candida albicans</i>	62.5	>250
<i>Rhodotorula pilimanae</i>	62.5	>250

^a not determined.

Hemolysis

Hemolytic activity was determined using methods described by Dartois et al. (2005) and Sorensen et al. (1996) with modification. Sheep red blood cells (RBCs) were obtained by centrifuging whole blood at $1,000 \times g$, washed four times with phosphate-buffered saline (PBS), and resuspended in PBS to a final concentration of 10^8 erythrocytes mL^{-1} . The RBC suspension ($80 \mu\text{L}$) was added to wells of a 96-well polystyrene microtiter plate containing $20 \mu\text{L}$ of serially diluted FG03, FG08, and SRE in water. The plate was incubated at 37°C for 60 min. Wells with added deionized water and Triton X-100 (1 %, w/v) served as negative (blank) and positive controls, respectively (data not shown). The percent of hemolysis was calculated using the following equation:

$$\% \text{ hemolysis} = \frac{[(\text{absorbance of sample}) - (\text{absorbance of blank})] \times 100}{(\text{absorbance of positive control})}$$

Fifty percent hemolysis (HD_{50}) values were calculated as the sample concentrations required to lyse 50% of the RBC.

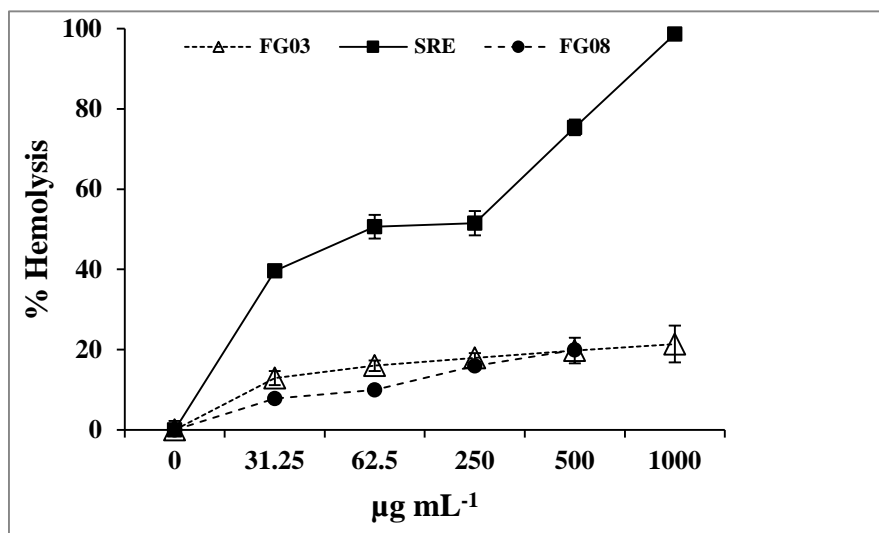


Figure.C-2. Hemolytic activity of FG03, SRE and FG08 against sheep erythrocytes

Mammalian cell growth inhibition assay

C6181.9 (melanoma) cells were grown in DMEM/Ham's F12 (1:1) containing 10% FBS. NIH3T3 cells were grown in DMEM (high glucose) media containing 10% FBS in Corning Cell Bind Flasks. The confluent cells were then trypsinized with 0.25 % w/v trypsin and resuspended in fresh medium. The cells were transferred into 96-well plates at a density of 2×10^5 CFU mL⁻¹. They were mixed with FG03 at final concentrations of 10, 20, 50, 100 and 250 $\mu\text{g mL}^{-1}$ or equivalent volume of sterile double distilled water (negative control). The cells were incubated for 24 h at 37°C with 5% CO₂ in a humidified incubator. After 24 h incubation, 10 μL of 3-(4,5-dimethylthiazol-2-yl)-2,5-diphenyltetrazolium bromide (Sigma Aldrich, St. Louis, MO) was added to each well and incubated for 4 h. In living cells, mitochondrial reductases convert the MTT tetrazolium to formazan, which precipitates. Formazan is dissolved using acidified Na₂S₂O₄ (0.01 M HCl) and the A₅₇₀ using a Gen 5 spectrophotometer (Synergy 4, BioTek). Triton X-100 (1 %, v/v) gave complete loss of cell viability and was used as a positive control.

FG03 did not show toxicity to NIH3T3 and C6181.9 cell lines at and above its antifungal activity against fungi.

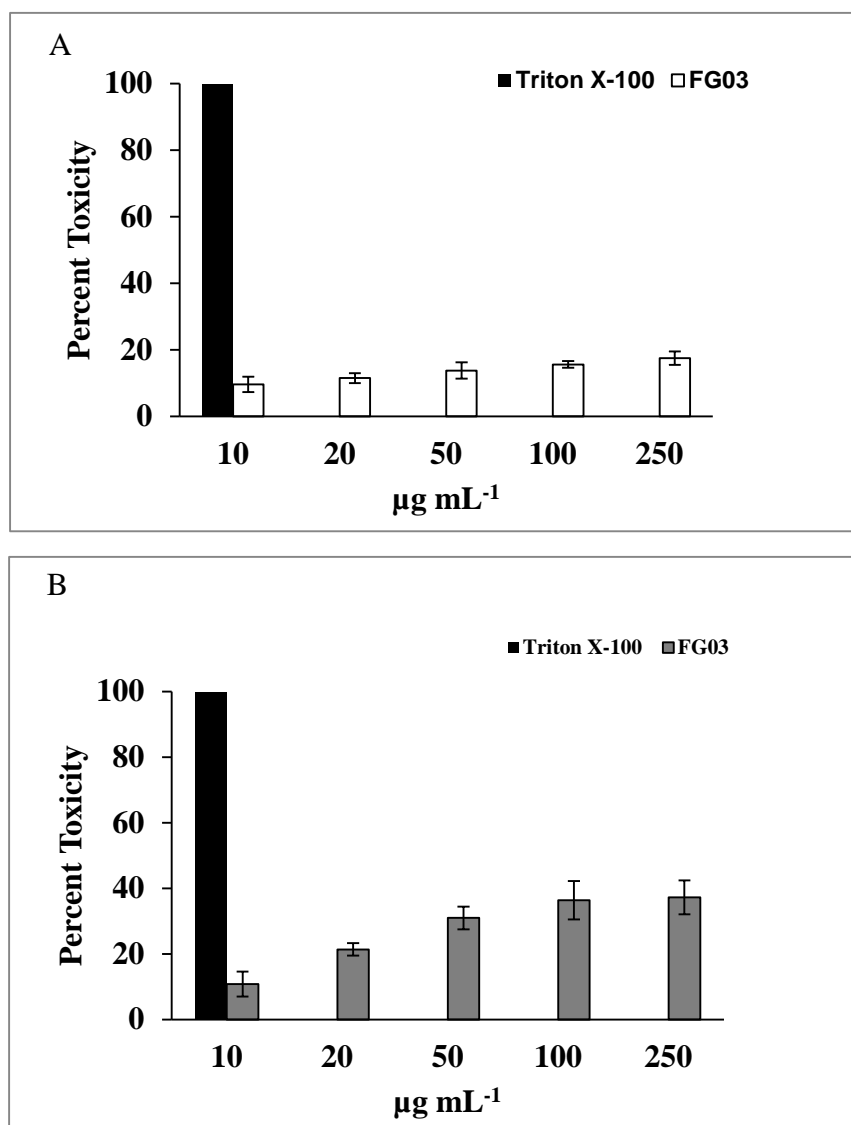


Figure. C-3. Mammalian cell cytotoxicities of FG03. (A) MTT cytotoxicities of C8161.9 melanoma cells (White bars) and (B) NIH3T3 mouse fibroblast cells (Grey bar) with 24 h exposure to FG03 at various concentrations. Positive control (0% cell survival) was provided by treatment with Triton X-100[®] (1%, v/v) (black bar).

Membrane permeabilization assay

Spores (5×10^5 spore mL^{-1}) of *Fusarium graminearum* were grown for 18 h in PDB broth with continuous agitation. Aliquots (500 μL) were taken and centrifuged for 2 min at 10,000g. The hyphae were suspended in 10 mM HEPES, pH 7.4, centrifuged again, and suspended in 500 μL distilled water (Chang et al. 2010). Hyphae were incubated with 20 $\mu\text{g mL}^{-1}$ of FG03 for 1h at 28°C with continuous agitation. The FG03 treated hyphae were assessed 10 min after addition of 6 $\mu\text{g mL}^{-1}$ concentration of FITC (10 mg mL^{-1} stock in acetone) (Sigma Aldrich) as previously described (Mangoni et al. 2004) with slight modification. Glass slides were prepared with 10 μL of each mixture and observed in dark-field and fluorescence (using an Olympus MWIB filter, excitation and emission wavelength 488-512 nm) modes with an Olympus IX81 fluorescence microscope. Data was obtained from at least three independent experiments.

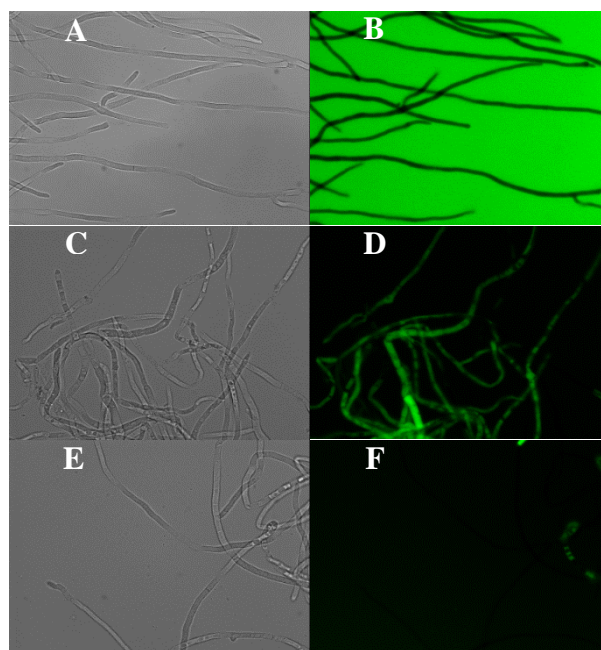


Figure C-4. Membrane perturbation effects of FG03 on *F. graminearum*.

FITC dye uptake without (A, B), with FG03 ($20 \mu\text{g mL}^{-1}$) (C, D), and kan B ($50 \mu\text{g mL}^{-1}$) (E, F) exposure for 10 min. Bright-field images (A, C, and E) and fluorescence images (B, D, and F). Image B (no FG03 and no kanamycin B) shows no fluorescent cells against a fluorescent background. Triton X-100[®] (1%, v/v) gave 100% dye influx (data not shown).

At two times MIC of $20 \mu\text{g mL}^{-1}$ for *F. graminearum*, FG03 caused significant FITC cell staining. In contrast, nearly no hyphae were stained when exposed to kanamycin B ($50 \mu\text{g mL}^{-1}$). Unexposed cells were negligibly stained (< 2%). The result indicates that FG03 also inhibits fungi by disrupting fungal cell membrane like FG08 and K20.

TEACHING EXPERIENCE

- Spring 2013 Graduate Teaching Assistant, Department of Biology, Utah State University, Logan, Utah
- Course: Microbial Physiology Lab BIOL 5300: Coordinated two student class experiments namely enzyme (Beta-galactosidase and alkaline phosphatase) cell localization and catabolite repression in *E.coli* using techniques such as enzyme assays, protein expression and extraction, SDS-PAGE, Western Blots etc. Evaluated and graded student's lab notebooks
- Fall 2012 Course: Biology Lab BIOL 1610: Supervised students doing experiments in the field of microbiology, genetics, plant science, animal science and biostatistics. Lectured on lab course topics and graded lab quizzes and assignments
- Spring 2008 Course: Microbiology Lab BIOL 3300: Responsible for conducting two labs of 30 students in each group. Taught microbiology techniques, lectured on lab topics, prepared exams and graded assignments
- Fall 2007 Worked in Media Kitchen: Maintained bacterial and fungal cultures, prepared different types of media and buffer for microbiology lab classes
- Spring 2007 Course: Plant Pathology Lab BIOL 5300: Maintained bacterial and fungal cultures and conducted lab experiments related to Plant Pathology

TECHNICAL SKILLS

Microbiology

- Performed antibacterial, antiviral and antifungal susceptibility testing for antimicrobials
- Experienced working with Gram-positive and G-negative bacteria.
- Skilled with the techniques such as disk diffusion, checkerboard and time kill curve assays.
- Maintained yeasts, molds, and mammalian cell cultures
- Skilled in identification of bacteria using traditional methods based on physiology and biochemical tests, selective media and morphology
- Worked in BSL 2 and BSL 3 laboratory set-up.

- Experienced working with mouse model (infections)
- Conducted bench-top bacterial fermentations (inoculum development, fermentor inoculation, pH calibration).

Molecular biology

- Performed DNA isolation from bacteria and fungi
- Acquired skills for PCR, gel electrophoresis, SDS-page, ELISA and Western Blotting
- Skilled in DNA analysis (isolation, purification, extraction, restriction analysis, primer design, cloning and vector transformation)
- Skilled in protein biochemistry (expression, purification and protein analysis)

Cell biology

- Skilled in mammalian cell culture (NIH 3T3, HEK 293, CHO and C6181.9 melanoma cells).
- Performed MTT assay to test the cytotoxicity of antimicrobials against animal cells.
- Skilled in extraction of red blood cell and measurement of hemolytic activities of antimicrobials

Instrumentation

- UV-visible absorption, flame atomic absorption spectroscopy and spectrofluorimeter
- Bioreactors
- Bright field and fluorescence microscopy
- HPLC, thin layer, column and gel filtration chromatography

AWARDS and FELLOWSHIPS

- Received Graduate Senate Student travel fund from Utah State University (Sep. 2013)
- USDA-NIFA- Utah Agricultural Experiment Station fellowship (2013-2014)
- Received Student travel grant from AAAS, Pacific Division meeting (June 2011)
- Second place, best poster award in AAAS, Pacific Division meeting
- Baicor, LC fellowship 2008 (June-Aug)
- Utah Science Technology and Research Initiative (USTAR) fellowship (2008-2012)

- Research assistant fellowship, National Academy of Science and Technology (NAST), Nepal (2005-2006)
- Reviewer for the Journal of Basic Microbiology

LEADERSHIP EXPERIENCE

- Experience in directing and training of undergraduate researchers
- Data analysis, interpretation and preparation of reports for publication
- Demonstrated ability to conduct independent research and publish results

COMPUTER SKILLS

- Proficient with MS office, Microsoft Excel and Power point

PUBLICATIONS

- **Shrestha S**, Grilley M, Fosso MY, Chang C-WT, Takemoto JY. **2013**. Membrane lipid-modulated mechanism of action and non-cytotoxicity of novel fungicide aminoglycoside FG08. PLoS ONE 8(9): e73843. doi:10.1371/journal.pone.0073843
- Chang C.-WT, Fosso M, Kawasaki Y, **Shrestha S**, Bensaci MF, Wang J, Evans CK, Takemoto JY. **2010**. Antibacterial to antifungal conversion of neamine aminoglycosides through alkyl modification. Strategy for reviving an old drug into agrofungicides. *J. Antibiot.* **63**, 667-672.
- **Shrestha S**, and Kropp BR. **2009**. Use of *Calvatia gigantea* to treat pack animals in Nepal. *Fungi* **2**: 59-60.
- **Shrestha S**, Chang C.-WT, Grilley M, Takemoto JY. Novel Aminoglycoside K20: Antifungal properties, mechanism of action, and suppression of murine pulmonary *Cryptococcus neoformans* infection. (**Submitted**).
- **Shrestha S**, Grilley M, Dhiman C, Chang C-WT, and Takemoto JY. Antifungal synergism between aminoglycoside K20 and azoles antifungals. (**In preparation**).
- Fosso M, Nziko V, **Shrestha S**, Kawasaki Y, and Chang C-WT: Exploring the optimal Sites for converting antibacterial kanamycin into antifungal agent. (**In preparation**)

PRESENTATIONS

- **Shrestha, S.**, Chang, C.-W. T., Grilley, M., and Takemoto, J. Y. **2013**. Synergism between aminoglycoside K20 and therapeutic azole antifungals. Presented at the Interscience Conference on Antimicrobial Agents and Chemotherapy (**ICAAC**), 53rd ICAAC, Denver, Colorado.
- **Shrestha, S.**, Chang, C.-W. T., Grilley, M., and Takemoto, J. Y. **2013**. Synergistic activity of azole and K20 against azole resistant *Candida albicans* 10231. Presented at the American Society for Microbiology (**ASM**), 113th General Meeting, Denver, Colorado.
- **Shrestha, S.** **2012**. Bioactive properties and mode of action of novel aminoglycoside analogs. Presented at the American Society for Microbiology Intermountain Branch Meeting, Pocatello, Idaho
- **Shrestha, S.**, Chang, C.-W. T., Fosso, M., Kawasaki, Y., Grilley, M., and Takemoto, J. Y. **2011**. Non-cytotoxicity of novel antifungal aminoglycosides in mammalian cells. Presented at the 92nd American Association for the Advancement of Science (**AAAS**), Pacific Division meeting, San Diego, CA.
- Fosso, M., Kawasaki, Y., **Shrestha, S.**, Takemoto, J. Y., and Chang, C.-W. T. **2011**. Synthesis and antifungal activity of kanamycin B analogs. Presented at the Gordon Research Conferences (GRC) “Carbohydrates”, Waterville, ME.
- **Shrestha, S.** **2011**. Bioactive properties and chemoenzymatic synthesis of novel aminoglycoside analog, FG08. Presented at the Intermountain Graduate Research Symposium, Utah State University, Logan, UT.
- **Shrestha, S.**, Takemoto, J. Y., and Chang, C.-W. T. **2010**. Synthesis and structural optimization of antifungal kanamycin B analogs. Presented at the 240th American Chemical Society National Meeting & Exposition, Boston, MA.

Patent

- Takemoto, J.Y., Chang, C-W. T., Grilley, M., and **Shrestha, S.** 2013. Aminoglycoside and Azole Compositions and Methods, Non-Provisional Patent Application, US61/824,847, U.S. Patent and Trademark Office, filed May 17, 2013

PROFESSIONAL MEMBERSHIPS

- American Society for Microbiology (ASM)

Languages:

- Fluent in English, Hindi and Nepali